# The role of endocannabinoid system in neuron-glial communication in the ageing and diseased brain

**Dissertation**

zur

Erlangung des Doktorgrades (Dr. rer. nat.)

der

Mathematisch-Naturwissenschaftlichen Fakultät

der

Rheinischen Friedrich-Wilhelms-Universität Bonn

vorgelegt von

**Frank Ativie**

aus

Uromi, Nigeria

Bonn, Juli 2017

Angefertigt mit Genehmigung der Mathematisch-Naturwissenschaftlichen Fakultät
der Rheinischen Friedrich-Wilhelms-Universität Bonn

1. Gutachter: PD Dr. Andras Bilkei-Gorzo

2. Gutachter: Prof. Dr. Gerhard von der Emde

Tag der Promotion: 29.11.2017

Erscheinungsjahr: 2017

## Affirmative declaration

I hereby solely declare that I prepared this thesis entitled: “The role of endocannabinoid system in neuron-glial communication in the ageing and diseased brain” entirely by myself except otherwise stated. All text passages that are literally or correspondingly taken from published or unpublished papers/writings are indicated as such. All materials or services provided by other persons are equally indicated.

Bonn, July 2017 _____

(Frank Ativie)

*The greatest scientific discovery was the discovery of ignorance*
*Yuval Noah Harari*

# Abbreviations

| | |
|---|---|
| AA | Arachidonic acid |
| 2-AG | 2-arachidonoyl-glycerol |
| AEA | Arachidonoyl ethanolamine (Anandamide) |
| ANOVA | Analysis of variance |
| ATP | Adenosine triphosphate |
| BCA | Bicinchoninic acid assay |
| BCP | 1-bromo-3-chloropropane |
| BDNF | Brain-derived neurotrophic factor |
| BMM | Bone marrow-derived macrophages |
| BSA | Bovine serum albumine |
| BrdU | 5-Bromo-2-Deoxyuridine |
| CA1 | cornu ammonis area 1 |
| CA3 | cornu ammonis area 3 |
| CB1 | Cannabinoid receptor 1 |
| CB2 | Cannabinoid receptor 2 |
| cm | Centimeter |
| Cnr1 | Cannabinoid receptor 1 gene |
| CNS | Central nervous system |

| | |
|---|---|
| DAG | Diacylglycerol |
| DAGL | Diacylglycerol lipase |
| DAPI | 4',6-diamidino-2-phenylindole |
| dH2O | Deionized H2O |
| DIG | Digoxigenin |
| DMEM | Dulbecco's Modified Eagl Medium |
| DMSO | Dimethylsulfoxid |
| DNA | Desoxyribonucleic acid |
| DTT | Dithiothreitol |
| eCB | Endocannabinoid |
| ECS | Endocannabinoid system |
| EDTA | Ethylene glycol tetraacetic acid |
| ELISA | Enzyme-linked immunosorbent assay |
| EtOH | Ethanol |
| FAAH | Fatty acid amid hydrolase |
| FCS | Fetal calf serum |
| FITC | Fluorescein isothiocyanate |
| GABA | γ-aminobutyric acid |
| g | Gram |
| GPR | G-protein coupled receptor |

| | |
|---|---|
| h | Hour |
| HBSS | Hank’s buffered salt solution |
| HCl | Hydrochloric acid |
| HRP | Horseradish peroxidase |
| IL-1β | Interleukin 1 beta |
| IL-6 | Interleukin 6 |
| i.p. | intraperitoneal |
| kg | Kilogram |
| M | Molar |
| m | Meter |
| mM | Millimolar |
| mA | Miliampere |
| MAGL | Monoacyl glycerol lipase |
| M-CSF | Macrophage colony-stimulating factor |
| MeOH | Methanol |
| min | Minutes |
| mRNA | Messenger RNA |
| ms | Milliseconds |
| MWM | Morris water maze |
| n | Number (sample size) |

| | |
|---|---|
| NAPE | N-acyl-phosphatidylethanolamine |
| NAPE-PLD | NAPE-phospholipase D |
| NeuN | Neuronal nuclear antigen |
| nM | Nanomolar |
| ns | Not significant |
| ng | Nanogram |
| PBS | Phosphate buffered saline |
| PCR | Polymerase chain reaction |
| PE | Phosphatidylethanolamine |
| PFA | Paraformaldehyde |
| PFC | Prefrontal cortex |
| PKA | Protein kinase A |
| PKC | Protein kinase C |
| PLC | Phospholipase C |
| RNA | Ribonucleic acid |
| RT | Room temperature |
| RT-PCR | Reverse transcriptase-PCR |
| s | Second |
| SDS | Sodium dodecyl sulfate |
| SEM | Standard error of the mean |

| | |
|---|---|
| SSC | Saline sodium citrate |
| TBS | tris buffered saline |
| TE | Tris EDTA |
| THC | Δ9-tetrahydrocannabinol |
| TNF-α | tumor necrosis factor alpha |
| Tris | Tris (hydroxymethyl) aminomethane |
| TRPV1 | Transient receptor potential vanilloid type-1 |
| U | Unit |
| UV | Ultraviolet |
| VTA | Ventral tegmental area |
| WHO | World Health Organization |
| WT | Wild type |
| µl | Microliter |

# Contents

# 1. Abstract (Summary)

The endocannabinoid system has been implicated in the regulation of glial activity and progression of brain ageing. Mice constitutively or specifically lacking the cannabinoid receptor 1 (CB1) on neurons or GABAergic neurons respectively have been reported to show symptoms of accelerated cellular and behavioural brain ageing. However, the particular cell type(s) and the mechanisms involved in this process have not been exhaustively elucidated. This study showed that inadequate regulation of immune response could be a possible phenomenon leading to the increased inflammation following GABA-CB1 deletion and this disturbed immune cell regulation becomes exacerbated in cases of chronic LPS challenge with increasing ageing. In addition, GABA-CB1 deletion caused enhanced accumulation of the ageing and senescence marker lipofuscin in isolated microglia, suggesting that microglial cells may be the major cell type containing the increased lipofuscin accumulation reported in hippocampal immunohistological staining. Moreover, a reduced 2-AG production following microglia-specific Daglα deletion led to upregulation of immune regulator proteins which neither influenced cytokine production nor affected social and cognitive abilities. Furthermore, increased anandamide level after FAAH deletion led to increased microglia activity with age-associated exacerbation. These findings, together, indicate that GABA-CB1 receptor-mediated cannabinoid signalling is crucial in the regulation of microglial activity in young as well as in aged animals, though the consequences of a deficient GABA-CB1 activity only become visible and eventually detrimental with increasing age.

# 2. Introduction

The endocannabinoid system (ECS) has emerged a pivotal regulator of glial activity. The role and implications of the ECS in the "normal" and "diseased" brain during ageing are increasingly of keen interest in the scientific community. Microglial cells, the resident immune cells of the central nervous system (CNS), play a central role in this ECS-related regulation of brain physiology in healthy, ageing and diseased state.

## 2.1 Ageing and brain ageing

The world report on ageing and health revealed that the majority of people across the world now live well beyond their 60s. This is as a result of safer childbirth and improved health care during childhood in developing countries, whereas in developed countries, it is rather a result of increasing life expectancy due to declining mortality in older individuals (World Health Organization, 2015). Irrespective of the specific regional and economic drivers of life expectancy, the common denominator is the ever-improving health care as a consequence of advances in medical research. Sadly but expected, increasing life expectancy also has its limitations and woes. Although advancement in medicine has led to increased longetivity, the down-side is that people now live long enough to be exposed to age-related diseases that were not prominent in the past when humans had a lower life expectancy. Thus, a growing concern in this modern society is the obvious threat posed by ageing, most specifically ageing of the brain with risk for neurodegeneration and cognitive impairment (Bishop, Lu and Yankner, 2010).

Ageing of the brain, however, occurs in individuals at varying rate, hence understanding the molecular mechanisms of ageing is fundamental to unravelling questions surrounding the process of brain ageing. Although "normal" brain ageing is not a pathological process, it shares some common characteristics with premature ageing diseases like in the Werner syndrome and

Bloom syndrome, where increasing life span is not a causative or contributing factor but increasing accumulation of damaged DNA. Various neurodegenerative disorders and cancers are also preceded by reduced integrity of molecular mechanisms akin to those observed during a non-pathological ageing process (Burtner and Kennedy, 2010; Lopez-Otin *et al.*, 2013)

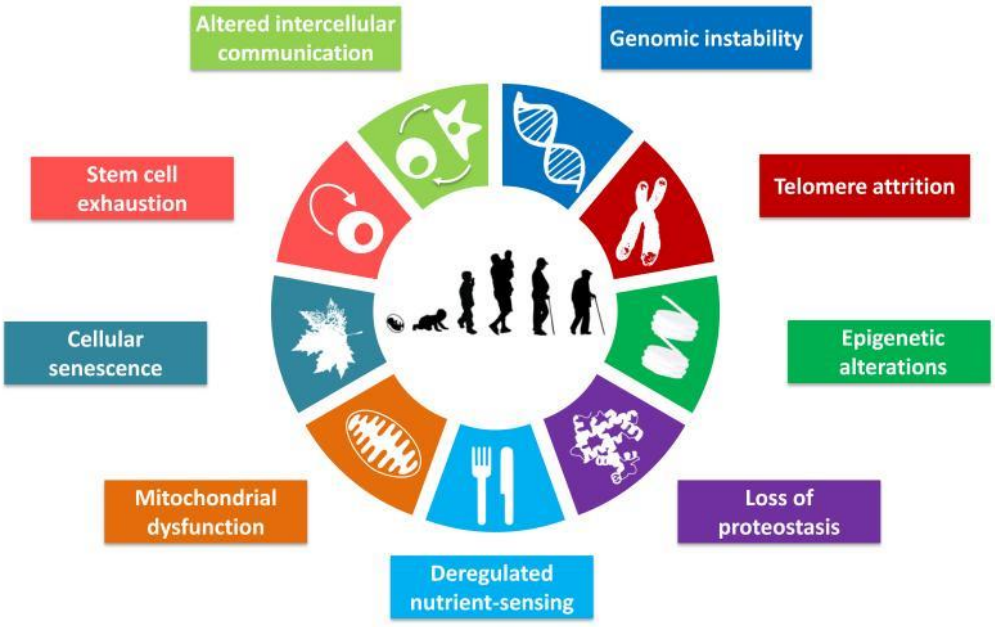


**Figure 2.1: The nine hallmarks of ageing** (Lopez-Otin *et al.*, 2013): Genomic instability, telomere attrition, epigenetic alterations, loss of proteostasis, deregulated nutrient-sensing, mitochondrial dysfunction, cellular senescence, stem cell exhaustion, and altered intercellular communication

In line with this, elucidating potential candidate hallmarks of ageing is essential to finding lasting solutions to age-related diseases. Over the years, research on ageing has identified quite a number of factors that may influence ageing. Reviewing known molecular mechanisms that have been implicated in the ageing process and acknowledging that none of the candidate hallmarks of ageing is mutually exclusive of the other, nine hallmarks of ageing were proposed by Lopez-Otin et al, 2013. They further divided the candidate hallmarks into three groups; - The primary hallmark which includes genomic instability, telomere attrition, epigenetic alterations and loss of proteostasis, are all obvious causatives of cellular damage (Lopez-Otin

*et al.*, 2013). Telomere attrition and genomic instability may be less detrimental in postmitotic cells like neurons or slowly dividing cells like microglia, whereas other more rapidly dividing glia cells such as oligodendrocytes and astrocytes in the CNS may be affected, leading to homeostatic imbalance (Miron *et al.*, 2013). The next group was termed the antagonistic hallmarks. Unlike the primary hallmarks, the antagonistic hallmarks are a response to damage. The effect of the response depends on the intensity of damage. Hence, the resulting response could elicit beneficial effects at low-level damage or detrimental effects at high-level damage. The hallmarks belonging to this group are; deregulated nutrient sensing, mitochondrial dysfunction and cellular senescence. The general role of the antagonistic hallmarks is to mitigate the damage they are responding to. However, should the damage become chronic, this could trigger additional negative effects where compensatory response was intended (Lopez-Otin *et al.*, 2013). Senescence of the cell captures perfectly the phenomenon presented above. Senescence in normal physiological conditions protects the cell from being cancerous. It sets an internal clock for the cell after which the cell is eliminated to prevent increase in the number of damaged cells due to accumulation of mutations over time (Delaney *et al.*, 2013; Soreq *et al.*, 2017). But increasing senescent cells may trigger senescence in neighbouring cells through gap-junction-mediated cell-cell contact thereby compounding the negative effects (Lefebvre *et al.*, 2012). Senescence in microglia, for instance, is especially harmful because the microglia do not only lose their function of clearance of debris and of other damaged cells, they further contribute to damaging neighbouring cells by becoming primed themselves and producing increasing levels of pro-inflammatory cytokines (Wynne, Henry and Godbout, 2009; Streit and Xue, 2014). The third category includes the integrative hallmarks. This group comprises of stem cell exhaustion and altered intercellular communication. They are also referred to as the culprit of the phenotype because they are the consequential manifestation of the effects of the two aforementioned categories and are responsible for the actual age-related functional decline (Villeda *et al.*, 2011; Lopez-Otin *et al.*, 2013). A declining regenerative capacity of tissues is a

characteristic shared by both neurodegenerative diseases and ageing (Lucin and Wyss-Coray, 2009). This can be as a result of microglia overreactivity, leading to increased neuroinflammatory milieu in the brain. Ultimately, cell viability reduces in such environment and the end result is that otherwise healthy cells are eliminated and regeneration is hampered, which further compounds ageing phenotype (Wynne, Henry and Godbout, 2009). Besides stem cell exhaustion, altered cell-cell communication leads to imbalance and disturbed signalling. Altered communication between neurons and microglia is more detrimental because of the important role of microglia in maintaining a healthy microenvironment in the brain. Subsequently, the milieu becomes increasingly inflammatory thereby resulting in neurotoxicity (Sheridan and Murphy, 2013).

## 2.2 Microglia in healthy, diseased and ageing brain

The central nervous system [CNS] is an immune privileged organ and is largely separated from the peripheral immune system. Hence, blood-borne immune cells such as macrophages are under healthy conditions prevented from getting into the CNS. In line with this, there is a need for microglia, the resident immune cells of the CNS (Ousman and Kubes, 2012). Microglial cells are immature macrophages originating from the primitive hematopoiesis of the yolk sac to populate the neuroepithelium during early stages of CNS development (Ginhoux *et al.*, 2010). They are smaller than other glial cells and make up for about 15 % of total cell population in the CNS (Carson *et al.*, 2006). Microglial cells are self-renewing, keeping their dividing capacity even in adulthood. On the contrary, other tissue macrophages derived from the yolk sac are replaced gradually by macrophages derived from monocytes of bone marrow origin. (Massberg *et al.*, 2007; Hoeffel *et al.*, 2012; Schulz *et al.*, 2012).

Since the brain tissue has a restricted regenerative capacity (Zhang *et al.*, 2007), it is highly sensitive to injuries and pathological conditions. Consequently, during events of brain-insults such as injuries or pathological conditions, the blood brain barrier is relaxed, thus macrophages and other blood-borne immune cells are recruited into the CNS (Ransohoff and Cardona, 2010). Microglia can either be in the resting or activated state. Under healthy conditions, microglial cells are in the ramified state otherwise referred to as the resting state. Moreover, contrary to the suggestion by the term "resting", ramified microglial cells are actually active. They survey their microenvironment with their long processes and are highly motile. However, if the brain is injured or in cases of immunological stimuli, microglial cells become activated. The now amoeboid-shaped microglia increase their body size and take on the role of a scavenger with increased reactivity (Hellwig *et al.*, 2016). In response to a stimulus, microglia may also recruit blood-borne immune cells, like the T cells by presenting antigens. In addition, reactive oxygen species may be produced, cytokines and chemokines released and the microglia can also become highly phagocytic (Wynne, Henry and Godbout, 2009). Numerous publications have suggested that microglia/macrophages are activated to M1or M2 phenotypes. On the one hand, M1 polarized microglia are characterized by increased pro-inflammatory responses with mainly cytotoxic properties. On the other hand, M2 polarization is further divided into three activation states. The M2a activation state is involved in repair and regeneration, the M2b activation state has a mainly immunoregulatory role, while the M2c state has an acquired-deactivation property (Chhor *et al.*, 2013). Yet, recent publications warn against this characterization as it is simplistic and no data so far have conclusively supported this classification (Ransohoff, 2016). In order for microglia to respond appropriately to a cue, they express cannabinoid receptors (Palazuelos *et al.*, 2009) and a wide range of other receptors that are up-regulated during various pathologies of the CNS (Vinet et al. 2012). Microglia do express a functional endocannabinoid signalling system, which upon activation may drive certain characteristics in microglia such as proliferation, migration, cytokine release or a phagocytic response (Stella, 2009). Indeed,

microglia express diacylglycerol lipases (DAGLs) and therefore can produce 2-arachidonoylglycerol [2-AG], which has been reported to promote microglial acquisition of M2 phenotype at least in cell culture systems (Mecha *et al.*, 2015).

A primary role of microglia is the immune defence thereby supporting survival of neurons and promoting maintenance of the microenvironment as well as other cells in the CNS. Nonetheless, microglial cells are increasingly being implicated as causatives or at the least contributors to neural damages in various neurodegenerative diseases and ageing. Accumulating evidence shows that microglia while responding to a stimulus may become overreactive depending on the strength and duration of the stimulus, causing damage to the cells they should otherwise be maintaining (Block, Zecca and Hong, 2007).

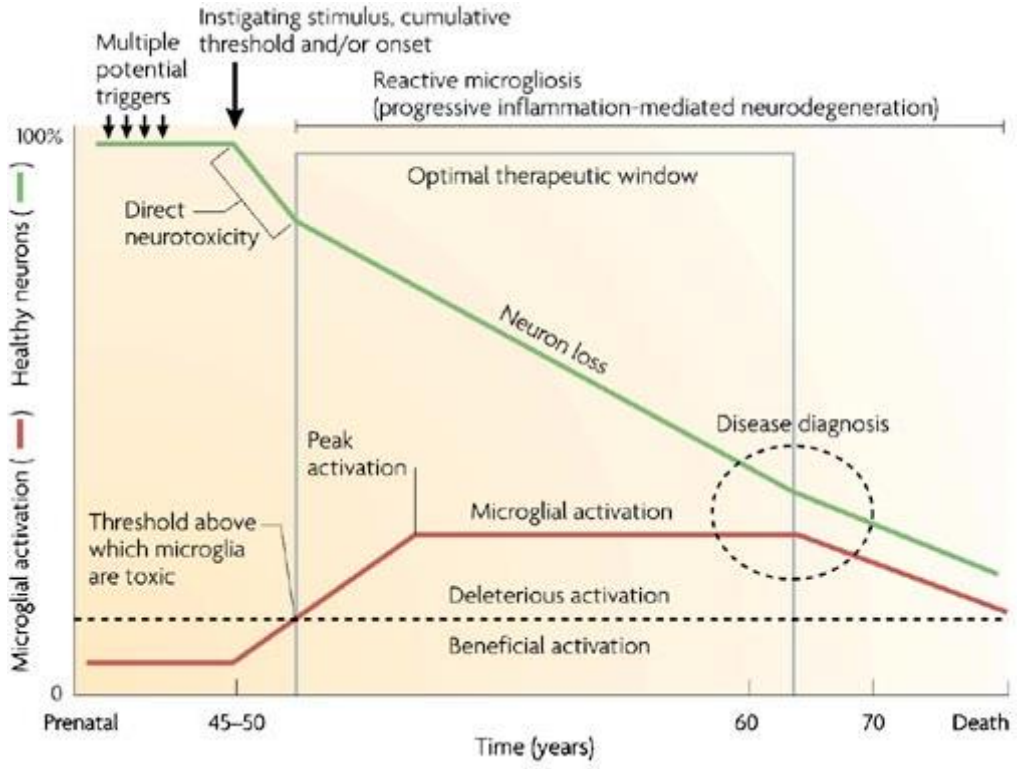


**Figure 2.2: Reactive microgliosis drives progressive neurotoxicity** (Block, Zecca and Hong, 2007)

Similarly, the risk of neurodegenerative disease has been shown to be higher with increasing age and there are mounting evidences that microglia play a central role in the progression of neurodegeneration. However, microglial cells have been reported to be more activated with

progressing ageing and it has been shown that microglial ageing progresses in a region-dependent manner with the hippocampus mostly affected (Grabert *et al.*, 2016). Hence, some studies have hypothesized that microglial reactivity in a normal ageing process mimics that observed in deteriorating brains that ultimately result in neurodegenerative disorders like Alzheimer's disease and Parkinson's disease (Block, Zecca and Hong, 2007; Wyss-Coray, 2016).

A large number of microglia in the aged brain and in neurodegenerative diseases are primed and senescent (Niraula, Sheridan and Godbout, 2016). Primed microglia, also referred to as "sensitized" microglia are reported to have a heightened reactivity to a stimulus as compared to microglia that have not been previously sensitized (Jurgens and Johnson, 2012). They damage the neurons in their microenvironment and then become even more activated in response to the damaged neurons. This process, which is termed reactive microgliosis (Block, Zecca and Hong, 2007), leads to increased production of pro-inflammatory cytokines such as interleukin 1β (IL-1β), interleukin 6 (IL-6) and tumour necrosis factor-α (TNF-α) but also reactive oxygen species (ROS) and nitric oxide (NO). The resulting toxic microenvironment now further promotes degeneration and age-related brain deterioration (Lucin and Wyss-Coray, 2009; Villeda *et al.*, 2011; Piyanova *et al.*, 2015).

## 2.3 The endocannabinoid system

The plant, *cannabis sativa,* has remained a source of controversy in societies since its first recorded use dating back to over 4000 years (Murray *et al.*, 2007). Depending on the society in question, the use of cannabis has been viewed as an "evil emergence" or "God's own gift" to mankind. Despite this divergence in attitude, a recent World Drug Report from the United Nations Office on Drugs and Crime estimated that about 181 to 232 million people age 15 – 64 use cannabis for nonmedical purposes globally (UNODC, 2015), while the acceptance of cannabis for medicinal use is on the rise. The main psychoactive component of this plant, $\Delta^9$-

tetrahydrocannabinol (THC), was first isolated in 1964 (Gaoni and Mechoulam, 1964). Yet, only after a prolonged period of about two and a half decades was the molecular target of THC identified. The first target to be identified and characterized was termed cannabinoid receptor 1 (CB1) (Devane *et al.*, 1988), while the second to be characterized about half a decade after the first, was referred to as cannabinoid receptor 2 (CB2) (Munro, Thomas and Abu-Shaar, 1993). These two receptors, their two main endogenous ligands (2-arachidonoylglycerol [2-AG] and Anandamide [AEA]) and the synthesis and degradation enzymes of these endocannabinoids make up the endocannabinoid system. The endocannabinoid system (ECS) is a retrograde and modulatory signaling system at the synapses (Katona *et al.*, 1999). While the endocannabinoids are produced on demand in the postsynapses, they are released into the synaptic cleft to activate cannabinoid receptors on the presynapses.

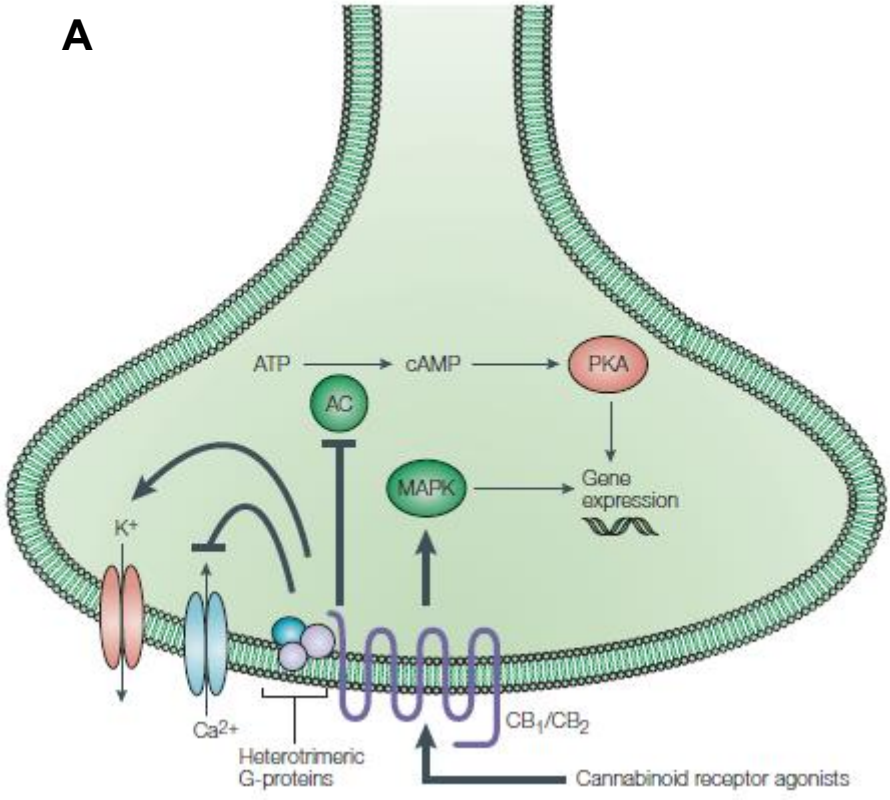


**Figure 2.3A: Signal transduction pathway of the cannabinoid receptors 1 and 2 activation at the pre-synapse (adapted from Di Marzo et al. 2004)**

The cannabinoid receptors 1 and 2 are members of the 7 transmembrane domain rhodopsin-like G-protein coupled receptors (GPCRs) that are mostly coupled to the $G_{i/o}$ proteins (Dalton *et al.*,

2009). CB1 receptor activation leads to an inhibition of adenylate cyclase, activation of MAP kinases and inhibition of the calcium influx (Mackie and Hille, 1992). Consequently, neurotransmitter release is inhibited leading to a reduced depolarization- induced suppression of inhibition (DSI) or suppression of excitation (DSE) (Ohno-Shosaku, Maejima and Kano, 2001). CB1 receptor is highly expressed in the brain with the highest density in cholecystokinin (CCK) positive GABAergic neurons (Lee and Soltesz, 2011; Keimpema *et al.*, 2012). However, CB2 receptor is mainly expressed on peripheral immune cells and by microglia in the brain (Munro, Thomas and Abu-Shaar, 1993; Atwood and Mackie, 2010). Yet, CB2 receptor has been reported to be expressed also on neurons in some parts of the brain, particularly in the brain stem and the CA2 region of the hippocampus (Ashton *et al.*, 2006; Suárez *et al.*, 2009; García-Gutiérrez *et al.*, 2010). Possible non-CB1 or non- CB2 cannabinoid receptors such as the transient receptor potential vanilloid type 1 (TRPV-1), the G-protein coupled receptor GPR55 and the GPR18 have been introduced , with GPR18 regarded to be a much likely candidate as a bona fide cannabinoid receptor (De Petrocellis and Di Marzo, 2010; Di Marzo and De Petrocellis, 2010, 2012; McHugh *et al.*, 2012; Köfalvi, 2016).

2-arachidonoylglycerol [2-AG] and Anandamide [AEA] are the two most-studied endocannabinoids and thus best-characterized ligands of the cannabinoid receptors. While 2-AG has a relatively high affinity for both CB1 and CB2 receptors, AEA has a higher affinity for CB1 but lower affinity for CB2 receptor (Felder *et al.*, 1993; Mackie, Devane and Hille, 1993; Atwood and Mackie, 2010). The efficacy of AEA at both CB1 and CB2 receptors and so with the strength of signal transduction is weaker compared to what is achieved with 2-AG which is a full agonist of both receptors. Hence AEA is a partial agonist of the cannabinoid receptors.

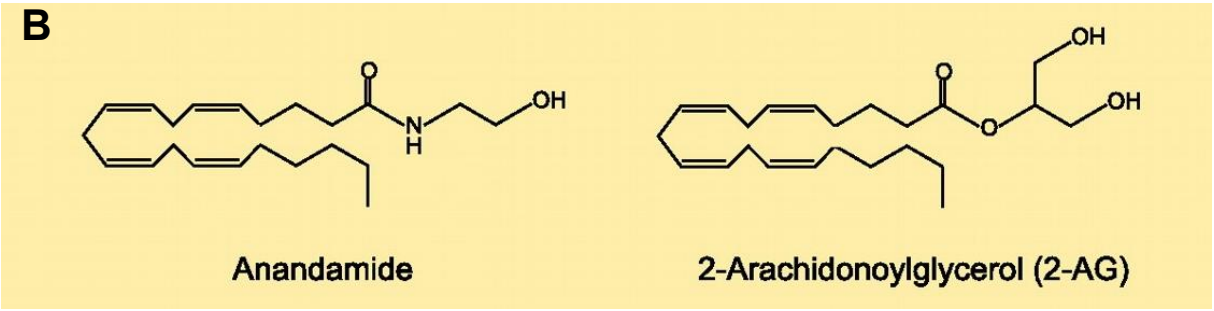


**Figure 2.3B: Structural formula of the major endocannabinoids (adapted from Kano et al. 2009)**

In addition, there is a higher production of 2-AG in the CNS as compared to AEA (Murataeva, Straiker and MacKie, 2014). There are four known distinct pathways associated with the biosynthesis of anandamide and the main degradation enzyme being the fatty acid amide hydrolase (FAAH) (Di Marzo, Bifulco and De Petrocellis, 2004). Although the synthesis of 2-AG occurs through a few known pathways, the best-studied pathway for 2-AG synthesis begins with the phospholipase-Cβ mediated hydrolysis of phosphatidylinositol 4,5-bisphosphate, resulting in an intermediate product termed diacylglycerol (DAG). This intermediate product is then further cleaved by either diacylglycerol lipase α (DAGLα) or diacylglycerol lipase β (DAGLβ) to the end product 2-arachidonoylglycerol (2-AG) (Murataeva, Straiker and MacKie, 2014; Köfalvi, 2016). Nevertheless, 2-AG can also be synthesized by dephosphorylation of arachidonoyl-LPA or through a chronological action of PLA1 and lyso phospholipase C (lyso-PLC) (Nakane *et al.*, 2002; Murataeva, Straiker and MacKie, 2014).

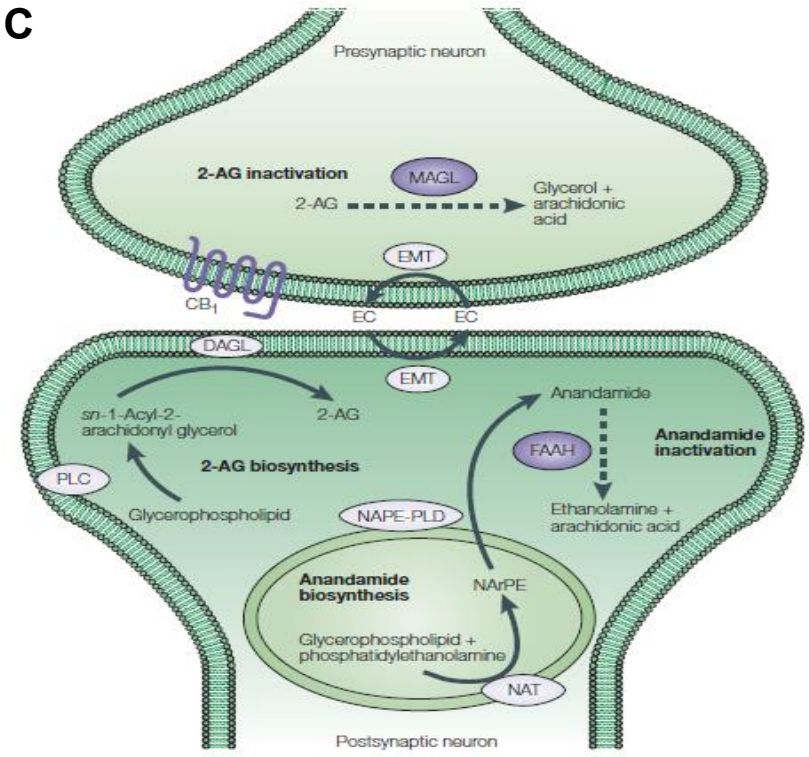


**Figure 2.3C: Depiction of the Synthesis and degradation pathways of endocannabinoids (adapted from Di Marzo et al. 2004)**

Most of the 2-AG produced in the CNS can be traced back to the activity of DAGLα, while DAGLβ is more active in some peripheral organs like the liver (Bisogno *et al.*, 2003). Both DAGL isoforms are highly conserved between species with mouse and human sharing a DAGLα homology of about 97 % while DAGLβ homology shared is at about 79 % (Murataeva, Straiker and MacKie, 2014). The degradation of 2-AG is based largely on the activity of monoacylglycerol lipase (MAGL) but other enzymes like serine hydrolase α-β-hydrolase domain 6 (ABHD6), serine hydrolase α-β-hydrolase domain (ABHD12) and fatty acid amide hydrolase (FAAH) also degrade 2-AG (Blankman, Simon and Cravatt, 2007; Kano *et al.*, 2009). The metabolic products of 2-AG through the aforementioned pathways are mainly arachidonic acid and glycerol (Gellman *et al.*, 2002; Freund, Katona and Piomelli, 2003). Several other degradation pathways for 2-AG are known that do not lead to arachidonic acid and glycerol as end products. COX-2 can oxidize 2-AG to produce prostaglandin glycerol esters, acyl glycerol

kinase phosphorylation of 2-AG yields lysophosphatidic acid (LPA) and lipoxygenases oxidize 2-AG to hydroperoxy derivatives. These metabolic products of 2-AG may activate other signalling pathways other than the endocannabinoid pathway, leading to excitatory instead of inhibitory effects. Hence alteration in 2-AG levels may not only affect the endocannabinoid system signalling but also the other signalling pathways mention above (Murataeva, Straiker and MacKie, 2014).

## 2.4 The endocannabinoid system in brain ageing

It is now widely accepted that disrupted intercellular communication is a major candidate-hallmark of ageing (Lopez-Otin *et al.*, 2013) and the profound role of the endocannabinoid system in the regulation of cell-cell interactions including neuron-neuron as well as neuron-glia communications cannot be overstated. In line with this, it could be expected that a reduced endocannabinoid activity would result in an accelerated progression of ageing. Similarly, impaired endocannabinoid system signalling has been reported to promote age-related and neurodegenerative diseases such as Alzheimer's, Huntington's and Parkinson's diseases to name but a few (Bisogno and Di Marzo, 2010; Bilkei-Gorzo, 2012). Interestingly, literature reports and findings in our lab have it, that CB1 receptor deficient mice exhibit age-related changes in learning and memory abilities. While learning and memory performance deteriorated in old CB1 receptor knockout mice in various learning and memory tests , these were rather significantly better in young CB1 receptor knockout mice compared to age-matched littermates (Reibaud *et al.*, 1999; Bilkei-Gorzo *et al.*, 2005). Concomitantly, loss of principal neurons, altered glial activation and increased level of pro-inflammatory cytokines were recorded in old CB1 receptor knockout mice. These observed early age-related changes were confined to the hippocampus and influenced cognitive functions but not motor or sensory abilities (Bilkei-Gorzo *et al.*, 2012). Consequently, it is most likely that CB1 receptor on GABAergic neurons influence the regulation of glial activity, thereby maintaining glial

homeostasis and providing a shield against early onset of age-associated dysfunctions (Bilkei-Gorzo *et al.*, 2005, 2012; Albayram *et al.*, 2011). Although CB2 receptor expression is higher in glial cells like microglia as compared to neurons (Stella, 2009) and the upregulation of the CB2 receptor has been linked to beneficial effects such as the restoration of tissue homeostasis during pathological neuroinflammatory conditions (Miller and Devi, 2011), deletion of CB2 receptors did not result in detrimental effects such as enhanced glial reactivity. Thus, it can be assumed that this receptor may not be responsible for the observed age-related changes. Nonetheless, it is not absolutely clear which of the endocannabinoids is more influential in the CB1 receptors mediated protection against early ageing. Owing to literature knowledge that endocannabinoids levels are reduced in ageing (Wang *et al.*, 2003; Maccarrone *et al.*, 2015), it is reasonable to think that an increased CB1 receptor signalling due to increased 2-AG or anandamide may delay ageing. Indeed, an increase in the activity of the cannabinoid system through anandamide elevation (Ortega-Gutiérrez, Molina-Holgado and Guaza, 2005; Tham *et al.*, 2007) has been shown to promote anti-inflammatory response *in vitro.* Moreover, anandamide levels were described to be reduced in age-associated diseases such as Alzheimer's disease, reporting a significantly low levels of this endocannabinoid in mid-frontal and temporal cortices in post-mortem samples (Jung *et al.*, 2012). Furthermore, 2-AG mediated cannabinoid signalling has been shown to be bias for microglial M2 polarization, leading to overall reduction in inflammation (Mecha *et al.*, 2015) . Similarly, several reports have demonstrated a beneficial effect of cannabinoids during ageing, reporting that the effects of cannabinoids on cognitive functions were age-dependent. Young individuals were more vulnerable to cannabinoid agonists as older individual (Trezza, Cuomo and Vanderschuren, 2008). A recent publication in our lab even went further to show that a chronic low dose of THC even improved cognitive ability in aged mice. Consequentially, exploration of the endocannabinoid system may open avenues for treatment of age-related pathologies including neurodegenerative diseases (Bilkei-Gorzo *et al.*, 2017).

## 2.5 Neuron-glial communication and the endocannabinoid system

The importance of bidirectional communications between neurons and neighbouring glial cells for healthy functioning of the CNS is a widely accepted knowledge. In order to maintain a healthy microenvironment in the CNS, neurons, microglia and astrocytes have been reported to regulate each other by indirect interaction through soluble mediators and by direct interaction through membrane-bound mediators (Perry and Holmes, 2014). Microglial expression of the two main cannabinoid receptors has been reported. However, it is still a subject of debate whether these receptors are expressed only after activation of microglia or if they are significantly upregulated following microglia activation. Either way, microglia express cannabinoid receptors and can, therefore, be regulated by the endocannabinoid system (Stella, 2009). There are a number of signalling pathways that may indirectly modulate immune functions in the CNS. Several neurotropic factors have been shown to modulate microglial reactivity. The brain-derived neurotrophic factor (BDNF) downregulates microglial expression of co-stimulatory molecule B7 and CD40 thereby modulating T cell recruitment and activation (Wei and Jonakait, 1999). Similarly, nerve growth factor (NGF) inhibits microglial expression of MHC class II (Neumann *et al.*, 1998). Now, microglial activity can also be modulated by neurons through an array of GABA receptors expressed on microglia. GABA A and GABA B receptors expressed on microglia upon activation decrease pro-inflammatory cytokine release (Stella, 2009; Lee, Schwab and Mcgeer, 2011). In addition, GABAergic neurons have been shown to play an important role in the cannabinoid system associated modulation of microglial reactivity in the ageing brain. Mice constitutively deficient for CB1 receptors show symptoms of accelerated ageing characterized by increased glial activity, increased cytokines levels and an accelerated neuronal cell loss with progressing ageing. Interestingly, specific deletion of CB1 receptors on GABAergic neurons sufficed to elicit similar conditions (Bilkei-Gorzo *et al.*, 2005; Albayram *et al.*, 2011; Albayram, Bilkei-Gorzo and Zimmer, 2012). However, similar

conclusions could not be reached in experiments with mice specifically deficient for CB1 receptors on glutamatergic neurons. In line with this, the important role of GABAergic neurons in microglia regulation in the ageing brain cannot be overstated (Albayram *et al.*, 2011; Piyanova *et al.*, 2013). Nevertheless, of equal importance is the neuron-glial cell-cell modulation. Direct communication membrane-bound proteins play a crucial role in the crosstalk between neurons and microglia. The CD200 ligand on neurons and its corresponding CD200 receptor on microglia are such membrane-bound proteins. The interaction between neuronal CD200 and microglial CD200R has been shown to maintain microglia in a quiescent state, preventing them from becoming overreactive (Hoek, 2000; Neumann, 2001; Jurgens and Johnson, 2012). Another membrane-bound communication protein between neurons and microglia is the fractalkine ($CX_3CL1$) on neurons and the corresponding receptor $CX_3CR1$ on microglia. Their interaction has been reported to promote microglial survival and the initiation of pathological pain (Milligan, Sloane and Watkins, 2008; Rowinska *et al.*, 2017). The receptors of these two neuroimmune regulator protein pairs (CD200R and $CX_3CR1$) that are always situated on the microglia are transmembrane proteins coupled to immunoreceptor tyrosine-based inhibitory (ITIM) motifs. ITIM acts via SHP-1 and SHP-2 phosphatases to inhibit or reduce microglia activation thereby modulating microglia reactivity (Billadeau and Leibson, 2002). $CX_3CR1$ activity has been reported to be crucial in hippocampal neurogenesis. Deletion or pharmacological blockade of $CX_3CR1$ resulted in reduction or complete attenuation of hippocampal neurogenesis with reduced cognitive ability as the consequence. Furthermore, $CX_3CR1$ expression levels have been shown to decrease during ageing and administering exogenous $CX_3CL1$ to ageing animals led to improvement of hippocampal neurogenesis (Bachstetter *et al.*, 2012; Justin *et al.*, 2012; Sheridan and Murphy, 2013). Moreover, deficient CD200-CD200R signalling has been linked to microglia over-reactivation, leading to dopaminergic neurodegeneration (Zhang *et al.*, 2011) and increasing ageing-associated properties.

## 2.6 Aim of this study

The first aim of this study was to clarify how cannabinoid system activity influences brain ageing. Since we hypothesized that decreased microglial 2-AG production leads to early onset of cognitive deficits and age-related histological changes in the brain, we compared the declarative learning ability of the conditional DAGLα knockout mice and wild-type littermates in a longitudinal study. We further characterized the spatial learning and working memory abilities of these animals. Secondly, we hypothesized that reduced cannabinoid signalling between microglia and the regulatory hippocampal GABAergic neurons leads to upregulation of microglial activity thereby promoting neuroinflammatory changes in the ageing brain. In order to test this hypothesis, we assessed microglial reactivity using organotypic hippocampal slice culture from GABA-specific CB1 knockout (GABA-Cnr1$^{-/-}$) and microglia-specific DAGLα knockout (Dagla$^{-/-}$) animals. Then we went further to compare the reactivity of microglia *in vivo* to LPS in the hippocampus of wild-type and GABA-Cnr1$^{-/-}$ mice in different age groups. We also hypothesized that increased cannabinoid signalling due to increased anandamide levels influences microglial reactivity. Thus, we assessed microglial reactivity in different age groups of FAAH knockout animals and wild-type littermates. Lastly, we hypothesized that disturbed endocannabinoid signalling leads to an early onset and/or exacerbated senescence-associated phenotype in microglia. Hence, we compared lipofuscin accumulation, expression of some GABA receptors and cytokines in isolated microglial cells of Dagla$^{-/-}$ and GABA-Cnr1$^{-/-}$ animals alongside their wild-type littermates in different age groups. This was followed by characterization of age-related histological changes of neuron-glial communication markers in Dagla$^{-/-}$ animals in different age groups

# 3. Materials and Methods

If not stated otherwise, all applied chemicals were acquired from Sigma-Aldrich, Invitrogen, Roche, Fluka, Applichem, Merck, Applied Biosystems and Carl Roth. Contact information are provided in the appendix.

## 3.1 Equipment

| | |
|---|---|
| Analytical balance | BP 121 S, Sartorius |
| BD FACSCanto$^{TM}$II Flow Cytometer | BD Biosciences |
| Bioanalyzer | Agilent 2100 bioanalyzer, Agilent |
| CCD camera | AxioCamMRm, Zeiss |
| | KY-F75U, JVC |
| Cell culture incubator | Binder GmbH |
| Centrifuges | Biofuge fresco, Heraeus Instruments |
| | Biofugepico, Heraeus Instruments |
| Cryostate | CM 3050 S, Leica |
| Hamilton micro syringes | Sigma-Aldrich |
| Homogeniser | Precellys® 24, Bertin Technologies |
| Laminar flow hood | Herasafe, Kendro |
| Vibratome | VT1200 S Microtome,Leica |
| Magnetic stirrer | MR 3001 K, Heidolph, Fisher |
| Microplateanalyzer | MRX TC II, Dynex Technologies |

| | |
|---|---|
| Microscope | Axiovert 200 M, Zeiss |
| Millicell insert | BD Falcon, USA |
| PCR iCycler | iCycler, Bio-Rad Laboratories |
| pH meter | inoLab, WTW |
| Real-Time Cycler | 7500 Real-Time PCR Detection System, Applied Biosystems |
| Spectrophotometer | NanoDrop ND-1000, Thermo scientific |
| Stereotaxic instrument | Stoelting, USA |
| Surgical thread | Ethicon Endo-Surgery Europe GmbH |
| Vortexer | Vortex-Genie 2, Scientific Industries |
| Ultrasonic bath | Ultrasonic cleaning bath USC-THD, VWR |

## 3.2 Software

| | |
|---|---|
| AxioVision LE | Carl Zeiss, Germany |
| EthoVision® | NoldusVersion XT 8.15 |
| ImageJ | Wayne Rasband, USA Version 1.47v |
| Mouse-E-Motion | Infra-E-Motion, Germany |
| Microsoft Office 2016 | Microsoft, Germany |
| Prism | GraphPad Software, Inc. Version 5.03c |
| Statistika | StatSoft, Inc. Version 6 (2001) |
| VideoMot | TSE Systems, Germany |

## 3.3 Chemicals and reagents

### 3.3.1 Chemicals

| | |
|---|---|
| Albumin bovine Fraction V, pH 7.0 standard | Serva grade, lyophil. (BSA) |
| Brilliant Blue R-250 | Sigma-Aldrich |
| 1-Bromo-3-chlorpropane (BCP) | Sigma-Aldrich |
| BrdU (B5002-250mg) | Sigma-Aldrich |
| Cremophor® EL/ Kolliphor®EL | Sigma-Aldrich |
| DAPI Fluoromount-G® | SouthernBiotech |
| D(+)-Glukose | Sigma-Aldrich |
| Ethidium bromide solution (10 mg/ml) | Sigma-Aldrich |
| Fluoromount-G® | SouthernBiotech |
| $H_2O_2$ | Sigma-Aldrich |
| 2-Methylbutan/ Isopentan | Sigma-Aldrich |
| KCl | Sigma-Aldrich |
| $MgCl_2$ Hexahydrate | Applichem |
| NaCl | Roth |
| NaOH | Millipore |
| Paraformaldehyd | Sigma-Aldrich |
| PBS tablets | Gibco life technologies |

| | |
|---|---|
| Percoll | GE Healthcare, Germany |
| Rnase free water | Gibco life technologies |
| SDS ultra pure | Roth |
| TRIzol® Reagent | Thermo Fisher |
| TRIS | Roth |
| TRIS-HCL | Roth |
| Triton-X 100 | Sigma-Aldrich |
| Tween-20 | Sigma-Aldrich |
| β-mercaptoethanol | Sigma-Aldrich |

### 3.3.2 Kits

| | |
|---|---|
| GoTaq® Green Master Mix | Promega |
| BCA Protein Assay Kit | Thermo Fisher (PierceTM) |
| Mouse TNF-α ELISA | eBioscience (88-7324) |
| Mouse IL-6 ELISA | eBioscience (88-7064) |
| Mouse IL-1β ELISA | eBioscience (88-7013) |

### 3.3.3 Buffers and Solutions

All buffers and solutions were prepared with $dH_2O$, whereas all chemicals were purchased from Applichem, Life Technologies, Merck, Carl Roth or Sigma-Aldrich except the contrary is stated.

**ELISA Coating buffer**

| | |
|---|---|
| 10x coating solution | 1.1ml |
| MilliQ water | 9.9ml |
| capture Ab (1:250) | 44 µl |

**ELISA Wash buffer**

| | |
|---|---|
| PBS | 1l |
| Tween-20 | 500µl |

**ELISA Assay diluent**

| | |
|---|---|
| 5x assay diluent | 8ml |
| MilliQ water | 32ml |

**ELISA Detection Ab solution**

| | |
|---|---|
| assay diluent | 11ml |
| detection Ab | 44 µl |

**ELISA Avidin-HRP solution**

| | |
|---|---|
| assay diluent | 11ml |
| Avidin-HRP | 44 µl |

**ELISA Stop solution**

1M $H_3PO_4$ or 2N $H_2SO_4$

**4% PFA pH = 6.9**

| | |
|---|---|
| 1 x PBS | 800ml |

| | |
|---|---|
| PFA power | 40g |
| Adjust to 1l with 1xPBS | |

### 3.3.4 Antibodies

| | |
|---|---|
| **Primary Antibodies** | |
| Anti-Iba1 (019-19741, rabbit) | Abcam |
| Anti-Iba1 (016-20001, rabbit) | Wako |
| Anti-CD200/OX2 (ab33734, rat) | Abcam |
| Anti-CD200R/OX102 (ab34097, mouse) | Abcam |
| Anti-$CX_3CL1$ (ab25088, rabbit) | Abcam |
| Anti-$CX_3CR1$ (c8354, rabbit) | Sigma-Aldrich |
| **Secondary Antibodies** | |
| Alexa Fluor® 488 goat anti-rabbit | Invitrogen, A11008 |
| Alexa Fluor® 488 goat anti-mouse | Invitrogen, A11007 |
| Alexa Fluor® 594 goat anti-rabbit | Invitrogen, A21207 |
| Alexa Fluor® 594 goat anti-rat | Invitrogen, A11001 |
| Alexa Fluor® 647 donkey anti-rabbit | Invitrogen, A3157 |
| Cy3 goat anti-rabbit | Invitrogen, A10520 |

### 3.3.5 Enzymes

| | |
|---|---|
| Proteinase K | NEB |
| Superscript II Reverse Transcriptase | Invitrogen |

| | |
|---|---|
| Taq Polymerase | NEB |
| Phusion High Fidelity DNA Polymerase | NEB |

## 3.4 Media and solutions

### 3.4.1 OHSCs media

**Dissection medium for OHSCs**

| | |
|---|---|
| MEM medium (Gibco) | 500ml |
| 200mM Glutamine (Gibco or Sigma) | 5ml |
| HEPES | 5ml |

**OHSCs medium**

| | |
|---|---|
| MEM (Gibco) | 100ml |
| HBSS (Gibco) | 50ml |
| Heat inactivated horse serum (GE Healthcare) | 50ml |
| Glutamine (Gibcoand Sigma) | 2ml |
| Glucose | 2ml |
| Amphotericin B (Sigma) | 3ml |
| Pen/Strep 100x (Gibco) | 2ml |

### 3.4.2 ACSF solution

**ACSF solution A without Ca/Mg**

| | |
|---|---|
| NaCl | 8.66g |
| KCl | 0.224g |

Fill up to 500ml with MilliQ water

**ACSF solution A with 1.1mM $Ca2^+$**

| | |
|---|---|
| NaCl | 8.66g |
| KCl | 0.224g |
| $CaCl_2$ x 2 $H_2O$ | 0.162g |
| $MgCl_2$ x 6 $H_2O$ | 0.163g |

Fill up to 500ml with MilliQ water

**ACSF solution B**

| | |
|---|---|
| $Na_2HPO_4$ x 7 $H_2O$ | 0.214g |
| $NaH_2PO_4$ x $H_2O$ | 0.027g |

Fill up to 500ml with MilliQ water

Mix A and B 1:1 for use

### 3.4.3 Microglia isolation solution / FACS solution

**Isolation medium**

| | |
|---|---|
| DMEM with 4.5g/l glucose | 450ml |

| | |
|---|---|
| FCS | 50ml |

**Collagenase solution from 10 mg/ml stock**

| | |
|---|---|
| Collagenase | 500µl |
| Medium | 5ml |

**Dispase solution from 10 mg/ml stock**

| | |
|---|---|
| Dispase | 500µl |
| Medium | 5ml |

**Inactivation solution (20% FCS)**

| | |
|---|---|
| Heat inactivated FCS | 20ml |
| 1 x HBSS | 80ml |

**Percoll 30%**

| | |
|---|---|
| Percoll | 30ml |
| PBS | 120ml |

**Percoll 70%**

| | |
|---|---|
| Percoll | 120ml |
| Medium | 30ml |

**FACS buffer**

| | |
|---|---|
| Heat inactivated FCS | 1ml |
| PBS | 50ml |

**Blocking solution**

| | |
|---|---|
| CD16/32 | 1µl |
| FACS buffer | 300µl |

**Fluorescent labelled antibodies mix**

CD11b-APC diluted 1:200 in FACS solution

CD45-e450 diluted 1:200 in FACS solution

## 3.5 Animals

Animals used in this study were, on the one hand, mice with GABAergic neuron specific deletion of cannabinoid receptor 1 (GABA-Cnr1$^{-/-}$), and on the other hand, mice with microglia-specific deletion of Dagla (LysM-Dagla$^{-/-}$) and inducible microglia-specific deletion of Dagla (Tam-CX3CR1-Cre-Dagla$^{-/-}$) together with their wild-type littermates. A constitutive FAAH deficient mouse line was also used. Mice were generated on a congenic C57BL/6J background, housed sex-isolated in groups of 2 to 5 mice, allowed access to water and food *ad libitum* and kept in a reversed light-dark cycle (lights on :19:00; lights off: 9:00) in the House of Experimental Therapy, University of Bonn. Housing conditions were stable at about 21°C and 55 % relative humidity. The experiments were performed with conditional mice and their corresponding littermates aged 2, 12 and 18 months. For the Organotypic Hippocampal Slice Cultures, 3 to 5 days old pups were used. The experiments and treatment of animals were carried out as stipulated by the guidelines of the European Union Council Directives 86/609/EEC and were approved by the Landesamt für Natur, Umwelt und Verbraucherschutz Nordrhein-Westfalen.

## 3.6 Behavioural experiments and animal treatment

### 3.6.1 Subcutaneous injection of Tamoxifen for Cre induction in Tam-CX3CR1-Cre-Dagla-/- mice

Approximately four weeks old mice were subcutaneously injected on day 0 and day 2. Mice were administered a total of 200 µl of 20 mg/ml Tamoxifen (Sigma) in corn oil (Sigma) on day 0. The injection was given in 50 µl volume at the flanks and shoulders of an anaesthetized mouse. The injection was repeated on day 2. A recombination of about 90 % is expected in three to four weeks.

### 3.6.2 Morris water maze (MWM)

In a longitudinal test of cognition, the spatial learning and memory ability of Tam-CX3CR1-Cre-Dagla$^{-/-}$ female mice was tested in the MWM task (Barnes, Suster et al. 1997). A circular pool (1.2 m in diameter and 0.6 m in height) made of white PVC was used. First, the tank was filled with water to a depth of about 30 cm maintaining a temperature of about 24 °C. Then a non-toxic white paint was employed to make the water opaque so as to veil the rescue platform. The rescue platform was 15 cm high and 8 cm in diameter painted white to camouflage with the opaque water. Now, the platform was placed inside the tank approximately 1.5 cm under the water level, serving as an escape platform. The pool was located in a closed sound proof room with numerous extra-maze visual cues. Plastic placards of various shapes and colours were attached to the wall of the tank and act as additional cues. A camera fixed on the ceiling above the pool was used to record video signal that was simultaneously transmitted to a computer. With the aid of an automatic tracking system installed on the computer, the swim paths are captured and escape latencies, total path length and swim speed are calculated.

In the acquisition phase, which is the first phase of the Morris water-maze test, the learning ability of the mice was compared in the test groups. The platform was positioned at a fixed spot in the pool during the entire acquisition period. The animals were tested for six days consisting

of four consecutive sessions per day. There are four points along the wall of the pool designated as North, South, East and West (N, S, E, W) that divide the pool into four equal quadrants and also serving as starting points. The mice were always released facing the wall of the circular pool during the entire trials. In the first two days, all four sessions were started from the same point (W). However, from the third day onwards, the animals were released from all starting points (W, N, E, W) during sessions. The goal is for the mouse to reach the rescue/escape platform and stay on it for a period of 5s in which case the experiment ends automatically. Mice were allowed to remain on the platform for 30 s before placing them back into their respective home cages. Should the mouse fail to locate the platform within 70 s, the mouse was guided gently with the hand to the platform and in this case, the trial was recorded as an escape failure with an arbitrary latency of 70 s. In the second phase, referred to as the probe trial on day 7, the memory strength is tested. For this purpose, the rescue platform is removed and the mice are allowed to swim for 70 s. The more time spent in the quadrant where the platform was placed indicates better memory strength. The third and last phase is the reverse phase. Here we test the flexibility of the spatial memory. On day 8 to 10, the rescue platform is placed back into the pool, but this time on the opposite side to where it was placed during the acquisition phase. Mice were tested when they were 2 and 12 months old. The experiments were performed during the hours of 10:00 a.m. and 14:00 a.m., which is the active phase of the animals.

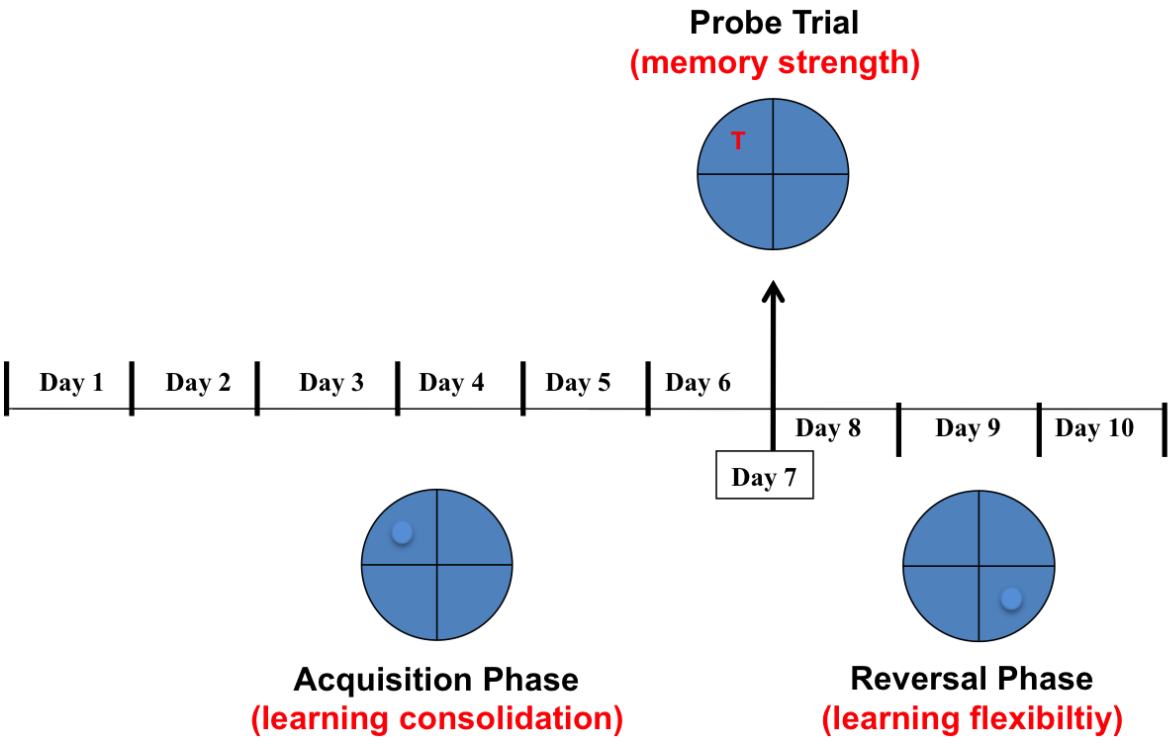


**Figure 3.5.2:** Depiction of a Morris Water Maze experimental set-up. During the acquisition and reverse phases, the platform is placed to the north and south, respectively. While the platform is removed during the probe trial (modified from Albayram *et al*, 2012)

### 3.6.3 Partner recognition test

In another longitudinal test, a social preference test was carried out with Tam-CX3CR1-Cre-Dagla$^{-/-}$ male mice when they were 2 and 12 months old. The trials were carried out in an open-field arena (44 cm x 44 cm) in a dimly illuminated and sound isolated environment. In order to exclude possible environment associated interference and result falsification (Haller, 2002; Thiemann, 2009), the test animals are habituated to the arena for five minutes daily on three consecutive days. Meanwhile, the sawdust, covering the floor of the arena remained unchanged, leading to saturation with mice odour. The trials, consisting of two sessions, started by putting male animals of the same age with test animals into grid cages. Now, a mouse in a grid cage was placed in a corner 12 cm away from the walls. This is labelled as " remain". On the opposite side to the remain cage, an object with similar size (in this case a Pepsi can) was placed. With the aid of the EthoVision XT software (Noldus, Information Technology Inc.), the

location of the test mice was recorded for 9 minutes. In the second session, the Pepsi can object was removed and replaced with a grid cage (termed New) containing a new mouse whilst the remain-cage was left untouched. After an interval of 30 minute (day one), 1 hour (day 2) and 2 hours (day three), the test mouse was placed again in the arena and allowed to explore for 3 minutes. Of interest, was the time the mice spend interacting (the nose of the mouse is not more than 1 cm from the wall of the grid cage) with the Pepsi can, remain and new mice. A sign for partner recognition is a significantly higher time spent investigating the new partner.

### 3.6.4 Social preference test after icv LPS treatment (Sickness behaviour)

In order to test the social preference of GABA-specific CB1 knockout mice (GABA-Cnr1$^{-/-}$) after intracerebroventricular (ICV) injection of LPS, animals age 3, 12 and 18 months old were housed in single cages and kept in reverse dark/light cycle for a period of one week. On the treatment day, animals were administered intraperitoneally (i.p) 0.1 mg/kg buprenorphine thirty minutes before surgery. The animals were then anaesthetized with ketamine/xylazine (0.1 ml ketamine, 0.2 ml xylazine from an injection solution diluted to 2 ml with saline or connected to a mask that supplies air with a mixture of 75 % $O_2$, 25 % N2 and 3-5 % of isoflurane after they were fixed to a stereotaxic instrument (Stoelting, USA). For an incessant and sustained anaesthetic effect, isoflurane was maintained at about 1.5-2 %. Now the scalp of the mouse was cut open with a scalpel, cleaned with a cotton swab and the skull treated with 3 % hydrogen peroxide to reveal the bregma and pattern of the skull. Employing the stereotaxic instrument, the skull was carefully punched above the right dorsal ventricle (coordinates: -0.6; -1.2 from bregma) with a fine drilling machine. Now with the aid of a Hamilton micro syringe (Sigma-Aldrich) , either 5 µl artificial cerebrospinal fluid (ACSF) or 100 ng LPS in 5 µl ACSF was injected into the punched hole (coordinates: -0.6; -1.2; -2 from bregma). The area of surgery was disinfected and stitched close with surgical suture on needle holder. The animal was then put back into the cage and allowed to recover. Behavioural test only followed 24 hours after

surgery. The sickness behaviour was assessed after the recovery and resting period. Similar to previous experiments, the trials were carried out in an open-field arena (44 cm x 44 cm) in a dimly illuminated and sound isolated environment. A mouse in a grid cage (same sex to test animals) was placed in a corner 12 cm away from the walls and on the opposite side to the mouse in the grid cage, an empty grid cage was positioned. Using the EthoVision XT software, the test mouse interaction with either the empty cage or the cage containing a mouse was recorded for 6 min. At the end of the tests, the animals were anaesthetized with isoflurane, followed by transcardial perfusion with ice-cold PBS. The brains were harvested, cut into two halves longitudinally and one-half directly shock frozen in dry ice for RT- PCR. The other half was processed for immunohistochemical staining. Here the brain half was fixed in 4 % PFA for 3 hours, cryoprotected in 20 % sucrose for 24 hours and lastly shock frozen in dry ice-cooled isopentane.

## 3.7 Molecular biological methods

### 3.7.1 Transcardial perfusion

Mice were collected and anaesthetized with a mixture of ketamine/xylazine. Now, the chest was cut open, allowing a catheter with a 25G needle to be inserted into the left ventricle. The right atrium was then cut open. The perfusion was then performed with cold phosphate-buffered saline (PBS) at a flow rate of 4 ml/min to wash out the blood, then at the same flow rate, 4 % paraformaldehyde (PFA) in PBS was used to fix the brain. A post fixation step followed, where the isolated brains were kept in a 4 % PFA solution for 24h at 4 $^{o}$C. Lastly, the brains were transferred into a 20 % sucrose solution for another 24 h for cryoprotection before finally snap frozen in ice cooled isopentane for storage at -80°C.

### 3.7.2 Microglia isolation and FACS analysis of lipofuscin

The deletion of CB1 receptors may lead to an early onset of age-related phenotypes in the brain with microglia cells readily showing senescent phenotype in the brain of GABA/Cnr1$^{-/-}$ mice as compared to their age-matched wild-type siblings. Here the amount of lipofuscin contained in the microglia is an indicator of the ageing process of these cells. For this purpose, we isolated microglia (precisely intracerebral lymphocytes), stained for microglia and proportion of lipofuscin accessed by FACS. Microglia isolation starts with transcardial perfusion and brain harvesting. Now a brain was homogenized in 1 ml of medium by chopping with a scalpel in a 35 mm dish, then 3 ml medium was added. An enzymatic solution ( Collagenase and Dispase) was added and placed in the incubator (37°C, 5 % $CO_2$ under stirring every 10 minutes). After 45 minutes, a DNase I solution was added for another 45 minutes. A 20 % fetal calf serum (FCS) in 1 x HBSS was used to stop the enzymatic reaction. The homogenate was collected in 50 ml falcon tube and centrifuged for 10 minutes at 4°C and 300 g. The pellet was resuspended in 1 ml medium and 4 ml medium was added. Using a 20G needle and a 20 ml syringe, the pellet was further dissociated to single cells. The homogenate was filtered through a 100 µm filter and 10 ml medium was used to wash the filter down. Again, a centrifugation step at 4°C and 300 g for 10 minutes was performed.

A discontinuous gradient density centrifugation step using Percoll was then performed. First the pellet was resuspended in 1 ml 70 % Percoll and then 14 ml Percoll was added. Now 15 ml of 30 % Percoll was gently added to the tube, taking care that the phases are not mixed together. On top of the 30 % Percoll phase, 15 ml 1 x PBS was added and centrifuged for 25 minutes at room temperature and 600 g without brakes. Thereafter, the material (myelin and debris) at the interphase between 30 % Percoll and 1 x PBS was carefully discarded. We now collected the interphase ring between the 70 % and 30 % phases (intracerebral lymphocytes) into a new 50 ml falcon tube and filled up to 45 ml with medium. Another centrifugation step at 4°C and 400

g was performed for 10 minutes. The pellet was resuspended in 1 ml FACS buffer in a 1.5 ml Eppendorf tube and centrifuged at 4°C and 1700 g for 5 minutes. Next, for the FACS analysis of lipofuscin levels, the isolated cells were stained for microglial markers (CD11b and CD45). While CD11b primary antibody was coupled with APC a far red dye, the CD45 primary antibody was coupled to a blue dye, e450. Lipofuscin displays it autofluorescence property at a wavelength range of 480-550. The isolated cells were incubated in CD16/32 blocking solution for 15 minutes to block the Fc- receptor binding sites on the cell surface. Afterward, 1 ml FACS-buffer was added and cells were centrifuged for 5 minutes at 1700 g rpm. The pellet was incubated in an antibody-mix of both CD11b-APC and CD45-e450. For control and FACS settings some samples were stained only with CD11b-APC, CD45-e450 and a negative control, where no antibody was added at all. The samples were incubated for 15 minutes after which 1 ml of FACS buffer was added to samples and centrifuged for 5 minutes at 1700 g rpm. The pellets were now resuspended in 200 ml FACS buffer and analysed by FACS. For each sample, we analysed 100-150 microglial cells by comparing the lipofuscin-like autofluorescence within the microglia.

### 3.7.3 Organotypic hippocampal slice culture

To investigate the interchanging role of the endocannabinoid system on microglia- neuron interaction, organotypic hippocampal slice culture experiments with GABA-Cnr1$^{-/-}$ mice (CB1 specifically knocked out in GABA neurons) and LysM-Dagla$^{-/-}$ mice (Dagla specifically knocked out in microglia) were performed. A laminar flow hood was cleaned and 6-well plates containing 1 ml of culture medium pre-warmed in the incubator were prepared. Thereafter, all instruments to be used were sterilised in 70 % ethanol. The instruments were, however, rinsed in dissection medium before use. Now, three to five days old pups were collected and sacrificed by decapitation and the head placed in a 10 cm petri dish, followed by sterilisation of the head with 70 % ethanol. Next, the head was dissected and the brain placed on ice in a petri dish with

wet filter paper, minding not to touch the brain with unsterilized instruments. Subsequently, the cerebellum was removed with a scalpel and two brains were fixed (dorsal side down) to the vibratome plate stabilised by agarose blocks. Then, the vibratome chamber was filled with cold dissection medium, while placing crunched ice blocks around the chamber. After this, the brains were cut into 350 µm slices, collecting the slices containing the hippocampus with a Pasteur pipette into a new petri dish containing dissection medium. Now, with the aid of a microscope, slices containing clearly hippocampal structure (dentate gyrus, CA1 and CA3) and entorhinal cortex were isolated without lesion to structure. Consequently, four to six slices were collected per brain with a Pasteur pipette and transferred into a petri dish filled with culture medium on ice. Now, the slices were picked with little culture medium alongside into a Millicell insert and excessive medium was removed with a pipette. Finally, the insert was placed into the prepared 6-well plate with forceps and placed back into the incubator (35°C and 5 % $CO_2$). Medium was changed a day after preparation but subsequently every two to three days. Slices were kept in culture for two weeks before starting experiments. For the experiment, we activated the microglia in the slices by stimulating with 5 µg/ml LPS for three consecutive days. Each day, the medium was collected in Eppendorf tubes, shock-frozen in liquid nitrogen and replaced with fresh medium before the next LPS stimulation. Collected samples were stored in -80°C pending further experiments. Four conditions were investigated; wild-type, wild-type (stimulated), Knockout and knockout (stimulated). Thereafter, glial activity was assessed as time-dependent increase in TNF, IL-1β and IL-6 in the media using ELISA.

### 3.7.4 LPS injection

As a further approach, we evaluated the effect of CB1 receptor deletion from GABAergic neurons on microglial activity in situ. Here, 2 months old knockout and wild-type mice were intraperitoneally injected with 0.8 mg/kg LPS or saline, once for the single injection paradigm or 4 times on four consecutive days for the multiple injection paradigm. Mice were sacrificed

24 hours after the last injection and microglial activity was assessed. Change in microglial number in the hippocampus and expression of cytokines were determined.

### 3.7.5 Enzyme-linked immunosorbent assays (ELISA)

Employing the Read-Set-Go ELISA Kit, TNFα, IL-1β and IL-6 levels in the collected media samples were measured. ELISA is an antibody-mediated characterisation of protein in a given sample, whereby the levels of the proteins of interest is in direct correlation with the light-sensitive signals that are detected by enzymatic oxidation of 3,3', 5,5'-Tetramethylbenzidine (TMB). The experiment was performed as instructed by the manufacturer. For short, a 96-well plate was coated with coating solution and incubated for 24 hours at 4°C, washed several times with washing buffer and assay diluent applied for 1 h at room temperature for blocking, then washed again. OHSC media sample were used at a 1:10 dilution while assay standards were diluted according to manufacturer's instructions. Now, 100 µl/well of standards and samples was used in duplicates. The measurements were done at a wavelength 450 nm, whereas the reference was at 570 nm.

### 3.7.6 RNA isolation

Total RNA from frozen half-brain tissue or isolated primary microglia was extracted using the TRIzol® reagent (Life Technologies). For half-brain, tissue was transferred into 2 ml Precellys tubes with 1.4 mm ceramic beads (peqLab, Erlangen) containing 1 ml TRIzol®. The tubes were placed into the Precellys centrifuge and the tissues were homogenized in 2 cycles for 20 sec. The homogenization step was repeated again for optimum outcome. For isolated microglia, 500 µl TRIzol® is added to the cells in 1.5 ml Eppendorf tubes and pipetted up and down several times. From this point on samples were handled similarly, irrespective of sample initial state. Homogenized samples were centrifuged at 12000 g for 10 min at 4°C. The

supernatants were then transferred into fresh 1.5 ml Eppendorf tubes after which 200 µl 1-bromo-3-chloropane (BCP) was added. Now, the samples were then continually vortexed for 30 s and later incubated at RT for 5 min. This was followed by another centrifugation step at 12000 g for 10 min at 4°C, leading to formation of phases. The upper phase, containing the RNA was transferred into a new tube and isopropanol was added at a ratio of 1:1 for precipitation of RNA. Again, the samples were vortexed for 30 s, but this time incubated for 10 min at RT before centrifugation (12000 g, 10 min, 4°C). The supernatant was discarded and the precipitated RNA washed three times in 1 ml 75 % ethanol. Subsequently, another centrifugation step was done at 12000 g for 5 min. The RNA pellet was dried for 30 min at 47°C and dissolved in 50 µl RNase-free water and the concentration was determined by optical density measurement using the NanoDrop 1000.

### 3.7.7 RT- cDNA synthesis

In order to transcribe the isolated and purified RNA into cDNA, a reverse transcription polymerase chain reaction was performed, using the SuperScript® II for RT-PCR (Life Technologies). First, RNA was prepared to contain an equal concentration at a maximum of 1000 ng per sample in a total volume of 11 µl in DEPC. Then, 1 µl of 0.5 µg/µl Oligo-dt and 1 µl of 100 mM dNTPs (Sigma-Aldrich) was added to each reaction before the thermo cycler was run under the cycler parameters indicated below:

**Cycling parameters**

| | |
|---|---|
| 65°C | 5 min |
| 4°C | 3 min |

Now, the master mix illustrated below was added to each sample.

**Master mix for a sample**

| | |
|---|---|
| 5 x first strand buffer (Life Technologies) | 4 µl |

| | |
|---|---|
| DTT 0.1 M (Life Technologies) | 2 µl |

Thereafter, the following program was applied:

| **Cycling parameters** | |
|---|---|
| 42°C | 2 min |
| 4°C | 3 min |

At this point, we added 1 µl SuperScript® II Reverse Transcriptase to each sample and the following program was run.

| **Cycling parameters** | |
|---|---|
| 42°C | 50 min |
| 70°C | 15 min |
| 4°C | 10 min |

The transcribed cDNA was diluted as required with RNase-free water and stored at -20°C pending usage. For the gene expression analysis, 4 µl of each sample containing 30 ng cDNA was used per well for the TaqMan reaction.

### 3.7.8 Real time quantitative polymerase chain reaction (RT-qPCR)

The expression levels of the cytokines of interest were determined using the TaqMan® Gene Expression Assay from Applied Biosystems, Darmstadt, Germany. Here, 4 µl of each sample containing 30 ng cDNA was added to 6 µl master mix:

| **Master mix for a sample** | |
|---|---|
| TaqMan® master mix | 5 µl |
| 20 x TaqMan® Gene Expression primer (Table x) | 0.5 µl |
| RNase-free water | 0.5 µl |

Lastly, samples were placed in the LightCycler® 480 from Roche, Germany and ran, applying a defined set of parameters (95°C for 10 min; 45 cycles at 95°C for 15 s and 60°C for 1 min). GAPDH being used as the housekeeping gene, relative gene expression levels were calculated with the 2−ΔΔCT method (Livak & Schmittgen, 2001).

**TaqMan® Gene Expression**

| Target genes | Assay ID |
|---|---|
| IL-1β | Mm00434228_m1 |
| IL-6 | Mm00446190_m1 |
| TNFα | Mm00443258_m1 |
| GAPDH | Mm99999915_g1 |

### 3.7.9 Immunohistochemical staining

The frozen brains or half-brains were serially cryosectioned into 16 µm coronal sections using a Cryostat (Leica CM3050 S; Leica Microsystems, Heidelberg, Germany). Sections were mounted onto glass slides and stored at -80°C, if not immediately processed.

**Iba1 Staining**

For Iba1 staining, sections were permeabilised with 0.5% Triton X-100 in PBS for 1 h at room temperature. After a short washing step, sections were blocked with 3% BSA in PBS and after washing, incubated with rabbit anti-Iba1 IgG (Wako, Japan) primary antibody diluted to 1:2000 in 3% BSA in PBS and incubated for 48 h at 4 °C. Next, after washing, slides were blocked by dipping them into 3% BSA in PBS and incubated with a secondary antibody (AF488 conjugated donkey IgG anti-rabbit, Invitrogen, USA) in 1:1000 dilution in 3% BSA in PBS for 2 h at room temperature. Finally, the slides were briefly washed and covered with Vectashield Mounting

Medium containing 4′,6-diamidino-2-phenylindole (DAPI) (Vector Laboratories Inc., Burlingame, CA).

**CX3CR1:CX3CL1 and CD200R:CD200L staining**

The sections were dried after collection from the freezer on a hot plate for 30 min at 40°C, and then washed in PBS for 10 min at RT. Sections were incubated in 10 mM sodium citrate (pH 8.5) for 30 min at 65°C. Now, sections were permeabilised in 0.5 % TritonX-100 in PBS for 20 min, washed and then blocked in 10 % normal goat serum (NGS) and 3 % BSA in PBS for 1 h all at RT. At this point, after washing, the various primary antibodies (Anti-CD200/OX2 [ab33734, rat], Anti-CD200R/OX102 [ab34097, mouse], Anti-CX3CL1 [ab25088, rabbit], Anti-CX3CR1 [c8354, rabbit]) were added diluted 1:500 in 3 % BSA in PBS and incubated for 24 h at 4°C. Afterwards, sections were washed 3 times in PBS and the respective secondary antibodies (Alexa Fluor® 488 goat anti-mouse, Alexa Fluor® 594 goat anti-rat, Cy3 goat anti-rabbit) were added diluted in the same solution and same concentration as the primary antibodies before incubating for 1 h at RT. Another washing step in PBS and Milli-Q water followed. Lastly, slides were covered with Vectashield Mounting Medium containing 4′,6-diamidino-2-phenylindole (DAPI) (Vector Laboratories Inc., Burlingame, CA).

## 3.8 Image acquisition and analysis

Fluorescence images were acquired using a Zeiss Axiovert 200 M fluorescent microscope (Carl Zeiss Microimaging, Germany) and the pictures were converted to 8-bit grey scale. For quantitative analysis, we determined microglia densities/sizes and in neuron-microglia communication markers (neuroimmune regulators) only the densities within the hippocampus using the Image J software (Image J 1.42q and 1.47v, NIH, USA). Neuroimmune regulators signal is given in average signal intensity of the areas covered in the hippocampus. Density of

microglia was given as number of Iba1 positive cells per $mm^2$. For statistical analysis, four to six representative slides were evaluated from each animal. Groups were compared using two-way ANOVA followed by Bonferroni test with post hoc test.

## 3.9 Statistics

In general, result data are presented as means ± SEM, whereby numbers of animals or samples are indicated in the respective figures. A Mann-Whitney U test, two-way ANOVA with Bonferroni´s post-hoc test or Students t-Test was used to assess data statistical significance, setting P-value at $p < 0.05$. GraphPad Prism 5.03 or Statistica software was used.

# 4. Results

## 4.1 GABA-CB1$^{-/-}$ leads to enhanced neuroinflammation in ageing

Constitutive deletion of CB1 receptor has been shown to promote aging. This was accompanied by increased neuroinflammation as a result of changing microglia reactivity. Microglial cells in constitutive Cnr1$^{-/-}$ mice had increased levels of activation and aging markers (Albayram et al. 2011). Here we asked whether a specific deletion of Cnr1$^{-/-}$ on GABA neurons may suffice to induce property-changes in microglia and the brain.

### 4.1.1 Disturbed regulation of cytokine production in GABA-Cnr1$^{-/-}$ mice in OHSC system

We hypothesized that the microglial reactivity is disturbed in the knockout model. Hence, we tested cytokines production regulation in organotypic hippocampal slice cultures that were obtained, prepared and maintained as detailed in materials and methods. ELISA was then performed as instructed by the manufacturer to measure cytokines levels.

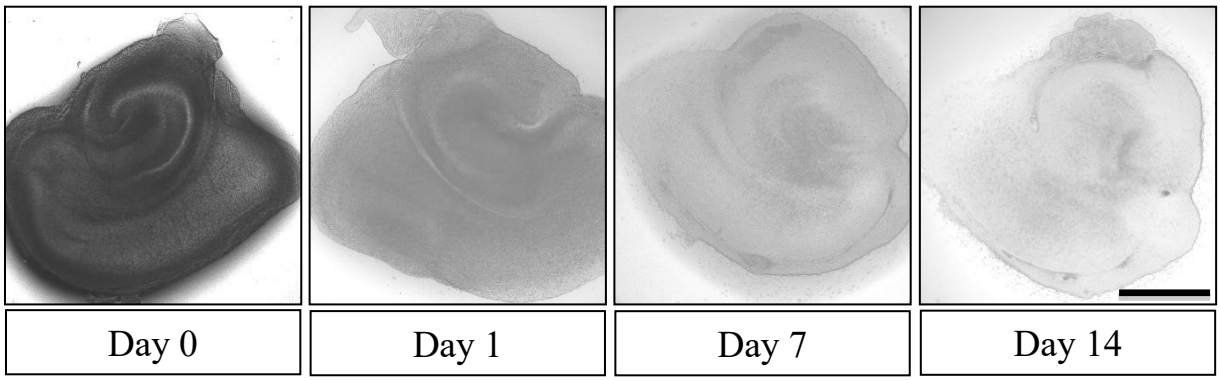


**Figure 4.1.1: Representative microphotograph of organotypic hippocampal slices in culture.The length of the scale bars is 200 µm**

One-way ANOVA revealed a highly significant LPS treatment effect in IL1β ($F_{(3, 30)} = 30.55$, $p < 0.001$), IL-6 ($F_{(3, 20)} = 54.49$, $p < 0.001$) and TNFα ($F_{(3, 20)} = 11.48$, $p > 0.01$) after 24h stimulation. Post hoc analysis of the data also showed that IL1β and IL-6 production was

significantly higher in the stimulated similarly in both genotypes ($p < 0.001$). TNFα production was significantly higher in the stimulated groups in the WT ($p < 0.01$) and in the GABA-Cnr$^{-/-}$ samples ($p < 0.05$). There was a significant increase in TNFα production in the unstimulated GABA-Cnr$^{-/-}$ samples compared to unstimulated WT control ($p < 0.01$). Figure 4.1.1A.

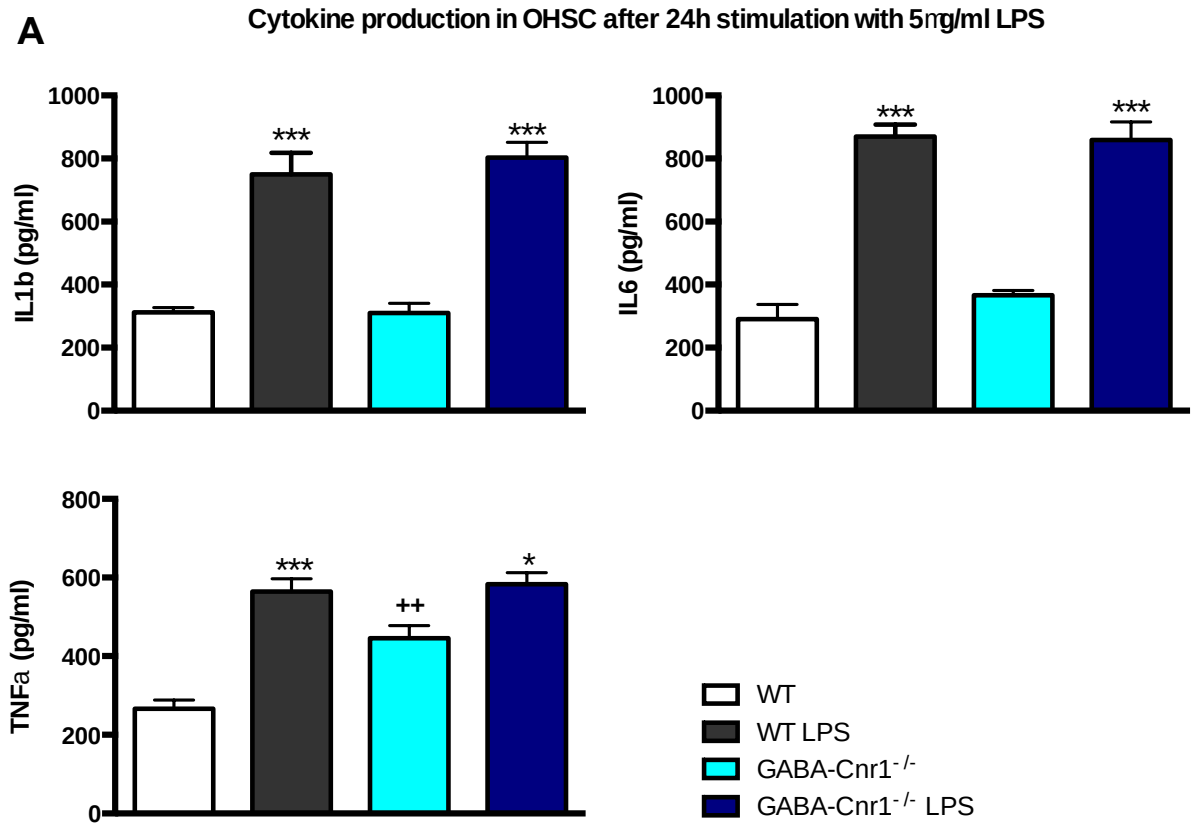


**Figure4.1.1A: ELISA measurement of OHSC supernatants for cytokine release after 24h LPS stimulation**. Stimulation with LPS for 24h led to increased production of IL1β, IL-6 and TNFα irrespective of genotype. TNFα level was higher in unstimulated GABA-Cnr1$^{-/-}$ compared to unstimulated WT. One-way ANOVA with Bonferroni's post-hoc test: WT stimulated compared to WT unstimulated (***$p < 0.001$), GABA-Cnr1$^{-/-}$ stimulated compared to GABA-Cnr1$^{-/-}$ unstimulated (***$p < 0.001$, *$p < 0.05$). Genotype effect for TNFα production when unstimulated WT and GABA-Cnr1$^{-/-}$ are compared ($^{++}p < 0.01$). Values represent mean ± SEM; n = 6 per group.

After 48h of LPS stimulation, one-way ANOVA revealed a significant LPS treatment effect in IL1β ($F_{(3, 30)} = 6.854$, $p < 0.01$) and IL-6 ($F_{(3, 20)} = 5.752$, $p < 0.001$) and in TNFα ($F_{(3, 20)} = 7.983$, $p < 0.01$). IL1β production in stimulated WT was higher than in WT unstimulated ($p < 0.05$) and stimulated GABA-Cnr1$^{-/-}$ was higher than in unstimulated GABA-Cnr1$^{-/-}$ group ($p < 0.01$). IL-6 production was also significantly changed when WT stimulated and WT unstimulated

controls were compared ($p < 0.05$), but stimulated GABA-Cnr1$^{-/-}$ group showed even higher IL-6 level compared to unstimulated GABA-Cnr1$^{-/-}$ group ($p < 0.01$). TNFα production was equally increased in both stimulated WT and stimulated GABA-Cnr1$^{-/-}$ as compared to unstimulated GABA-Cnr1$^{-/-}$ and WT controls groups ($p < 0.01$). Figure 4.1.1B.

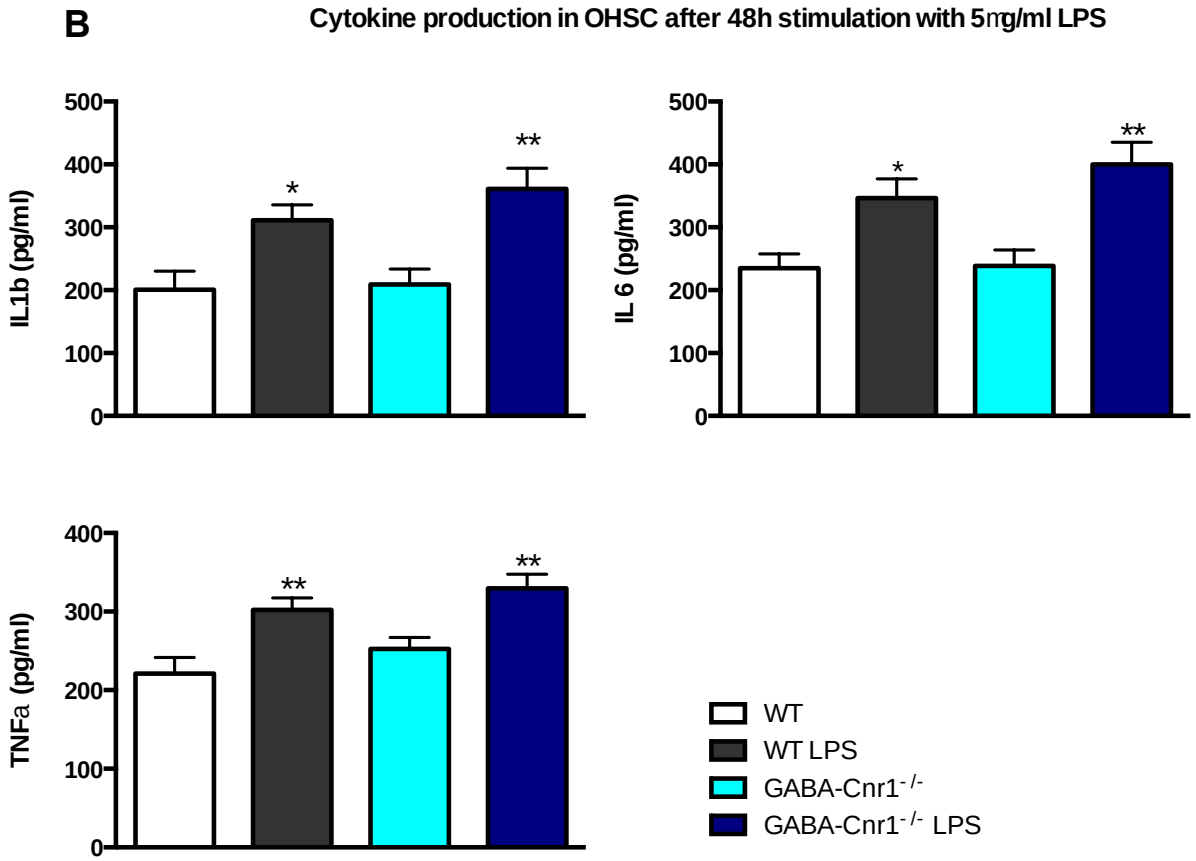


**Figure 4.1.1B: ELISA measurement of OHSC supernatants for cytokine release after 48h LPS stimulation**. Stimulation with LPS for 48h led to increased production of IL1β, IL-6 and TNFα irrespective of genotype. IL1β and IL-6 production was even higher in stimulated GABA-Cnr1$^{-/-}$ group. One-way ANOVA with Bonferroni's post-hoc test: $^{*}p< 0.05$,$^{**}p < 0.01$. Values represent mean± SEM; n =3-6 per group.

When LPS treatment effect was assessed after 72h of stimulation, one-way ANOVA showed a significant LPS treatment effect in IL1β ($F_{(3, 45)} = 4.887$, $p < 0.01$), IL-6 ($F_{(3, 20)} = 14.16$, $p < 0.001$) and TNFα ($F_{(3, 20)} = 9.015$, $p < 0.001$). IL1β production in stimulated WT was not significantly higher than in WT unstimulated ($p > 0.05$), while stimulated GABA-Cnr1$^{-/-}$ showed significantly increased IL1β compared to unstimulated GABA-Cnr1$^{-/-}$ group ($p < 0.001$). IL-6 production was not significantly changed when WT stimulated and WT unstimulated controls

were compared ($p > 0.05$), but stimulated GABA-Cnr1$^{-/-}$ group showed higher IL-6 level compared to unstimulated GABA-Cnr1$^{-/-}$ group ($p < 0.001$). TNFα production was higher in stimulated GABA-Cnr1$^{-/-}$ compared to unstimulated GABA-Cnr1$^{-/-}$ group ($p < 0,01$), while there was no significant change in TNFα level in the WT groups ($p < 0.05$). Stimulated GABA-Cnr1$^{-/-}$ samples revealed significantly higher production of IL1β ($p < 0.01$), IL-6 ($p < 0.001$) and TNFα ($p < 0.001$) compared to stimulated WT samples. Figure 4.1.1C.

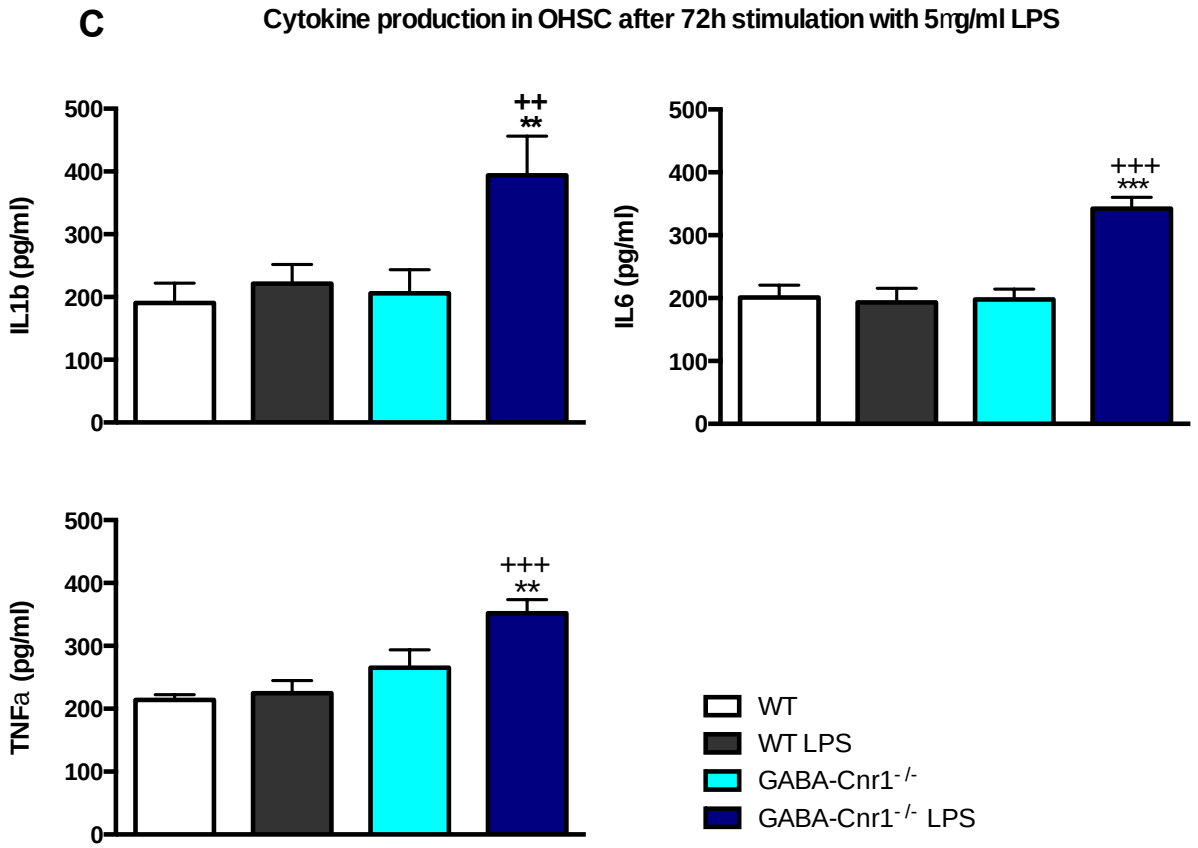


**Figure 4.1.1C: ELISA measurement of OHSC supernatants for cytokine release after 72h LPS stimulation**. Stimulation with LPS for 72h led to significantly increased production of IL1β, IL-6 and TNFα only in stimulated GABA-Cnr1$^{-/-}$ group. One-way ANOVA with Bonferroni's post-hoc test: Treatment effect: **$p < 0.01$;***$p < 0.001$. Genotype effect: $^{++}p < 0.01$; $^{+++}p < 0.001$. Values represent mean± SEM; n =3 per group.

### 4.1.2 Multiple intraperitoneal LPS injection leads to altered microglia reactivity in GABA-Cnr1$^{-/-}$ mice

Neuron-glia interaction is crucial in the regulation of inflammation responses in the CNS. Perturbed neuron-glial communication as a result of a disturbed cannabinoid system activity may affect microglia response to acute insult, here, a single LPS injection. Microglial response to an incessant (chronic) insult, here multiple LPS injection, may also change, leading to an altered cytokine production and/or microgliosis. We tested this hypothesis in a GABAergic neuron-specific Cnr1 knockout model.

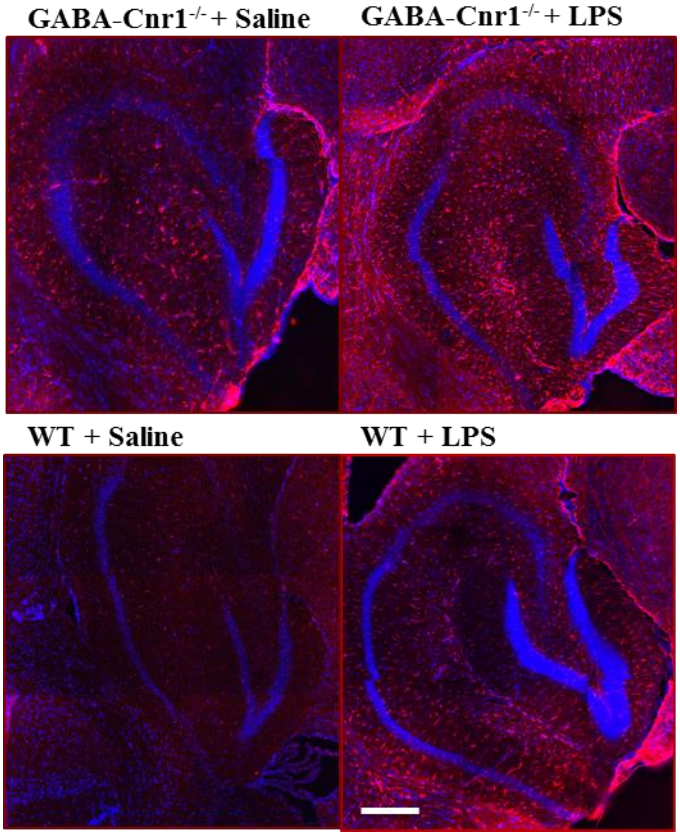


**Figure 4.1.2: Representative depiction of microglia density in the hippocampus. The length of the scale bar is 200 µm.**

Microglial density increased after single intraperitoneal (i.p) LPS injection in both WT control and GABA-Cnr1$^{-/-}$ mice. Two-way ANOVA showed that there was a significant treatment effect ($F_{(1, 8)} = 23.01$, $p < 0.01$; Fig. 4.1.2.1A) and genotype effect ($F_{(1, 8)} = 10.81$, $p < 0.05$; Fig. 4.1.2.1A). No interaction between treatment and genotype was seen ($F_{(1, 8)} = 0.1971$, $p > 0.05$;

Fig. 4.1.2.1A). After multiple i.p injection, similar to after single injection, significant treatment effect ($F_{(1, 8)}$ = 45.92, p < 0.001; Fig. 4.1.2.1B), and genotype effect ($F_{(1, 8)}$ = 25.41, p < 0.01; Fig. 4.1.2.1B) was revealed. As in the previous test, the interaction between treatment and genotype was not significant ($F_{(1, 8)}$ = 1.546, p > 0.05; Fig. 4.1.2.1B).

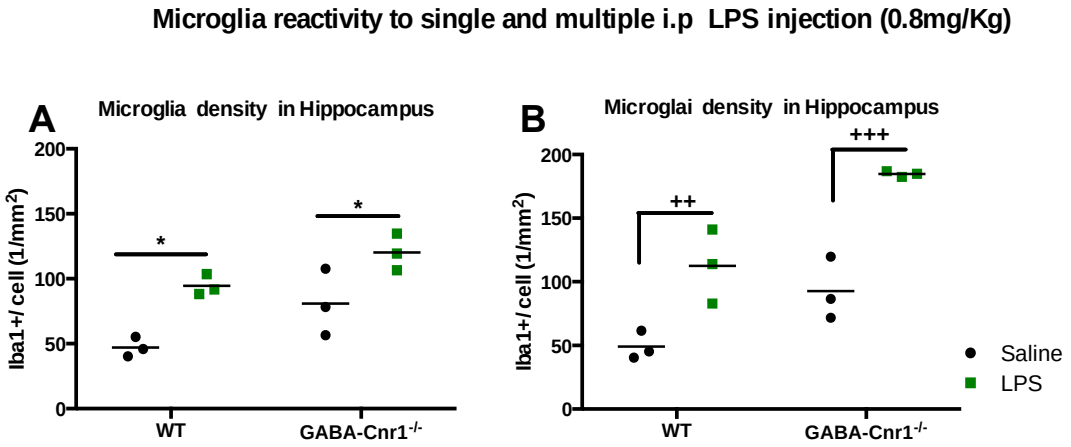


**Figure 4.1.2.1: Microglia reactivity in terms of density is stronger in GABA-Cnr1-/- and even strongest after multiple injection.** (A) Single LPS treatment led to a significantly increased microglia number in WT and GABA-Cnr1$^{-/-}$mice as compared to their untreated counterparts (*p < 0.05). (B) Multiple LPS treatment led to increased microglia number in the hippocampus of treated WT when compared to untreated WT mice ($^{++}$p < 0.01). The increase was exacerbated when GABA-Cnr1$^{-/-}$treated and untreated groups were compared ($^{+++}$p < 0.001). Analysis was performed by two-way ANOVA followed by Bonferroni's post hoc test. Lines represent mean value; n = 3 per group.

Next we sought to understand whether the exacerbated microglial reactivity in the GABA-Cnr1$^{-/-}$ mice after LPS treatment, as observed in the increased microglia density, is reflected in the levels of production of prominent pro-inflammatory cytokines like IL-6, IL-1β and TNF-α. RT-PCR was performed with the brains of single and multiple injected mice and their WT littermates.

Following single and multiple LPS injection, there was significant decrease in IL-6 production in the single injected mice ($F_{(1, 27)}$ = 15.35, p < 0.001; Fig. 4.1.2.2A) but not in the multiple injected mice ($F_{(1, 20)}$ = 3.876, p > 0.05; Fig. 4.1.2.2B). No genotype effect was observed ($F_{(1, 27)}$ = 0.3778, p > 0.05; Fig. 4.1.2.2A) for single injection and ($F_{(1, 20)}$ = 0.0630, p > 0.05; Fig. 4.1.2.2B) for multiple injection. Bonferroni's multiple comparison test showed that after single

injection, IL-6 production decreased significantly in the treated WT group as compared to the untreated WT control group ($p < 0.05$). This effect was exacerbated in the treated GABA-Cnr1$^{-/-}$ group compared to untreated GABA-Cnr1$^{-/-}$ group ($p < 0.01$). IL-1β production was significantly increased after LPS treatment with treatment effect observed to be ($F_{(1, 28)} = 52.93$, $p < 0.0001$; Fig. 4.1.2.2C) for single injected and ($F_{(1, 20)} = 96.39$, $p < 0.0001$; Fig. 4.1.2.2D) for multiple injected. There was no significant genotype effect ($F_{(1, 28)} = 0.1281$, $p > 0.05$; Fig. 4.1.2.2C) for single injected group and ($F_{(1, 20)} = 0.01402$, $p > 0.05$; Fig. 4.1.2.2D) for multiple injected group. Bonferroni's multiple comparison test indicated that single LPS injection led to significantly increased IL-1β production in the treated WT group as compared to the untreated WT control group ($p < 0.0001$) in both single and multiple injection paradigms. This effect was similar in the treated GABA-Cnr1$^{-/-}$ group when compared to untreated GABA-Cnr1$^{-/-}$ group ($p < 0.0001$). After single LPS treatment, TNF-α production increased significantly ($F_{(1, 27)} = 45.06$, $p < 0.0001$; Fig. 4.1.2.2E) and after multiple injection the treatment effect was also significant at ($F_{(1, 27)} = 12.83$, $p < 0.01$; Fig. 4.1.2.2F). No genotype effect was observed in any of the groups ($F_{(1, 20)} = 0 .7159$, $p > 0.05$; Fig. 4.1.2.2). Bonferroni's multiple comparison test showed that single LPS injection led to significantly increased TNF-α production in the treated WT group as compared to the untreated WT control group ($p < 0.001$). The same effect was recorded in the treated GABA-Cnr1$^{-/-}$ group when compared to untreated GABA-Cnr1$^{-/-}$ group ($p < 0.001$). Whereas, after multiple injection, TNF-α production significantly increased in the treated WT group as compared to the untreated WT control group ($p < 0.01$), but not in the treated GABA-Cnr1$^{-/-}$ group when compared to untreated GABA-Cnr1$^{-/-}$ group ($p > 0.05$).

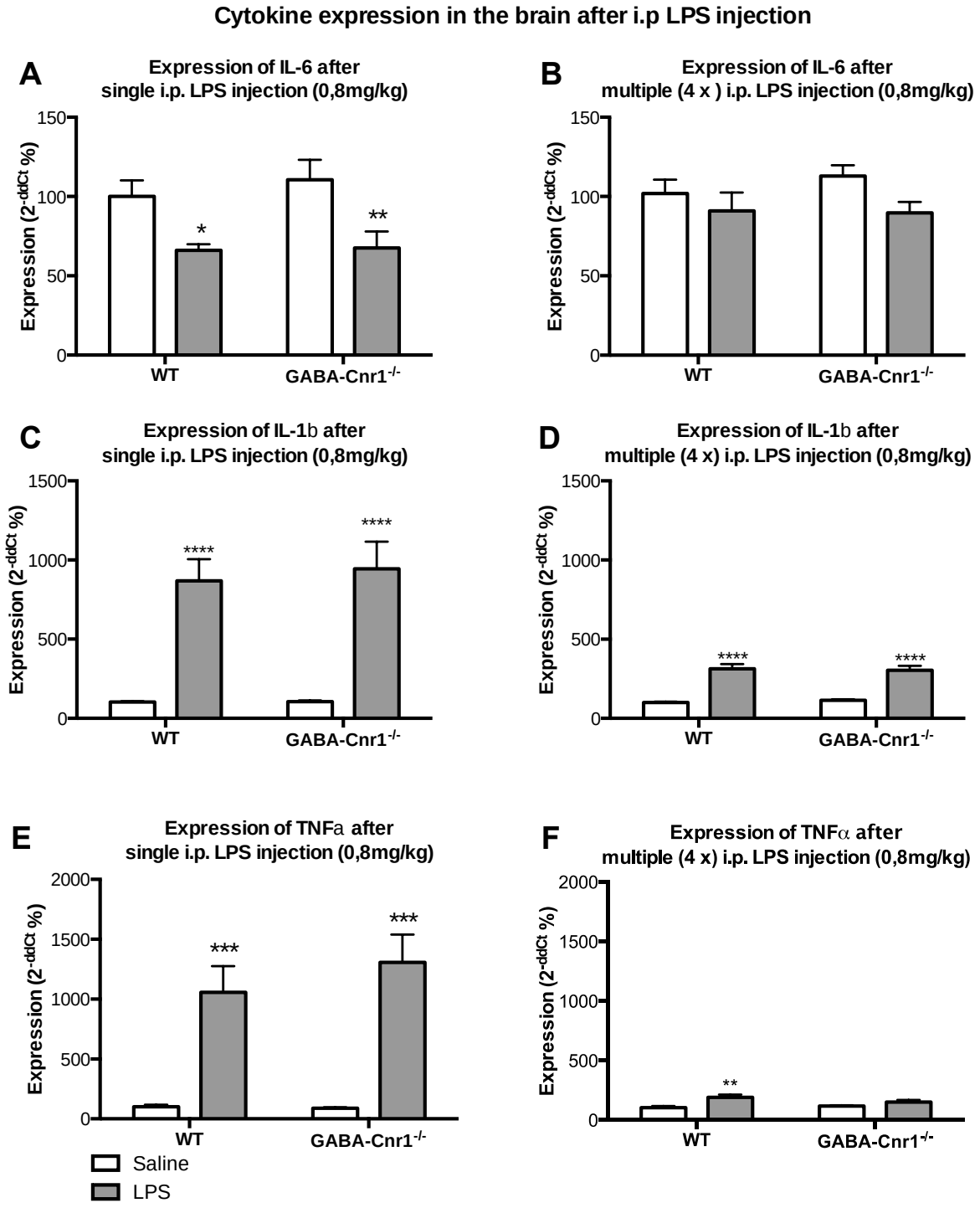


**Figure 4.1.2.2: Gene expression of IL-6, IL1β and TNF-α are differentially altered after LPS treatment of GABA-Cnr1$^{-/-}$ mice.** LPS treatment led to a decreased production of IL-6 in WT as well as in GABA-Cnr1$^{-/-}$ mice after single injection; Two-way ANOVA with Bonferroni's post-hoc test: $p > 0.05$, *$p < 0.05$, **$p < 0.01$.IL-1β increased dramatically irrespective of treatment paradigm and genotype; Two-way ANOVA with Bonferroni's post-hoc test: ****$p < 0.0001$. Two-way ANOVA with Bonferroni's post-hoc test revealed that TNF-α increased after single injection irrespective of genotype (***$p < 0.001$) but in the multiple injection paradigm, it only increased in WT treated group (**$p < 0.01$), not the GABA-Cnr1$^{-/-}$ group ($p > 0.05$).Values represent mean ± SEM; n = 6 - 8 per group.

### 4.1.3 Sickness behaviour and microglia reactivity to intracerebroventricular (ICV) LPS injection

After ascertaining microglia reactivity to intraperitoneal LPS in GABA-Cnr$^{-/-}$ mice, we sought to investigate microglia reactivity after direct injection of LPS into the brain (ICV). Furthermore, the role of ageing and its possible correlation to sociability of the mice were tested.

We assessed sickness behaviour as reduced motility and social preference. 2-way ANOVA revealed no significant genotype related change in motility of 2 months old mice (genotype effect: $F_{(1, 45)} = 1.578$, $p > 0.05$; Fig. 4.1.3.1A). Treatment with LPS significantly reduced the motility of 2 months old mice (Treatment effect: $F_{(1, 44)} = 4.121$, $p < 0.05$; Fig. 4.1.3.1A) Hence, there was no interaction between genotype and treatment (Treatment x genotype: $F_{(1, 45)}= 0$ .09699, $p > 0.05$; Fig. 4.1.3.1A). Social preference, which is assessed as a difference between the interaction time with an object or a partner mouse, was highly significant in 2 months old WT mice as mice interacted more with a partner mouse as with an object ($F_{(1, 44)} = 27.18$, $p < 0.001$; Fig. 4.1.3.1A). Furthermore, untreated WT mice spent more time investigating the partner mouse as compared to the time spent by LPS treated WT mice investigating a partner mouse (Treatment effect: $F_{(1, 44)} = 4$ .121, $p < 0.05$; Fig. 4.1.3.1A). GABA-Cnr1$^{-/-}$ mice also showed a strong preference for the partner mouse ($F_{(1, 44)} = 18.52$, $p < 0.001$; Fig. 4.1.3.1A) with no significant treatment effect observed ( Treatment effect: $F_{(1, 44)} = 2$ .037, $p > 0.05$; Fig. 4.1.3.1A).

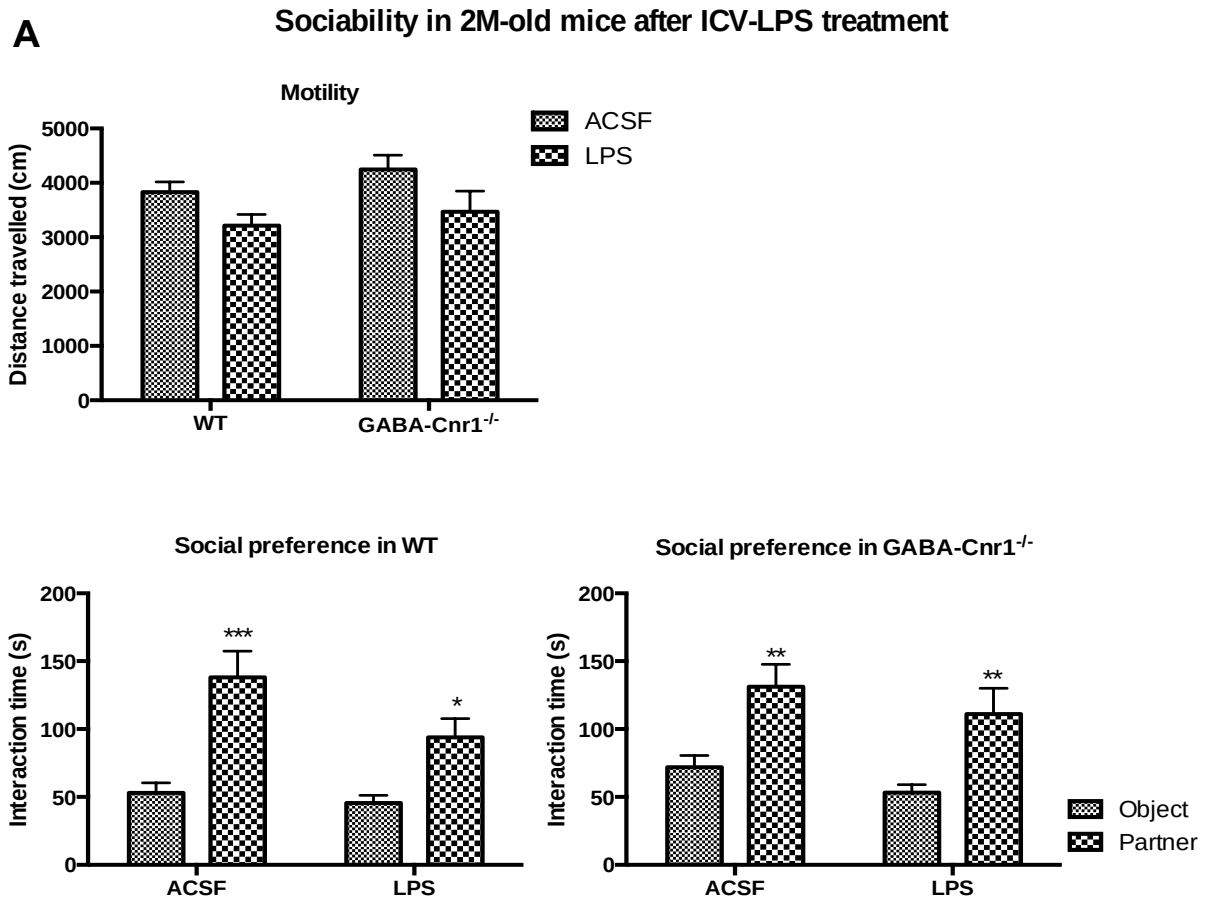


**Figure 4.1.3.1A: LPS treatment led to sickness behaviour in 2 months old WT mice, but not in 2 months old GABA-Cnr1$^{-/-}$ mice. P**reference for partner mice was significantly higher in untreated WT mice as compared to treated WT. Preference for partner mice was the same for both treated and untreated GABA-Cnr1$^{-/-}$ mice. Two-way ANOVA with Bonferroni's post-hoc test: $p > 0.05$; $^{**}p < 0.05$; $^{**}p < 0.01$; $^{***}p < 0.001$.Values represent mean ± SEM; n = 12 per group.

In 12 months old mice, the distance travelled was significantly reduced in LPS treated groups (Treatment effect: $F_{(1, 46)} = 4.469$, $p < 0.05$; Fig. 4.1.3.1B) in both genotypes (Genotype effect: $F_{(1, 46)} = 1.722$, $p > 0.05$; Fig. 4.1.3.1B). Preference for a partner mouse was similarly strong in both WT and GABA-Cnr1$^{-/-}$ mice ($F_{(1, 46)} = 14.83$, $p < 0.001$; Fig. 4.1.3.1B) for WT and ($F_{(1, 46)} = 20.83$, $p < 0.001$; Fig. 4.1.3.1B) for transgenic mice. After LPS treatment, preference for a partner mouse was reduced in both genotypes ($F_{(1, 46)} = 0.3753$, $p > 0.05$; Fig. 4.1.3.1B) for WT and ($F_{(1, 46)} = 0.2874$, $p > 0.05$; Fig. 4.1.3.1B) for GABA-Cnr1$^{-/-}$.

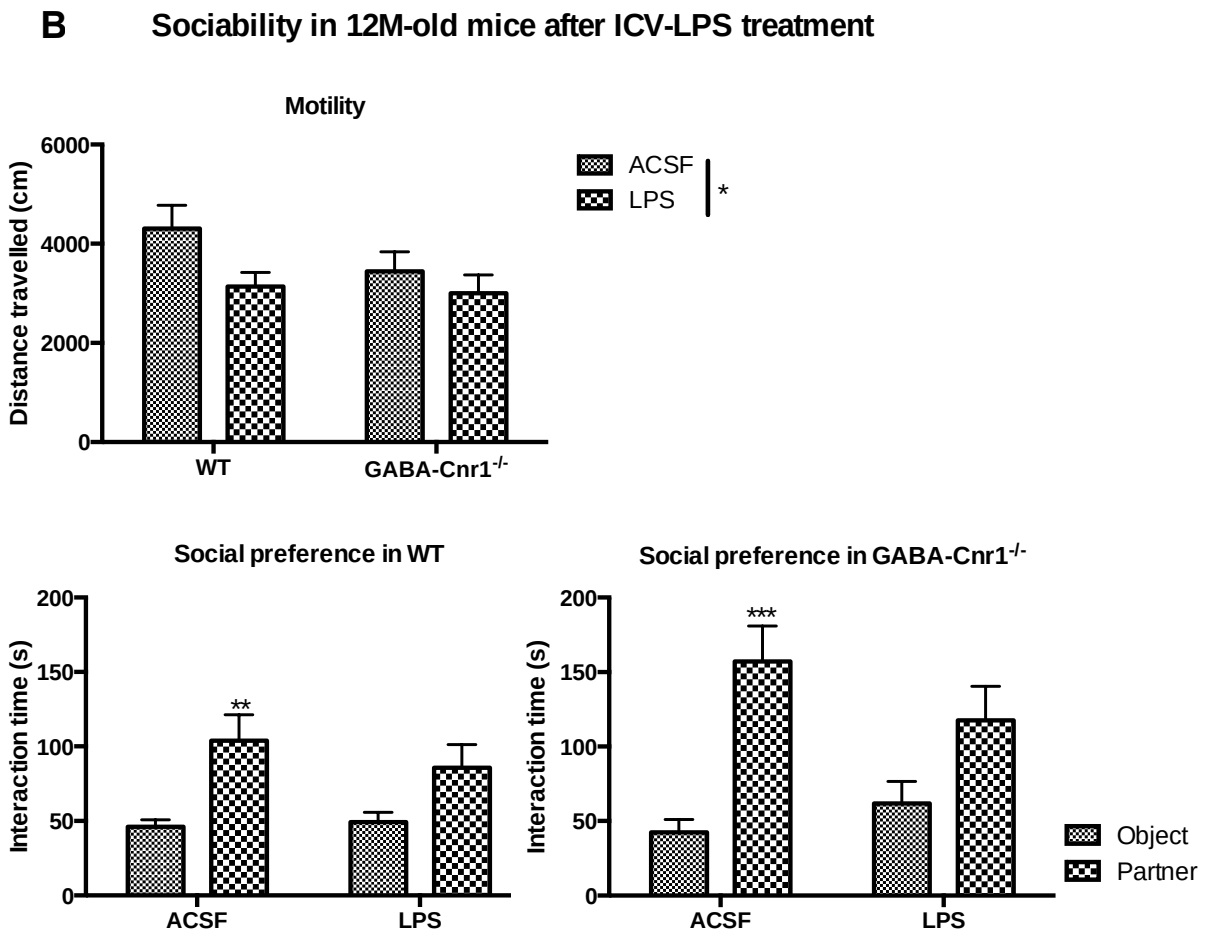


**Figure 4.1.3.1B: LPS treatment elicited similar sickness behaviour in 12 months old WT and GABA-Cnr1$^{-/-}$ mice.** Mice mobility was reduced after LPS treatment in both genotypes. **P**reference for partner mice was decreased in LPS-treated mice. The preference for a partner mouse over an object was highly significant in both genotypes. Two-way ANOVA with Bonferroni's post-hoc test: $p > 0.05$; $^{**}p < 0.01$; $^{***}p < 0.05$.Valuesrepresentmean±SEM; n = 12- 13 per group.

The distance travelled by 18 months old mice, was not significantly reduced in LPS treated groups compared to the untreated groups (Treatment effect: $F_{(1, 30)} = 3.18$, $p > 0.05$; Fig. 4.1.3.1C). There was also no genotype effect ($F_{(1, 30)} = 2.279$, $p > 0.05$; Fig. 4.1.3.1C). Interaction between genotype and treatment was not significant ($F_{(1, 30)} = 1.9$, $p > 0.05$; Fig. 4.1.3.1C). Preference for a partner mouse was significantly high for both WT and GABA-Cnr1$^{-/-}$ mice ($F_{(1, 30)} = 16.4$, $p < 0.001$; Fig. 4.1.3.1C) for WT and ($F_{(1, 30)} = 13.81$, $p < 0.001$; Fig. 4.1.3.1C) for transgenic mice. There was a significant LPS treatment induced decrease in partner preference in the treated WT and transgenic mice ( $p < 0.05$; Fig. 4.1.3.1C). Untreated

WT and GABA-Cnr1$^{-/-}$ mice maintained a strong preference for a partner over an object ($p < 0.01$) for WT and ($p < 0.001$) for GABA-Cnr1$^{-/-}$ mice. Fig. 4.1.3.1C.

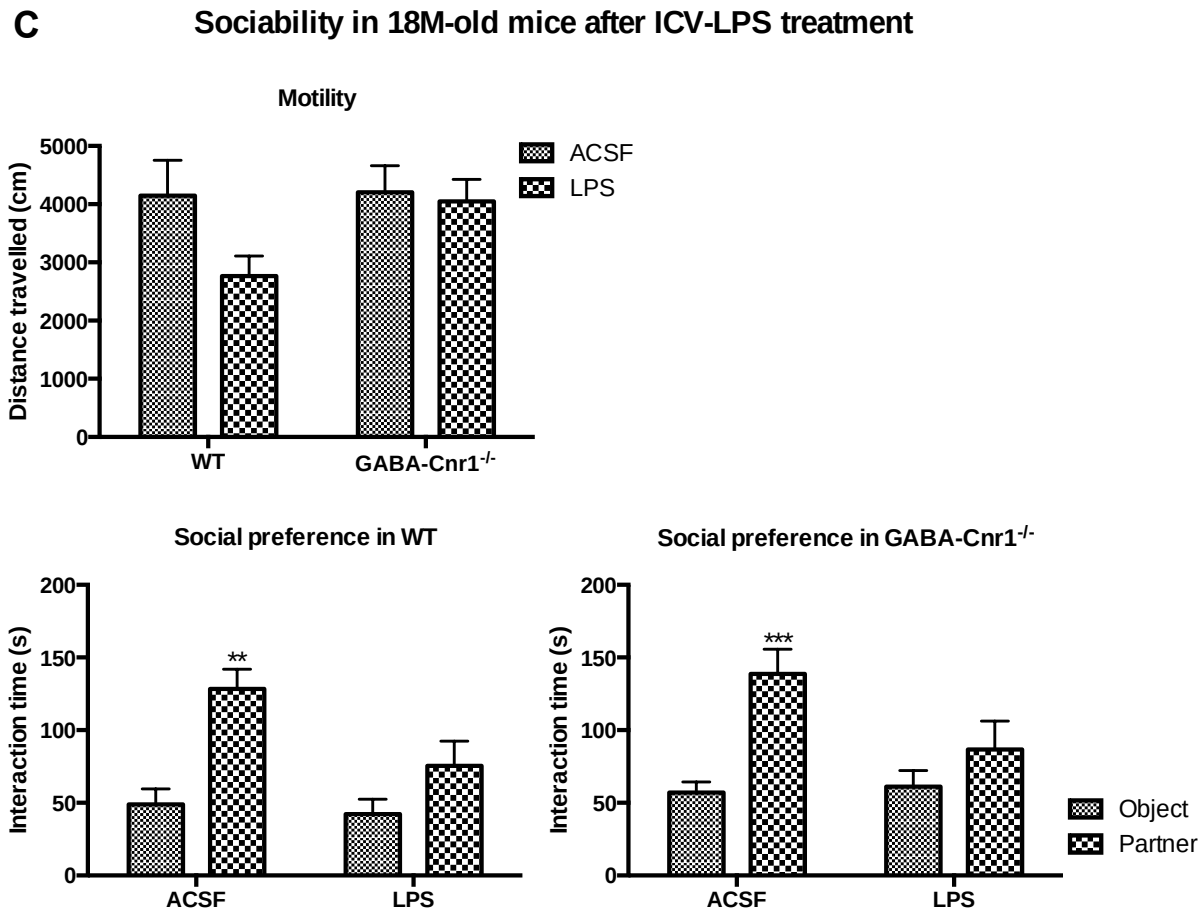


**Figure 4.1.3.1C: LPS treatment led to sickness behaviour in 18 months old WT and GABA-Cnr1$^{-/-}$ mice.** Mice mobility was not significantly reduced after LPS treatment in both genotypes. **P**reference for partner mice was significantly reduced in treated mice as compared to untreated mice. While preference for a partner mouse over an object was highly significant in both genotypes. Two-way ANOVA with Bonferroni's post-hoc test: $p > 0.05$; $^{**}p < 0.01$; $^{***}p < 0.05$. Values represent mean ±SEM; n = 7- 10 per group.

After showing that ICV-LPS treatment effects lead to sickness behaviour as evident in the reduced sociability in both genotypes, we investigated whether the sickness behaviour can be traced back to increased microglia reactivity as a result of increasing microglia density in the hippocampus.

Two-way ANOVA showed that the density of microglia in the hippocampus is significantly increased in 2-month-old mice after LPS treatment ($F_{(1, 8)} = 18 .14$, $p < 0.01$; Fig. 4.1.3.2A).

Microglia density differed between the genotypes ($F_{(1, 8)} = 15.9$, $p < 0.01$; Fig. 4.1.3.2A), no treatment x genotype interaction was detected ($F_{(1, 8)} = 0.8786$, $p > 0.05$; Fig. 4.1.3.2A). However, Bonferroni's multiple comparison test revealed that while LPS treatment led to a significantly higher microglia density in the WT ($p < 0.05$), there was no significant change in the GABA-Cnr1$^{-/-}$ animals ($p > 0.05$). Additionally, there was a significantly higher density of microglia present in hippocampus of untreated GABA-Cnr1$^{-/-}$ animals compared to their untreated WT siblings ($p < 0.05$). This genotype effect was not seen in the treated groups ($p > 0.05$). Figure 4.1.3.2A.

Analysis of 12 months old mice resulted also in a significant treatment effect ($F_{(1, 8)} = 20\ .97$, $p < 0.01$; Fig. 4.1.3.2B) and genotype effect ($F_{(1, 8)} = 23\ .56$, $p < 0.01$; Fig. 4.1.3.2B). Bonferroni's multiple comparison test now revealed that LPS treatment led to a significantly higher microglia density in both WT and GABA-Cnr1$^{-/-}$ groups ($p < 0.05$). Furthermore, microglia density was significantly higher in untreated and treated GABA-Cnr1$^{-/-}$ groups compared to WT of similar treatment ($p < 0.05$).

In the 18 months old mice groups, LPS treatment effect was highly significant ($F_{(1, 8)} = 57.26$, $p < 0.001$; Fig. 4.1.3.2C), and also the genotype effect was significant ($F_{(1, 8)} = 16.45$, $p < 0.01$; Fig. 4.1.3.2C). However, Bonferroni's multiple comparison test revealed that, while LPS treatment led to an exacerbated increase in of microglia density in the GABA-Cnr1$^{-/-}$ group ($p < 0.001$), this was only slightly significant in the WT group ($p < 0.05$). Consequently, the microglia density in treated GABA-Cnr1$^{-/-}$ animals was significantly higher than in their treated WT siblings ($p < 0.001$). There was no significant genotype-related change in the untreated groups ($p > 0.05$). Figure 4.1.3.2C.

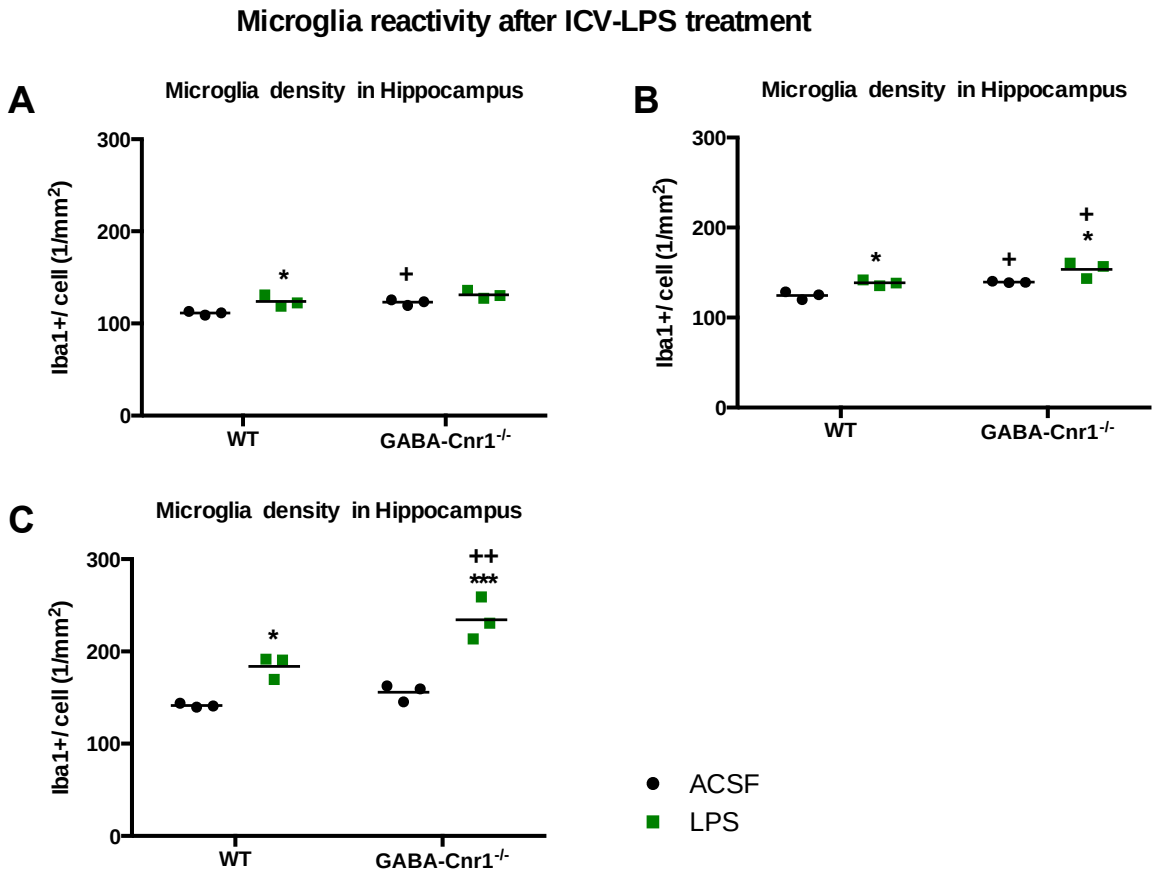


**Figure 4.1.3.2: LPS treatment associated increase in microglia density in the hippocampus was age-dependent in GABA-Cnr1$^{-/-}$ mice.** (A) ICV-LPS treatment led to a significantly increased microglia density in the treated 2 months old WT mice as compared to untreated WT mice (*$p < 0.05$). There was no significant change in microglia density when the 2 months old treated and untreated GABA-Cnr1$^{-/-}$ groups are compared ($p > 0.05$). The density of microglia in the hippocampus of untreated GABA-Cnr1$^{-/-}$ animals was higher than in the untreated WT siblings ($^{+}p < 0.05$). (B) In the 12 months old groups, LPS treatment led to similarly increased microglia density in the hippocampus of both treated WT and GABA-Cnr1$^{-/-}$ groups when compared to untreated WT and GABA-Cnr1$^{-/-}$groups, respectively (*$p < 0.05$). Treated and untreated GABA-Cnr1$^{-/-}$ animals showed significantly increased microglia density compared to WT littermates of similar treatment ($^{+}p < 0.05$). (C) Microglia density in the hippocampus of treated WT 18 months old mice was significantly increased compared to untreated WT (*$p < 0.05$). The treatment effect was exacerbated in GABA-Cnr1$^{-/-}$ animals (***$p < 0.001$). The density of microglia in treated GABA-Cnr1$^{-/-}$ animals was significantly increased compared to treated WT group ($^{++}p < 0.01$). Analysis was performed by two-way ANOVA followed by Bonferroni's post hoc test. Horizontal lines represent mean value; n = 3 per group.

Next, we sought to elucidate the role attributed to the morphological changes of microglia observed in the hippocampus. Hence, we analysed the cytokine expression levels in the different genotype and age groups, treated and untreated. Two-way ANOVA revealed that LPS treatment effect on IL-1β expression was significant in the 2 months old groups ($F_{(1, 39)} = 18$

.57, $p < 0.001$; Fig. 4.1.3.3A), while there was no significant genotype effect ($F_{(1, 39)} = 0.02796$, $p > 0.05$; Fig. 4.1.3.3A) and no age x genotype interaction ($F_{(1, 39)} = 0.0092$, $p > 0.05$; Fig. 4.1.3.3A). Bonferroni's post hoc test showed that LPS treatment led to a similarly increased IL-1β expression in the treated WT compared to untreated WT mice ($p < 0.01$) and in the treated GABA-Cnr1$^{-/-}$ compared to untreated GABA-Cnr1$^{-/-}$ mice ($p < 0.01$). IL-1β expression in the 12 months old mice was affected by LPS treatment $F_{(1, 36)} = 10.79$, $p < 0.01$; Fig. 4.1.3.3A). No genotype effect was attained ($F_{(1, 36)} = 1.106$, $p > 0.05$; Fig. 4.1.3.3A) and interaction between treatment and genotype was not significant ($F_{(1, 36)} = 1.272$, $p > 0.05$; Fig. 4.1.3.3A). Bonferroni's post hoc test, however, revealed a significant increase in IL-1β expression in the treated WT group compared to untreated WT group ($p < 0.01$) but not in the GABA-Cnr1$^{-/-}$ group. LPS treatment induced IL-1β expression was highly significant in 18 months old mice ($F_{(1, 27)} = 31.94$, $p < 0.0001$; Fig. 4.1.3.3A), but no significant genotype effect or interaction was obtained ($F_{(1, 27)} = 0.0084$, $p > 0.05$; Fig. 4.1.3.3A) and ($F_{(1, 27)} = 0.085$, $p > 0.05$; Fig. 4.1.3.3A). Bonferroni's multiple comparison test showed a significantly increased IL-1β expression in the treated WT group compared to untreated WT group ($p < 0.01$) and an even higher significant when treated GABA-Cnr1$^{-/-}$ group was compared to untreated GABA-Cnr1$^{-/-}$ group ($p < 0.001$).

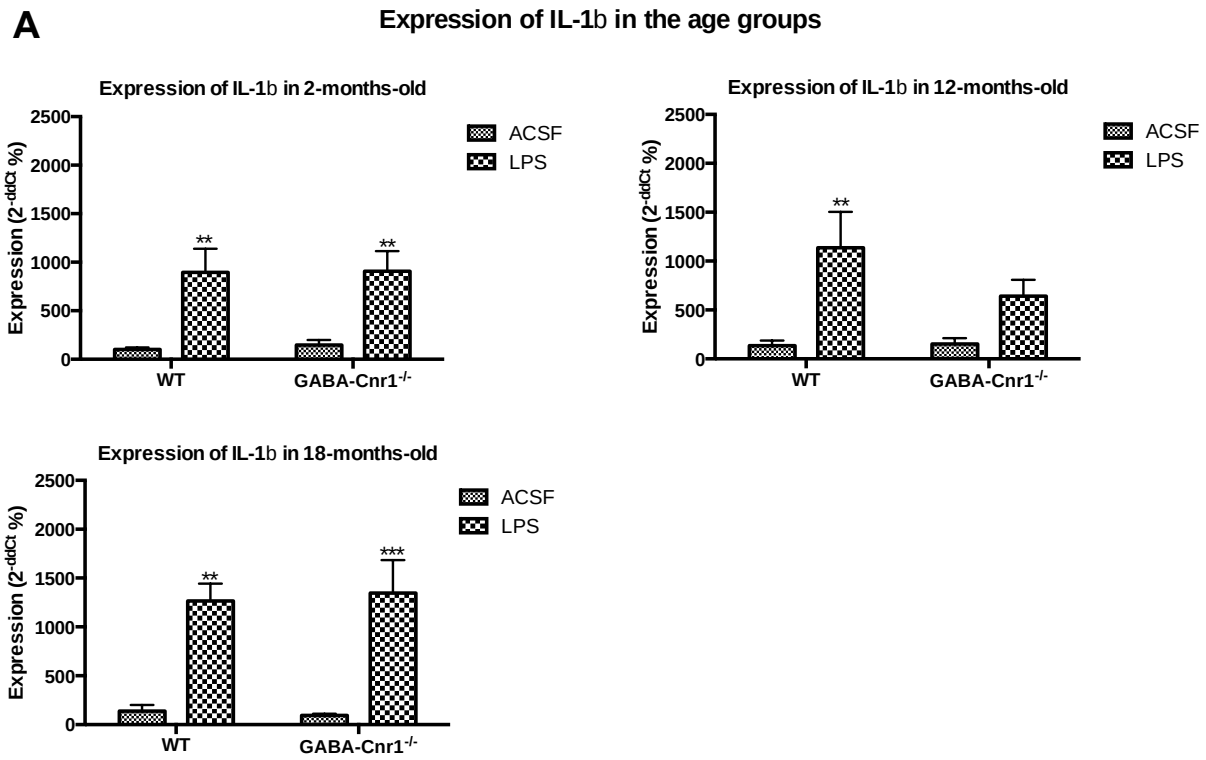


**Figure 4.1.3.3A: LPS treatment led to an increased IL-1β expression in each age group of the WT mice, whereas the effect of LPS was age-dependent in GABA-Cnr1$^{-/-}$.** IL-1β expression after ICV-LPS treatment was stably increased in WT mice across all age groups (**p < 0.01). The expression of IL-1β in GABA-Cnr1$^{-/-}$ mice was significantly increased in treated 2 months old group (**p < 0.01) and then not significant in 12-month-old mice (p > 0.05) to be highly significant in 18 months old mice group (***p < 0.001). Analysis was performed by two-way ANOVA followed by Bonferroni's post hoc test and values represent mean ±SEM; n = 7 - 11 per group.

For IL-6 expression in 2 months old mice groups, two-way ANOVA showed that there was no treatment effect ($F_{(1, 39)} = 3.571$, p > 0.05; Fig. 4.1.3.3B), no genotype effect ($F_{(1, 39)} = 2.722$, p > 0.05; Fig. 4.1.3.3B) and no interaction between treatment and genotype ($F_{(1, 39)} = 0.1701$, p > 0.05; Fig. 4.1.3.3B). Bonferroni's multiple comparison test showed no significant change in IL–6 expression in all groups, treated and untreated (p > 0.05). In the 12 months old mice groups, LPS led to a significant treatment effect ($F_{(1, 36)} = 7.391$, p < 0.05; Fig. 4.1.3.3B). No genotype effect ($F_{(1, 36)} = 1.647$, p > 0.05; Fig. 4.1.3.3B) or interaction effect ($F_{(1, 36)} = 2.64$, p > 0.05; Fig. 4.1.3.3B) was obtained. Bonferroni's multiple comparison test revealed that while IL–6 expression was significantly increased in treated WT mice group compared to untreated WT group (p < 0.01), treated GABA-Cnr1$^{-/-}$ group did not produce a significantly higher IL-6 as compared to untreated GABA-Cnr1$^{-/-}$ group (p > 0.05). Two-way ANOVA revealed a

significant LPS treatment effect in IL-6 expression of 18 months old mice groups ($F_{(1, 26)}$ = 5.627, $p < 0.05$; Fig. 4.1.3.3B). There was no genotype effect or interaction ($F_{(1, 29)}$ = 0.0855, $p > 0.05$; Fig. 4.1.3.3B) and ($F_{(1, 29)}$ = 0.0333, $p > 0.05$; Fig. 4.1.3.3B), respectively.

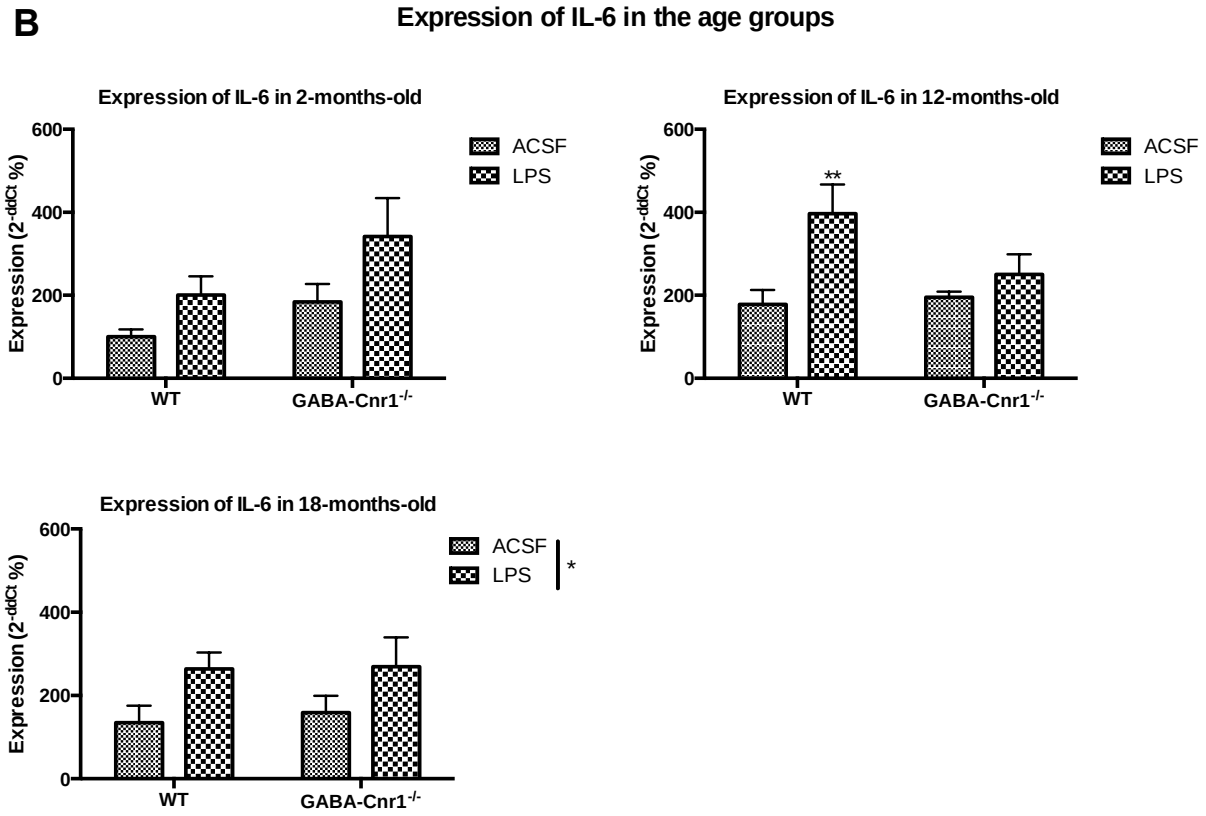


**Figure 4.1.3.3B: LPS treatment did not lead to a generally increased IL-6 expression.** IL-6 expression after ICV-LPS treatment was not significantly increased in GABA-Cnr1$^{-/-}$ mice regardless of age ($p > 0.05$). IL-6 expression was not significantly increased in 2 months old WT and GABA-Cnr1$^{-/-}$ mice both in the treated groups ($p > 0.05$). Treated 12 months old WT but not GABA-Cnr1$^{-/-}$ mice group produced significantly higher IL-6 compared to untreated (**$p < 0.01$). In 18 months old mice, IL-6 production in both treated groups was enhanced compared to untreated groups (*$p < 0.05$). Analysis was performed by two-way ANAOVA followed by Bonferroni's post hoc test and values represent mean ±SEM; n = 8 - 10 per group.

After two-way ANOVA analysis, it was obtained that ICV-LPS treatment of 2 months old mice resulted in a significant treatment effect on TNF-α expression ($F_{(1, 34)}$ = 14.66, $p < 0.001$; Fig. 4.1.3.3C), whereas, no significant genotype effect nor interaction was seen ($F_{(1, 34)}$ = 0.1645, $p > 0.05$; Fig. 4.1.3.3C) and ($F_{(1, 34)}$ = 0.4268, $p > 0.05$; Fig. 4.1.3.3C) for genotype and interaction respectively. Bonferroni's multiple comparison test further showed that LPS treatment led to a significant increase in TNF-α expression only in the WT groups ($p < 0.01$) but not in the

GABA-Cnr1$^{-/-}$ groups ($p > 0.05$). TNF-α expression in 12 month old mice was significantly increased after LPS treatment ($F_{(1, 36)} = 16.08$, $p < 0.001$; Fig. 4.1.3.3C). No significant genotype effect ($F_{(1, 36)} = 0.000$, $p > 0.05$; Fig. 4.1.3.3C) nor interaction ($F_{(1, 36)} = 0.0555$, $p > 0.05$; Fig. 4.1.3.3C) was seen. Bonferroni's multiple comparison test revealed that LPS treatment let to a significant increase in TNF-α expression in the WT groups ($p < 0.05$) and also in the GABA-Cnr1$^{-/-}$ groups ($p > 0.01$). Now, in the 18 months old mice, treatment effect after two-way ANOVA for TNF-α expression was obtained to be highly significant ($F_{(1, 28)} = 33.76$, $p < 0.0001$; Fig. 4.1.3.3C). No significance was obtained for genotype effect ($F_{(1, 28)} = 0.2121$, $p > 0.05$; Fig. 4.1.3.3C) and no significant interaction was observed ($F_{(1, 28)} = 0.0521$, $p > 0.05$; Fig. 4.1.3.3C). Bonferroni's post hoc test also showed a significant LPS treatment effect for both genotypes.

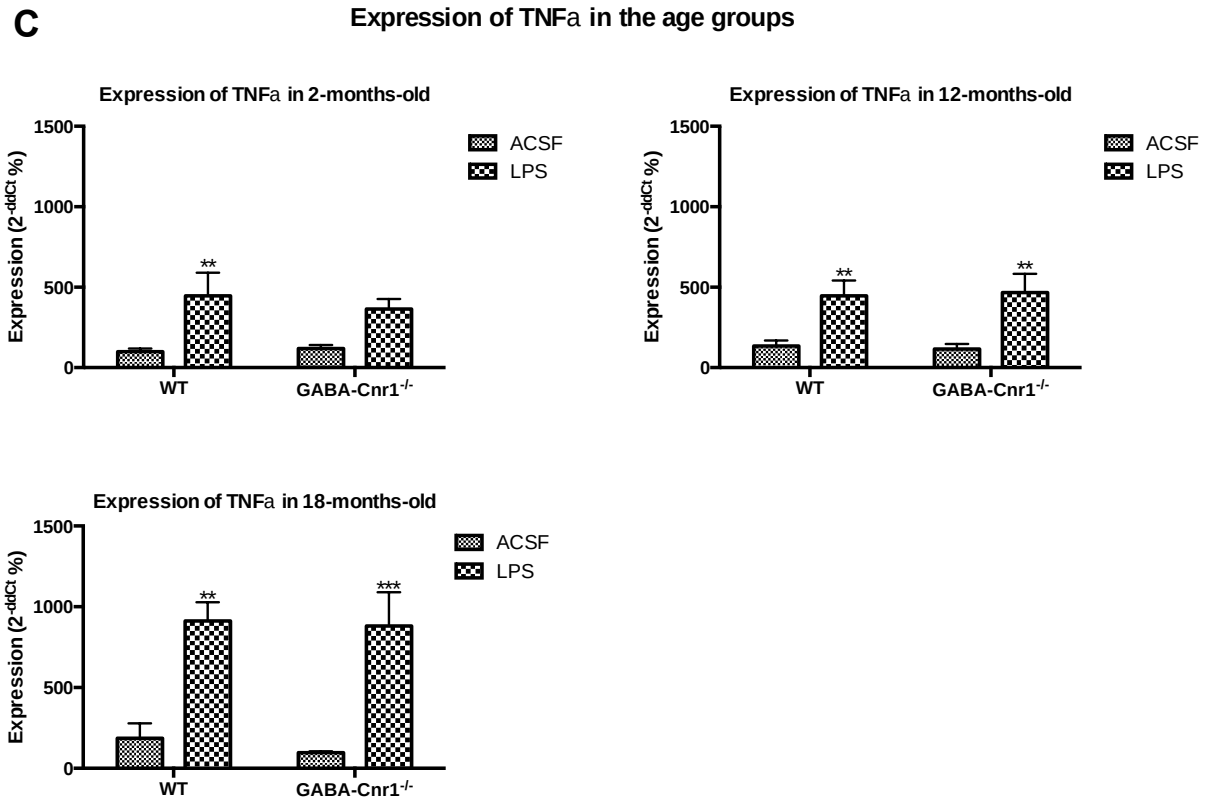


**Figure 4.1.3.3C: LPS treatment led to a relatively stable increased of TNF-α production in WT mice but increased in GABA-Cnr1$^{-/-}$ mice in an age- dependent manner.** TNF-α expression after ICV-LPS treatment was stably increased in WT mice across all age groups (**$p < 0.01$). The expression of TNF-α in GABA-Cnr1$^{-/-}$ mice did significantly increase in the treated groups in an age-dependent manner (**$p < 0.01$ and ***$p < 0.001$). Analysis was performed by two-way ANOVA followed by Bonferroni's post hoc test and values represent mean ±SEM; n = 7 - 10 per group.

### 4.1.4 Increased lipofuscin accumulation in isolated microglia of older GABA-Cnr1$^{-/-}$ mice

Increasing lipofuscin content of a cell has been reported to correlate with advancing age, as the clearance mechanism in cells is weakened, leading to accumulation of lysosomal degradation products with autofluorescence property at wavelengths around 400 to 560 nm. These accumulated complex of misfolded and oxidized proteins, as well as lipids, influence microglia reactivity, resulting in age-related microglia senescence as observed in progressing aging (Hartl et al., 2011; Mizushima et al., 2008). Here, we wanted to elucidate the role of GABAergic neuron-specific CB1 receptor knockout in microglial lipofuscin accumulation as an indication for early onset of aging.

In a set of FACS experiments, using microglia autofluorescence from 2 months old WT littermates as a base line, the number of cells containing lipofuscin was measured at 488 nm (FITC) in 2 and 12 months old GABA-Cnr1$^{-/-}$ mice as well as 12 months old WT littermates. ANOVA analysis revealed no significant genotype effect ($F_{(1, 23)} = 2.171$, $p > 0.05$; Fig. 4.1.4A). There was, however a significant age effect ($F_{(1, 23)} = 55.82$, $p < 0.0001$; Fig. 4.1.4A). No significant age-genotype interaction effect was observed ($F_{(1, 23)} = 0.9676$, $p > 0.05$; Fig. 4.1.4A). Lipofuscin autofluorescence measurement at 561 nm (PE) showed no significant genotype effect ($F_{(1, 23)} = 2.211$, $p > 0.05$; Fig. 4.1.4B). Again a significant age effect was reached ($F_{(1, 23)} = 109.3$, $p < 0.0001$; Fig. 4.1.4B) and no significant age-genotype interaction effect was observed ($F_{(1, 23)} = 0.1188$, $p > 0.05$; Fig. 4.1.4B). Lastly, lipofuscin accumulation measured at 496 nm (PerCP-Cy5.5) revealed a significant genotype effect ($F_{(1, 23)} = 10.93$, $p < 0.01$; Fig. 4.1.4C) and a significant age effect ($F_{(1, 23)} = 199.3$, $p < 0.0001$; Fig. 4.1.4C). Here, the age-genotype interaction effect was significant ($F_{(1, 23)} = 6.345$, $p < 0.05$; Fig. 4.1.4C). Bonferroni's post hoc test revealed that there was a significant genotype effect between the 12 months old groups ($p < 0.01$) but not in the 2 months old groups (p= ns).

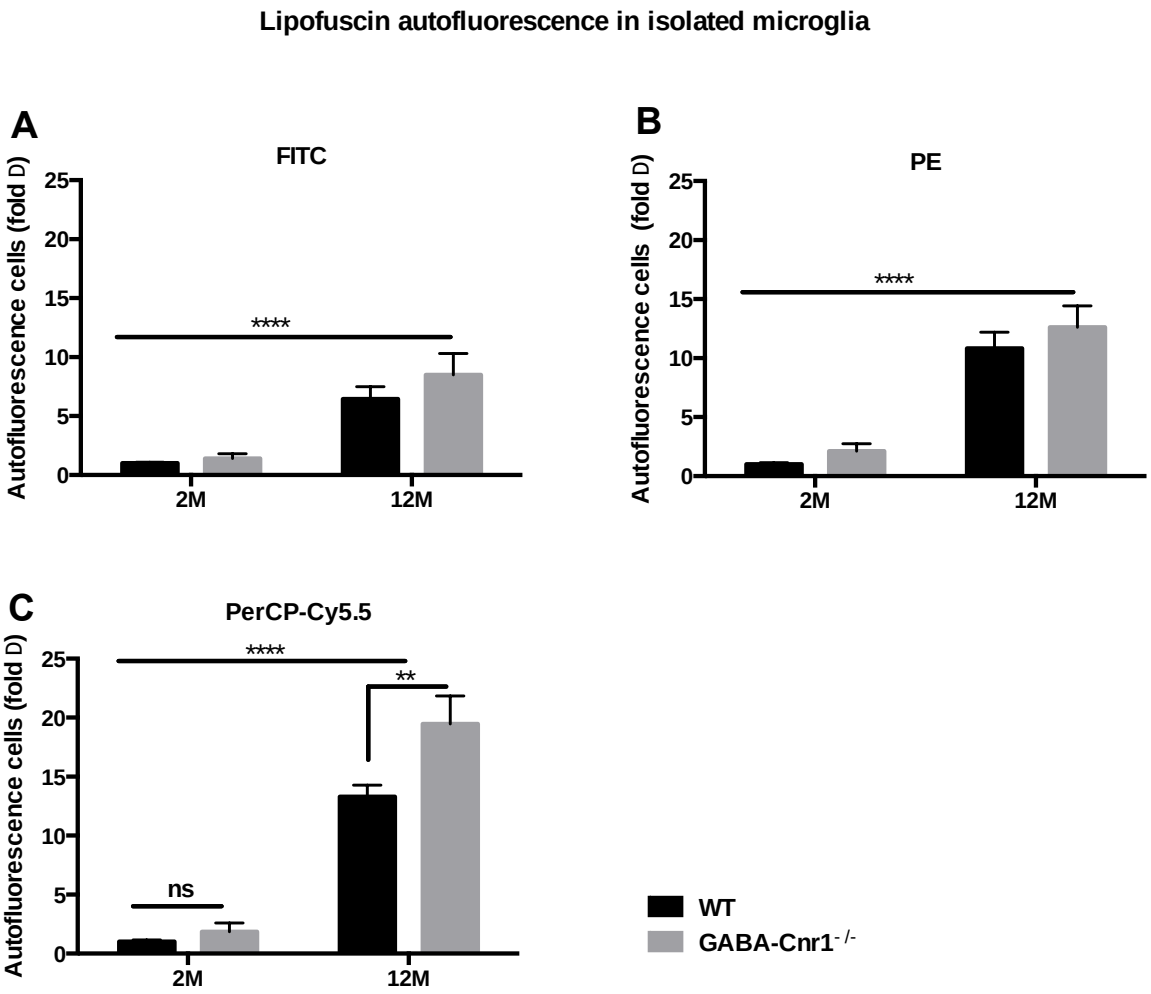


**Figure 4.1.4: Lipofuscin accumulation was exacerbated in 12 months old GABA-Cnr1$^{-/-}$ mice compared to age-matched WT littermates.** Lipofuscin accumulation was significantly increased in 12 months old mice groups at all three wavelengths measured (****$p < 0.0001$). A genotype attributed increase in lipofuscin accumulation was significant only in 12 months old mice measured at 496 nm (**$p < 0.01$). An age-genotype interaction effect was also significant for measurement at wavelength 496 nm. Analysis was performed by two-way ANOVA followed by Bonferroni's post hoc test and values represent mean ±SEM; n = 8 - 12 per group.

## 4.2 Neuron-microglial bidirectional regulation

### 4.2.1 Impaired neuroimmune regulators (NIReg) expression in hippocampus of microglia-specific Dagla$^{-/-}$ mice

After establishing that the deletion of a component of the endocannabinoid system, here CB1 receptor on GABAergic neurons, is enough to induce senescence-related characteristics in microglia, we asked whether this was due to deregulated interaction between neurons and

microglia, leading to reduced neuronal control. Hence, we investigated the expression of two major neuroimmune regulator proteins pairs (CD200/CD200R and $CX_3CL1/CX_3CR1$) in the hippocampus of microglia-specific $Dagla^{-/-}$ mice. In a previous experiment performed in our lab, we already found out that the expression of neuroimmune regulators are differentially changed during ageing. CD200 and CD200R expression was decreased in the hippocampus in WT 12 months old mice ($p < 0.001$) for CD200 and ($p < 0.05$) for CD200R compared to their age-matched GABA-$Cnr1^{-/-}$ siblings. Although CX3CL1 expression was unchanged in 12 months old WT mice during ageing, GABA-$Cnr1^{-/-}$ animals in similar age showed an increased expression ($p < 0.01$). CX3CR1 expression was not changed during ageing neither in the WT nor in the GABA-$Cnr1^{-/-}$ animals. (Bachelor project, Till Zimmer, 2013). We, thus, asked whether these changes were reproducible if another component of the endocannabinoid system, here Daglα on microglia, is altered.

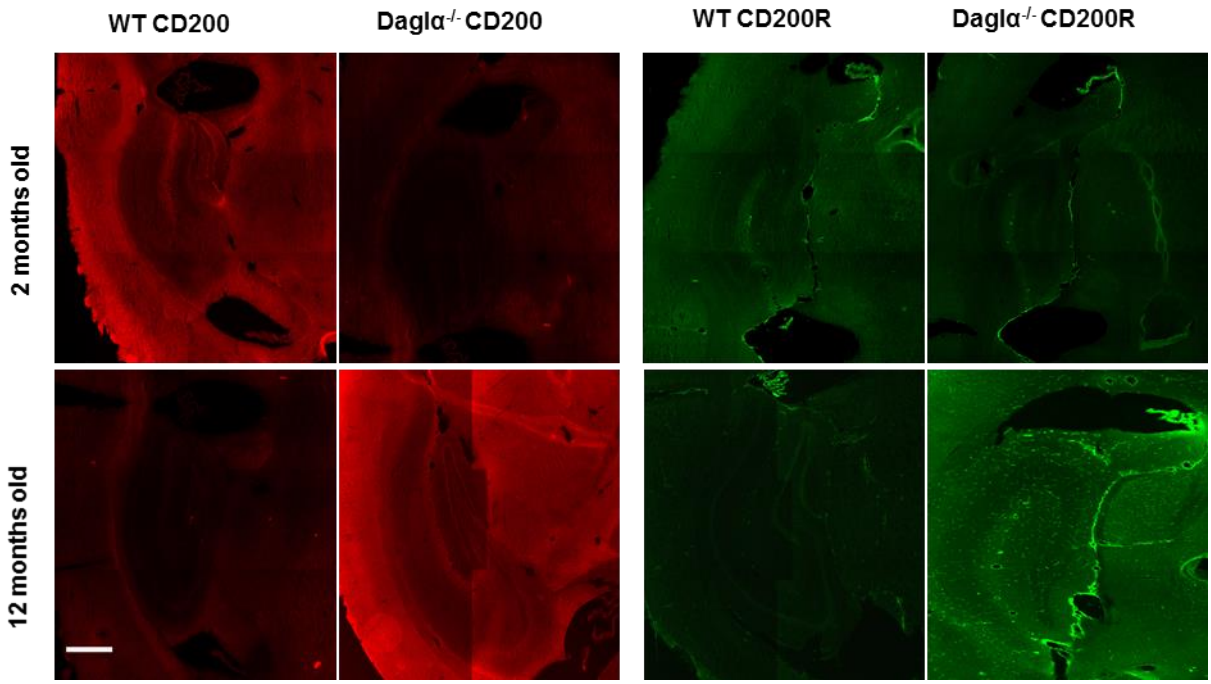


**4.2.1C: Representative micrographs of CD200 and CD200R immunostainings in the hippocampus of WT and Daglα$^{-/-}$ mice. The length of the scale bar is 500 µm**

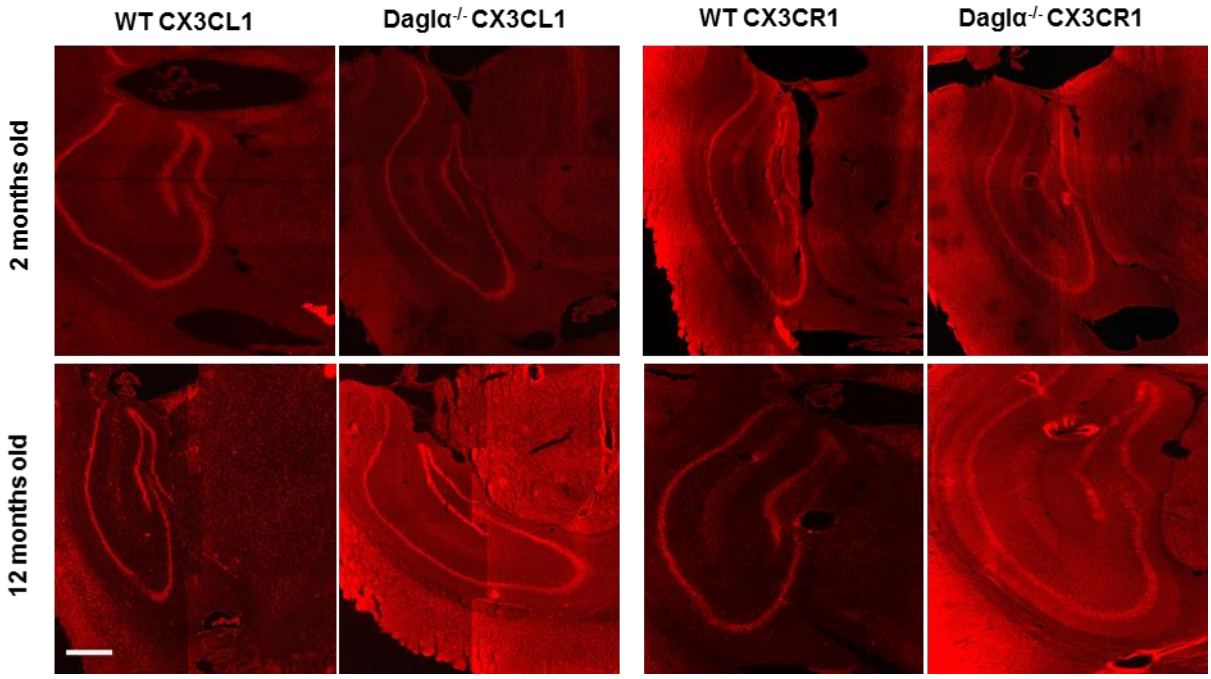


**4.2.1D: Representative micrographs of CX3CL1 and CX3CR1 immunostainings in the hippocampus of WT and Daglα$^{-/-}$ mice. The length of the scale bar is 500 µm**

Immunohistological experiments showed that protein levels of CD200 ligand produced by neurons and the corresponding CD200R on microglia are not significantly different in 2 months old WT and Dagla$^{-/-}$ mice ($U = 20$, $p > 0.05$; Fig. 4.2.1A) and ($U = 26$, $p > 0.05$; Fig. 4.2.1A) for CD200 and CD200R respectively. There was also no significant difference in fractalkine ($CX_3CL1$) and fractalkine receptor ($CX_3CR1$) in 2 months old WT and Dagla$^{-/-}$ mice ($U = 54$, $p > 0.05$; Fig. 4.2.1B) and ($U = 70$, $p > 0.05$; Fig. 4.2.1B) for $CX_3CL1$ and $CX_3CR1$ respectively. However, in 12 months old mice groups, CD200 and CD200R protein levels were significantly higher in Dagla$^{-/-}$ mice as compared to WT littermates ($U = 18$, $p < 0.05$; Fig. 4.2.1A) and ($U = 6$, $p < 0.0001$; Fig. 4.2.1A) for CD200 and CD200R respectively. Similarly, $CX_3CL1$ and $CX_3CR1$ protein levels were significantly higher in Dagla$^{-/-}$ mice as compared to WT littermates ($U = 12$, $p < 0.01$; Fig. 4.2.1B) and ($U = 23$, $p < 0.05$; Fig. 4.2.1B) for $CX_3CL1$ and $CX_3CR1$ respectively.

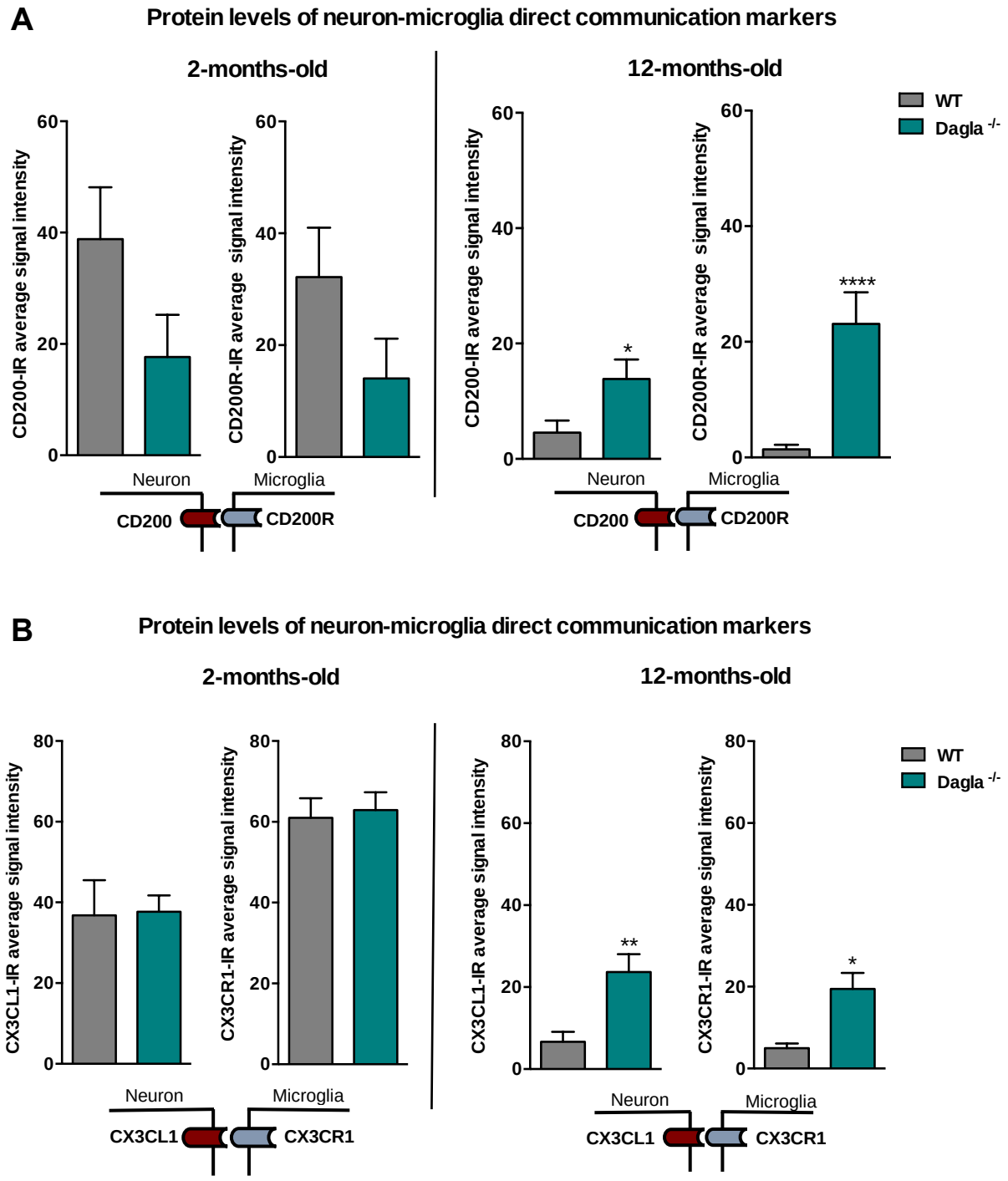


**Figure 4.2.1: 12 months old Dagla$^{-/-}$ mice showed a significant upregulation of neuron-microglia communication proteins as compared to WT littermates.**(A) CD200 and CD200R proteins were significantly increased in 12 months old Dagla$^{-/-}$ mice (Mann-Whitney U = 20 and 26, *p < 0.05, ****p < 0.0001,two tailed, values represent mean ± SEM, n = 9 - 12). (B) $CX_3CL1$ and $CX_3CR1$ proteins were significantly higher in 12 months old Dagla$^{-/-}$ mice as compared to WT (Mann-Whitney U = 12 and 23, **p < 0.01, *p < 0.05, two tailed, values represent mean ± SEM, n = 9 - 12).

### 4.2.2 Microglia-specific deletion of Dagla$^{-/-}$ led to upregulation of GABAergic receptors and pro-inflammatory cytokines in microglia of 12 months old mice

Following up on our findings that some neuron-microglia communication proteins are upregulated in 12 months old microglia-specific Dagla$^{-/-}$ mice, we asked what role GABA signalling play in this communication cascade and whether a pro-inflammatory or rather an anti-inflammatory microglia profile is encouraged. We investigated expression profiles of a selected set of GABA receptors as well as pro-inflammatory and anti-inflammatory cytokines in isolated microglia.

Expression levels of GABA B receptors and most important subunits of GABA A receptor (Gabbr1, Gabbr2, Gabra1, Gabrb2, Gabrg2 and Gabrd) were not significantly changed in both 2 months old WT and microglia Dagla$^{-/-}$ mice ($p > 0.05$). Expression of pro-inflammatory cytokines (IL-1β) and anti-inflammatory cytokine (IL-10 and Fizz) were not significantly altered ($p > 0.05$). Figure 4.2.2A.

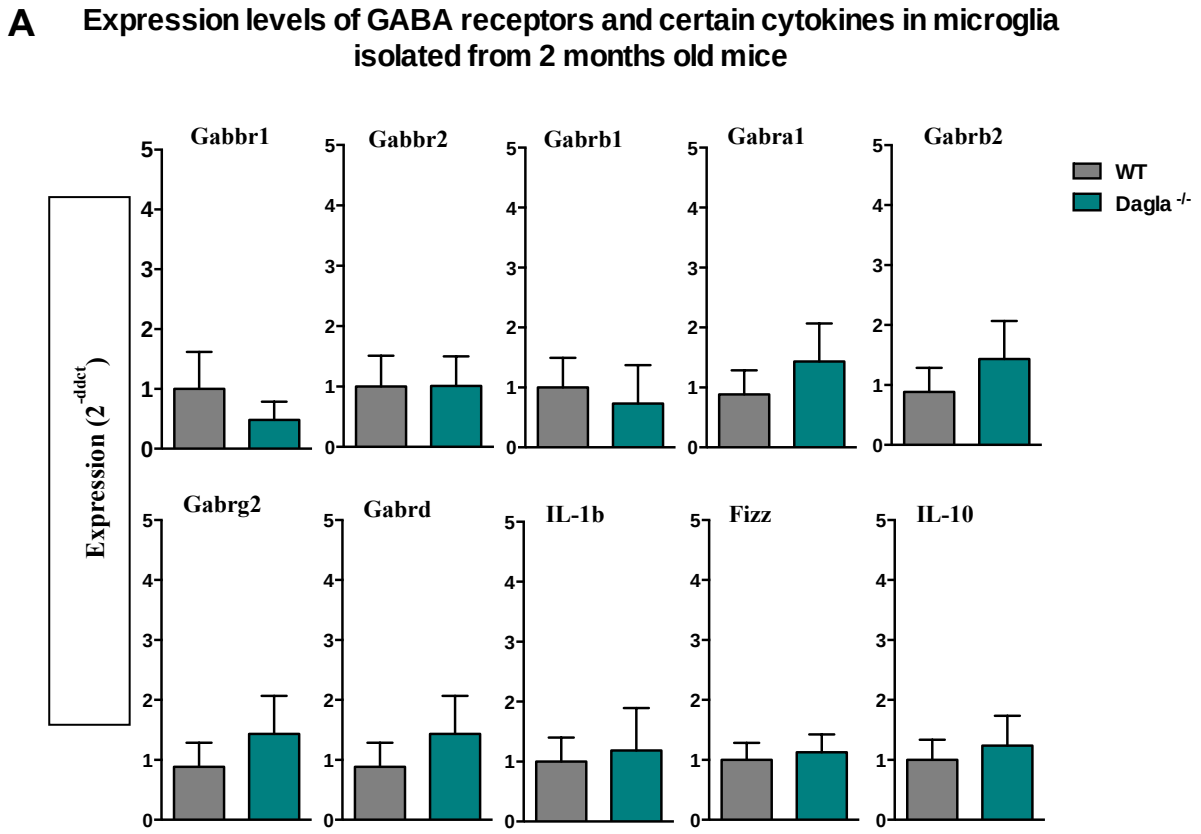


**Figure 4.2.2A: GABA receptors expression and cytokine levels were not altered in 2 months old microglia specific Dagla$^{-/-}$ mice.**

In 12 months old microglia specific Dagla$^{-/-}$ mice, expression of Gabrb2 ($t = 2.95$, $p < 0.05$; Fig. 4.2.2B), Gabrg2 ($t = 2.94$, $p < 0.05$; Fig. 4.2.2B) and Gabrd ($t = 2.94$, $p < 0.05$; Fig. 4.2.2B) were significantly increased as compared to WT littermates. Expression levels of cytokine proteins were also significantly increased ($t = 3.06$, $p < 0.05$; Fig. 4.2.2B) and ($t = 2.75$, $p < 0.05$; Fig. 4.2.2B) for IL-1β and Fizz respectively.

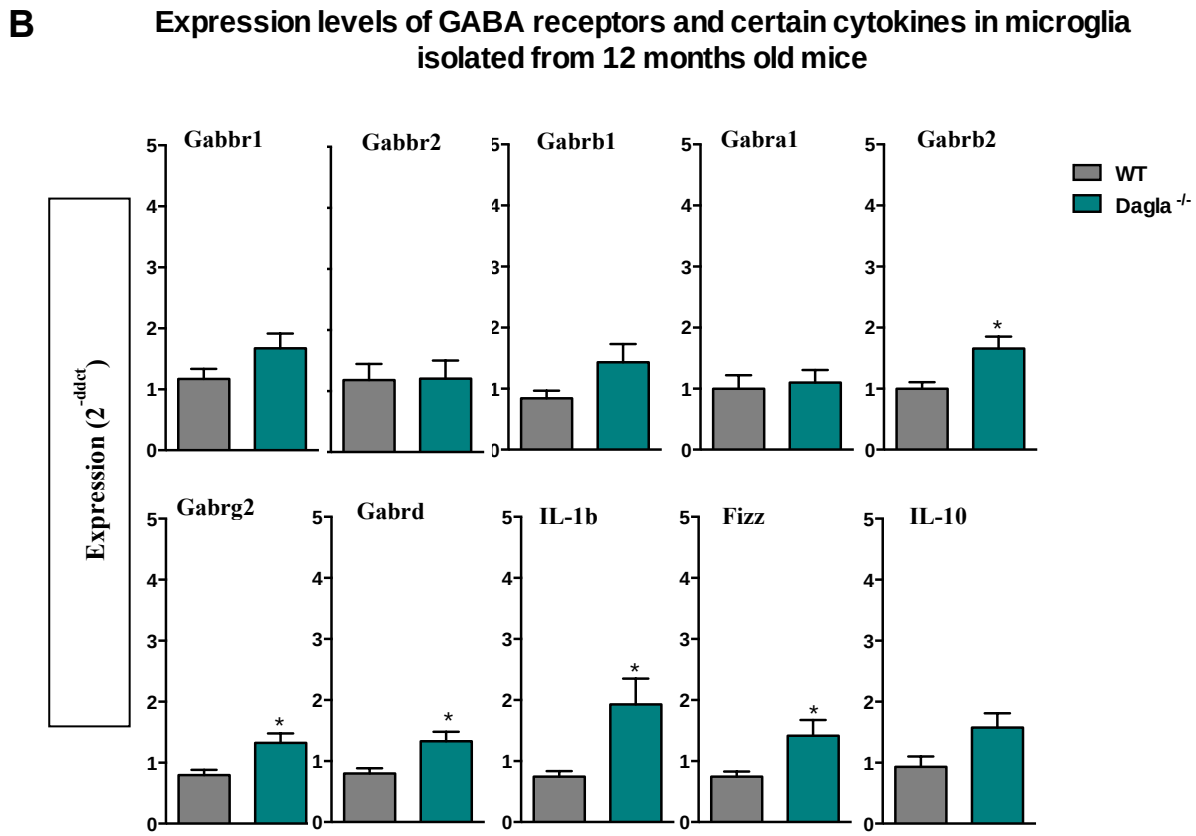


**Figure 4.2.2B: Some GABA receptors expression profile and cytokines levels were significantly increased in 12 months old microglia specific Dagla$^{-/-}$ mice (*p < 0.05).**

## 4.3 Cognitive ageing and microglia reactivity in microglia-specific Dagla$^{-/-}$ mice

As previously stated, a deletion of CB1, resulting in a disturbance of the endocannabinoid system, leads to early onset of aging and increased microglia reactivity. Here, we sought to understand whether the deletion of Dagla on microglia cells alone is sufficient to induce enhanced neuroinflammation and age-related cognitive and social deficits as observed in the

CB1 knockout mouse model. A microglia specific Dagla$^{-/-}$ mouse line and their wild-type siblings were used in these experiments.

### 4.3.1 Effects of a decreased microglial 2-AG production on the onset of recognition deficits

**Sociability**

In a longitudinal partner recognition test experiment, reduced 2-AG production in microglia-specific Dagla$^{-/-}$male mice did not affect the preference for a partner mouse over an object as both knockout mice and their wild-type siblings showed a similar strong significant preference for partner mice (U= 13, $p < 0.001$; Fig. 4.3.1.1A,B), which remained similar when the mice were 12 months old (U = 14, $p < 0.001$; Fig. 4.3.1.1C,D).The total distance covered by the mice exploring their surrounding was similar regardless of genotype and age(U = 96, $p > 0.05$; Fig. 4.3.1.1E,F).

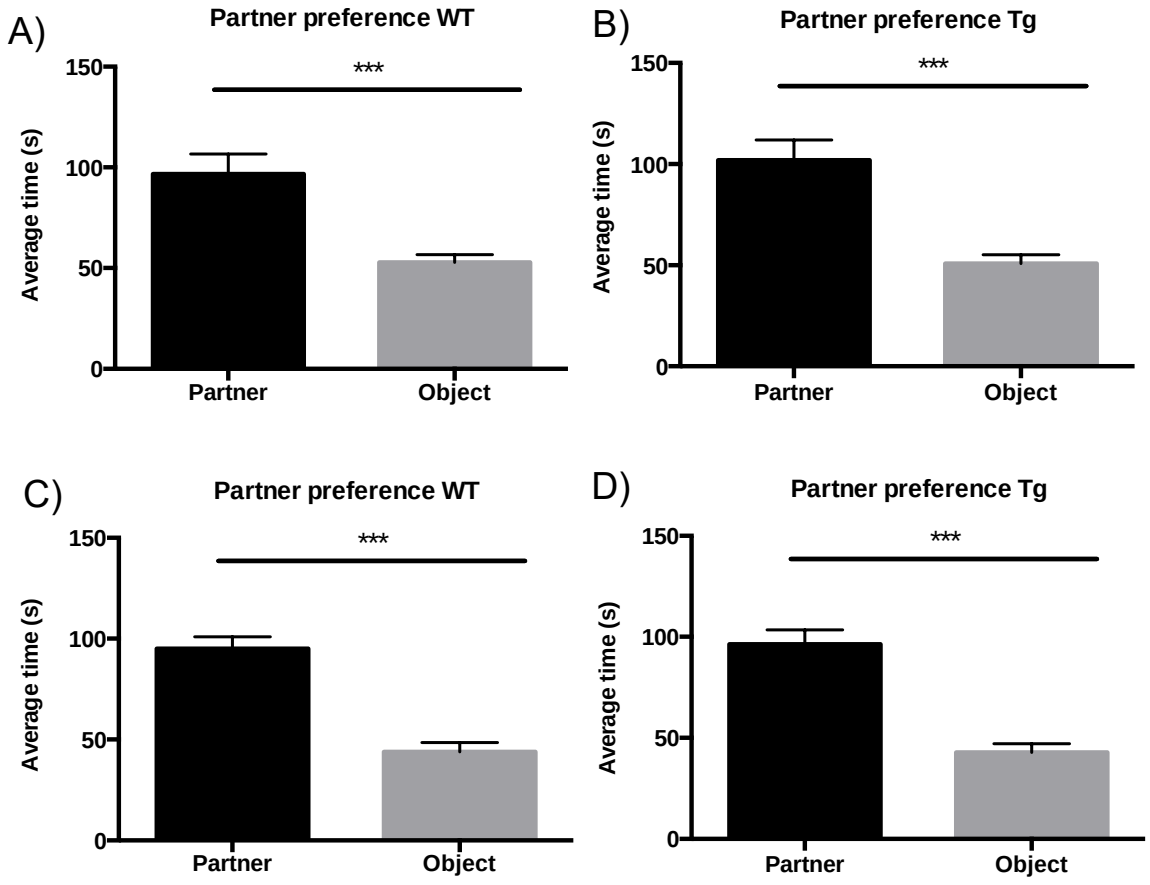

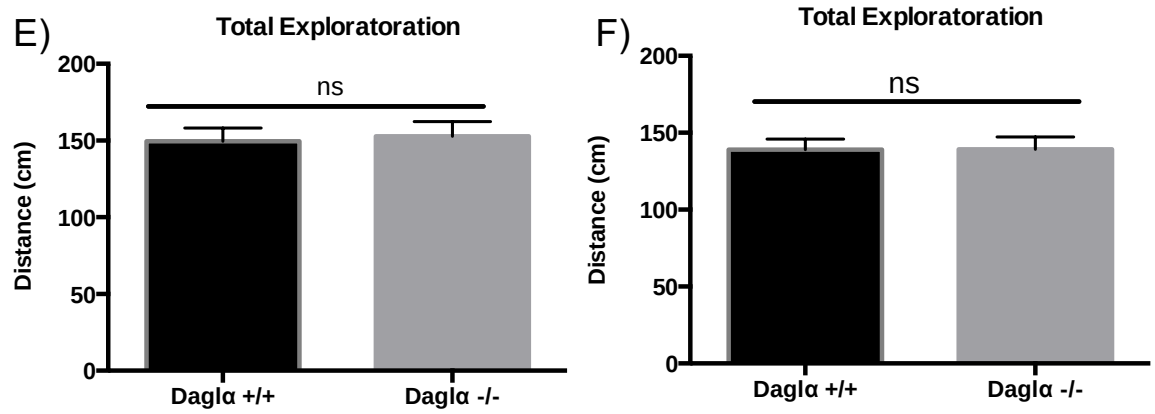


**Figure 4.3.1.1: Dagla$^{-/-}$ mice exhibited a normal social character.** (A,B) Both young 2 months old Dagla$^{-/-}$ and WT sibling control mice showed a strong preference for partner mice. The average time spent investigating the partner as opposed to an object was similar for both genotypes (Mann-Whitney U = 48, ***p < 0.001,two-tailed, values represent mean ± SEM, n = 13 – 17). (C,D) Mice when 12 months old showed a similar significance as observed in the young age group (Mann-Whitney U = 14, $^{***}$p < 0.001,two-tailed, values represent mean ± SEM, n = 12 – 17). (E,F) The total distance covered during exploration was similar for both genotypes and age groups with no significance (Mann-Whitney U = 96, p > 0.05, values represent mean ± SEM, n = 13 - 17). ns stands for not significant.

## Cognitive ability

The ability to recognise a previous partner was tested in both young and old mice. In 2 months old knockout mice, the recognition ability was strongly significant (U = 25, p < 0.001; Fig. 4.3.1.2B) but not in the wild-type littermates (U = 56, p > 0.05; Fig. 4.3.1.2A). When mice were 12 months old, the recognition ability was significant in the WT mice (U = 37, p < 0.05; Fig. 4.3.1.2C), while significance remained but less pronounced than in young ones in the knockout mice (U = 64, p < 0.01; Fig. 4.3.1.2D). Novelty preference was significantly higher in young microglia-specific Dagla$^{-/-}$ mice than in the age-matched wild-type littermate (U = 57, p < 0.05; Fig. 4.3.1.2E). There was no significance in novelty preference between mice of both genotypes when 12 months old (U = 94, p > 0.05; Fig. 4.3.1.2F)

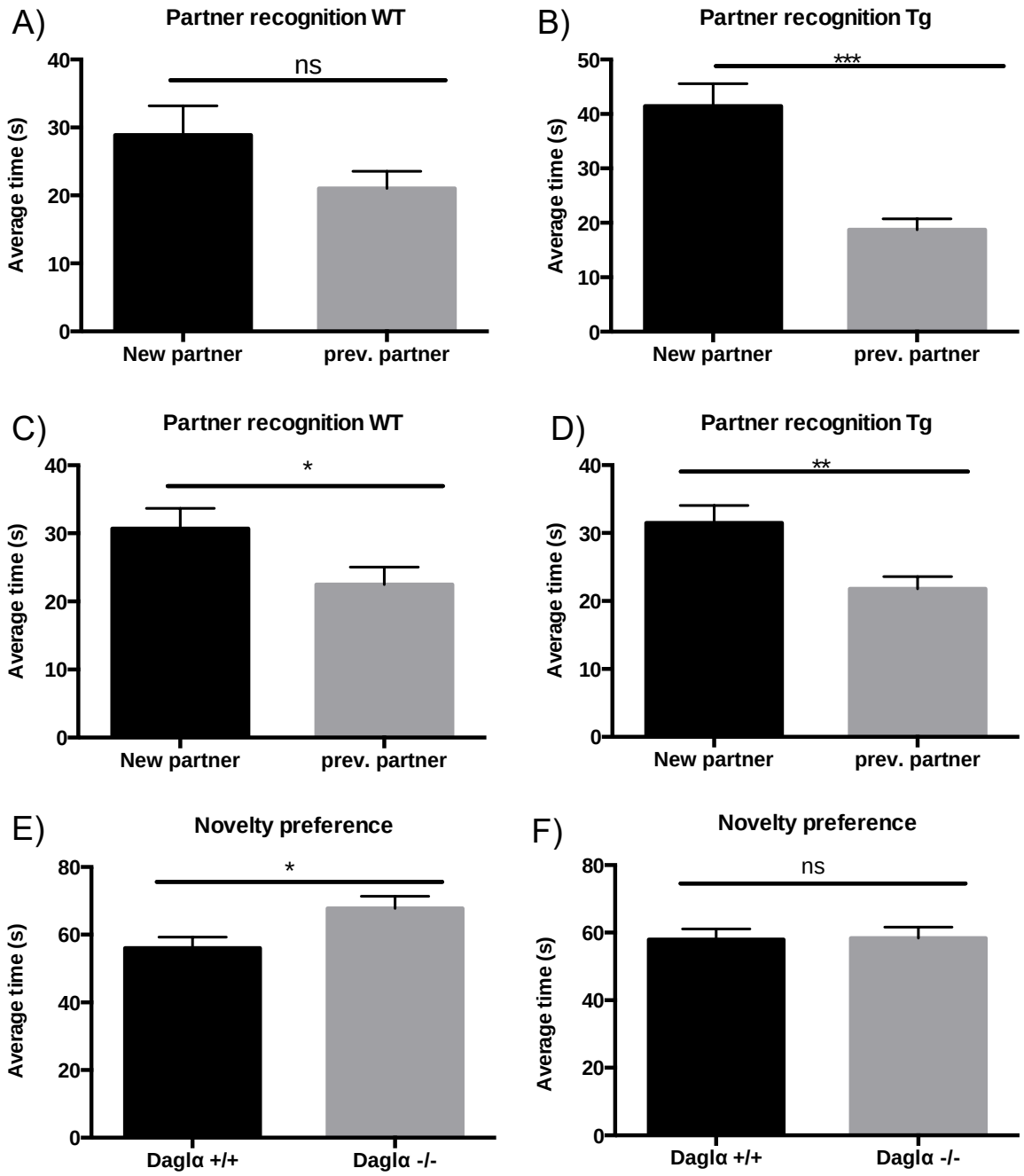


**Figure 4.3.1.2: A slightly reduced cognitive ability in 12 months old Dagla$^{-/-}$ mice.** (A)Young wild-type control mice did not show significant recognition ability (Mann-Whitney U = 56, $p > 0.05$, two tailed, values represent mean ± SEM, n = 13), (B) while there was a significant recognition ability in Dagla$^{-/-}$ mice (Mann-Whitney U = 25, $^{***}p < 0.001$,two tailed, values represent mean ± SEM, n = 17). (C) At age 12 month old, recognition ability was significant in WT mice (Mann-Whitney U = 37, $^{*}p < 0.05$, two tailed, values represent mean ± SEM, n = 12). 12 months old knockout mice also showed a significant but reduced recognition ability (Mann-Whitney U = 64, $^{**}p < 0.01$,two tailed, values represent mean ± SEM, n = 17). (E) In young 2 months old mice, there was a significant difference in novelty preference (Mann-Whitney U = 57, $^{*}p < 0.05$, two tailed, values represent mean ± SEM, n = 13 - 17). (F) There was no difference in novelty preference in 12 months old mice (Mann-Whitney U = 94, $p > 0.05$, two tailed, values represent mean ± SEM, n = 12 - 17). ns stands for not significant.

Next, we tested the effect of successive increase of intertrial duration on the cognitive ability of both WT and knockout 12-months-old mice. Test with 1 h intertrial interval revealed a similar significance in recognition ability for both wild-type controls and Dagla$^{-/-}$ mice (U = 37, p < 0.05; Fig. 4.3.1.3A,B). (C) After a 2 hours intertrial interval, no significance was recorded in Dagla$^{-/-}$ mice (U = 83, p > 0.05; Fig.4.3.1.3C), while the Wild-type littermates retained their significant recognition ability (U = 50, p < 0.05; Fig. 4.3.1.3D). Novelty preference decreased in Dagla$^{-/-}$ mice with increasing intertrial intervals (Fig. 4.3.1.4)

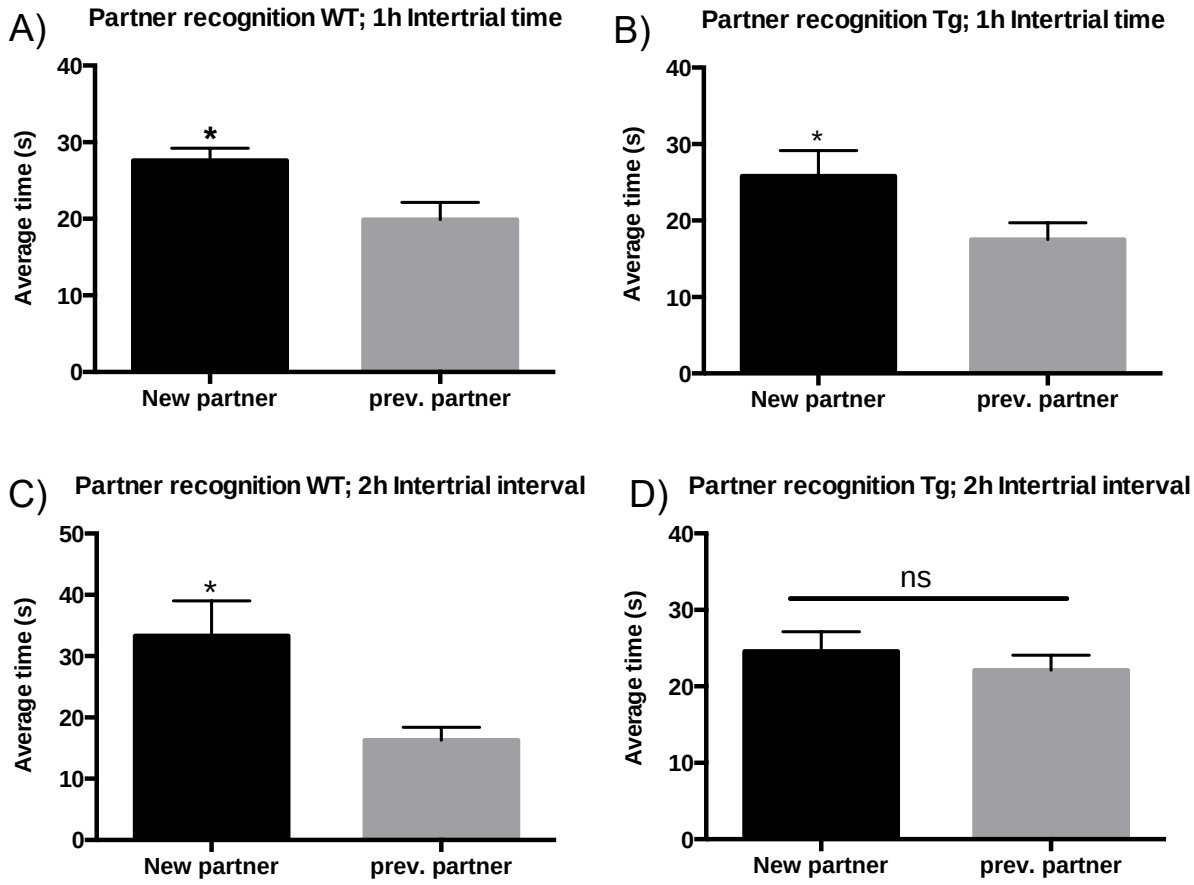


**Figure 4.3.1.3:** (A,B) After an hour intertrial interval, 12-months-old wild-type control mice and Dagla$^{-/-}$ mice showed a significant ability to recognise the previous mice (Mann-Whitney U = 37, *p < 0.05,two tailed, values represent mean ± SEM, n = 13 - 17). (C) At 2 hours intertrial interval, the wild-type control mice still recognised the previous mice (Mann-Whitney U = 50, *p < 0.05,two tailed, values represent mean ± SEM, n = 13), (D) while Dagla$^{-/-}$ mice no longer show significant recognition of previous mice(Mann-Whitney U = 83, p > 0.05,two tailed, values represent mean ± SEM, n = 14). ns stands for not significant.

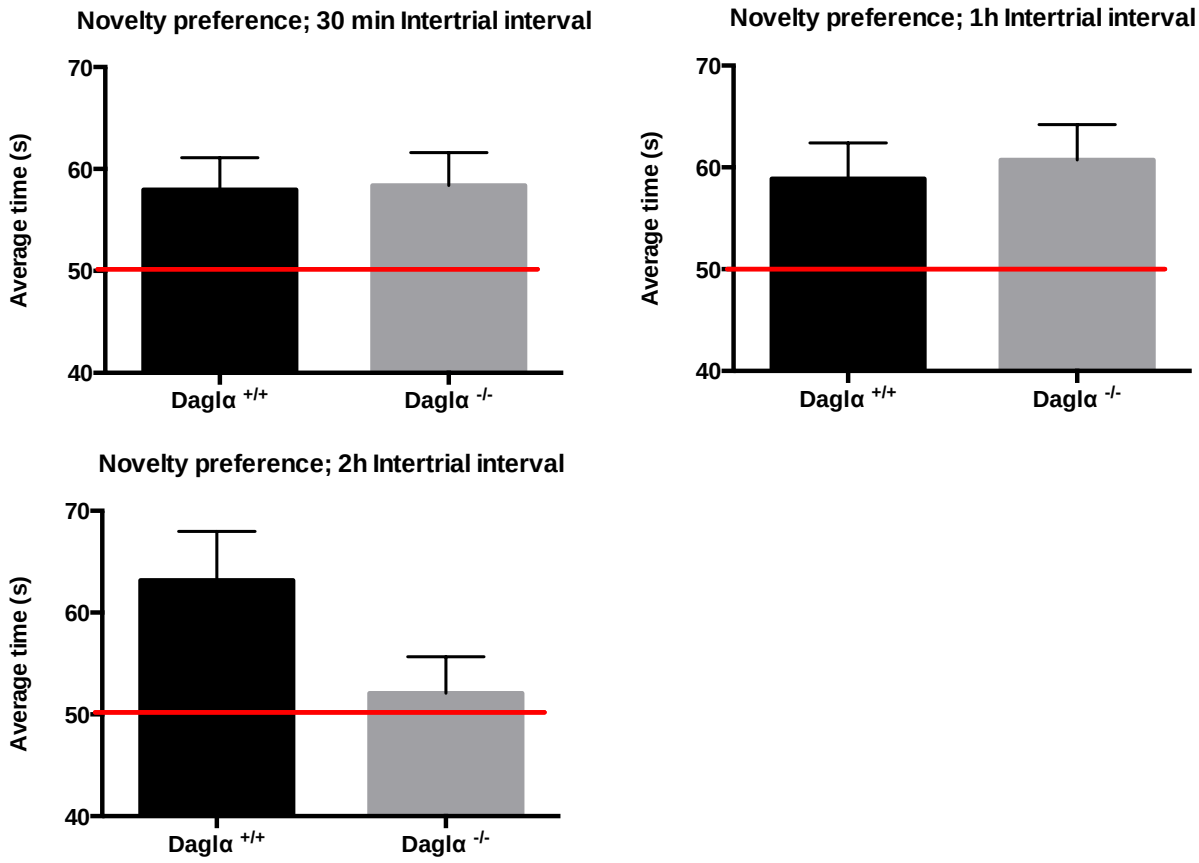


**Figure 4.3.1.4: Novelty preference decreases in Dagla$^{-/-}$ mice with successive increase in intertrial time.**

### 4.3.2 Effects of a decreased microglial 2-AG production in age-related spatial learning and memory deficits

Next, we tested the spatial learning ability and memory strength of female microglia-specific Dagla$^{-/-}$ mice alongside their wild-type siblings in the Morris water maze test. During the acquisition phase of MWM test (Fig. 4.3.2.-1A, 2A and 3A), we investigated, on the one hand, the spatial learning and memory consolidation abilities of the mice. On the other hand, we assessed in the reversal phase (Fig. 4.3.2.-1B, 2B and 3B) the learning flexibility of the mice. Meanwhile, the memory strength was tested in the probe trial as represented in figure 4.3.2.4.

When learning ability and memory consolidation were tested in the acquisition phase, the escape latency was similar for the 2 months old mice irrespective of genotype ($F_{(1.22)} = 0.02544$, $p > 0.05$; Fig. 4.3.2.1A). There was also no significant genotype difference observed in the 12

months old group ($F_{(1.17)} = 0.1889$, $p > 0.05$; Fig. 4.3.2.1B). In both age groups, regardless of genotype, the time needed to find the platform significantly decreased with progressing training days ($F_{(5.110)} = 21.92$, $p < 0.001$; Fig. 4.3.2.1A) and ($F_{(5.85)} = 11.77$, $p < 0.001$; Fig. 4.3.2.1A) for 2 and 12 months old groups, respectively. Escape latency was similarly not effected by genotype during the reversal phase, where memory flexibility is tested. For the young mice ($F_{(1.32)} = 0.01$, $p > 0.05$; Fig. 4.3.2.1B) and old mice ($F_{(1.21)} = 0.5215$, $p > 0.05$; Fig. 4.3.2.1B). The mice also find the platform in the reversal phase quicker with increasing training days in the 2 month old ($F_{(2.42)} = 10.22$, $p < 0.001$; Fig. 4.3.2.1B) and in 12 month old mice ($F_{(2.64)} = 9.002$, $p < 0.001$; Fig. 4.3.2.1B)

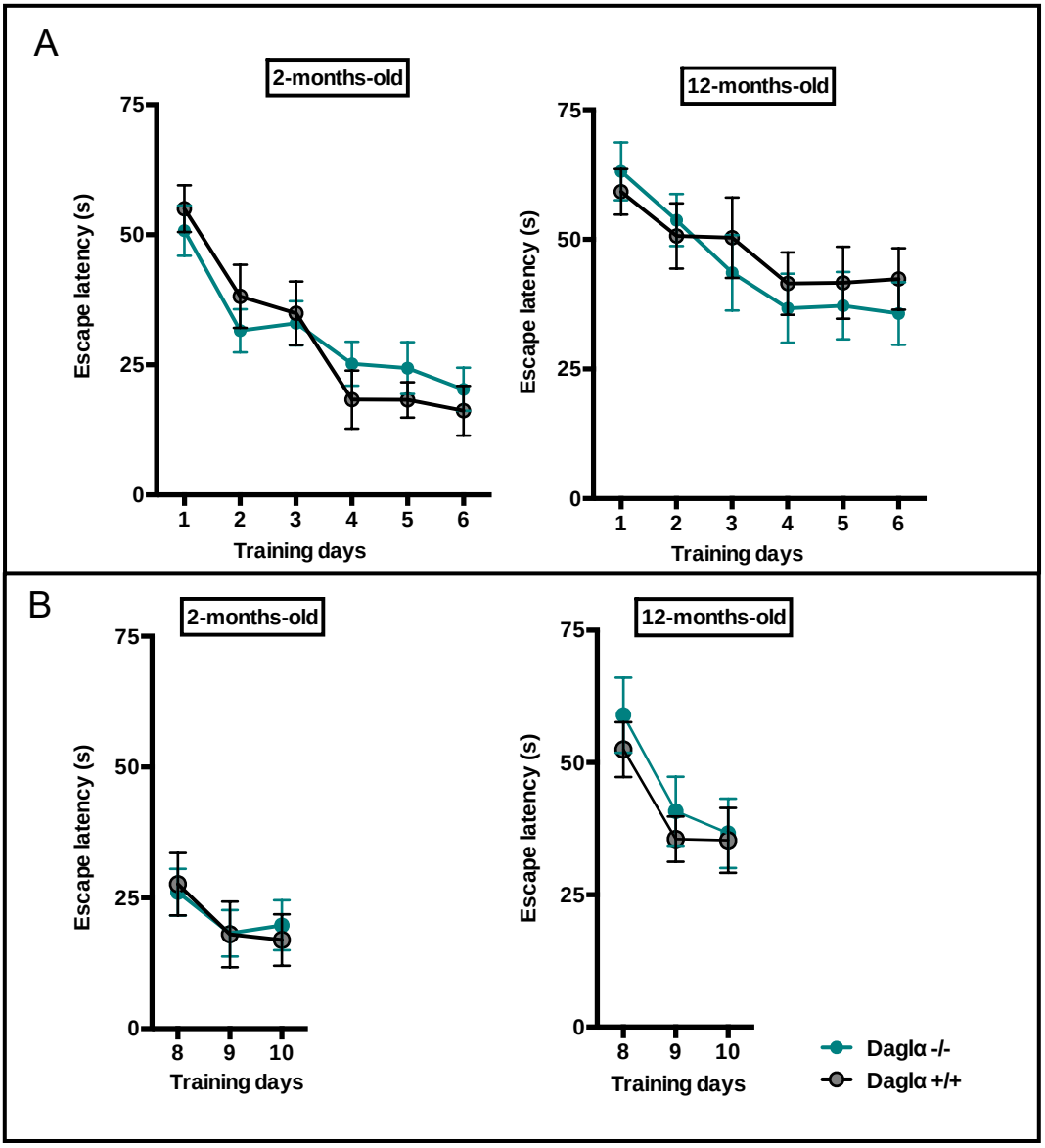


**Figure 4.3.2.1: Reduced microglia 2-AG production did not affect spatial learning and memory ability of microglia-specific Dagla$^{-/-}$ mice.** Escape latencies during the acquisition and reversal trials are depicted in A and B, respectively. There was no significant genotype effect in any of the age groups $p > 0.05$. (two-way ANOVA followed by Bonferroni's t-test; n=12 per group).

During the learning flexibility and memory consolidation phase, the distance covered by the mice was also evaluated. The path length was similar for both genotypes in the 2 months old as well as in the 12 months old mice. ($F_{(1.22)} = 1.491$, $p > 0.05$; Fig. 4.3.2.2A) and ($F_{(1.21)} = 0.01$, $p > 0.05$; Fig. 4.3.2.2A) for 2 and 12 months old groups, respectively. The path length in the reversal phase was also not different regardless of genotype and age group. $F_{(1.32)} = 0.01$, p

>0.05; Fig. 4.3.2.2B) and ($F_{(1.21)}$ = 0.2905, p > 0.05; Fig. 4.3.2.2B) for 2 and 12 months old groups, respectively.

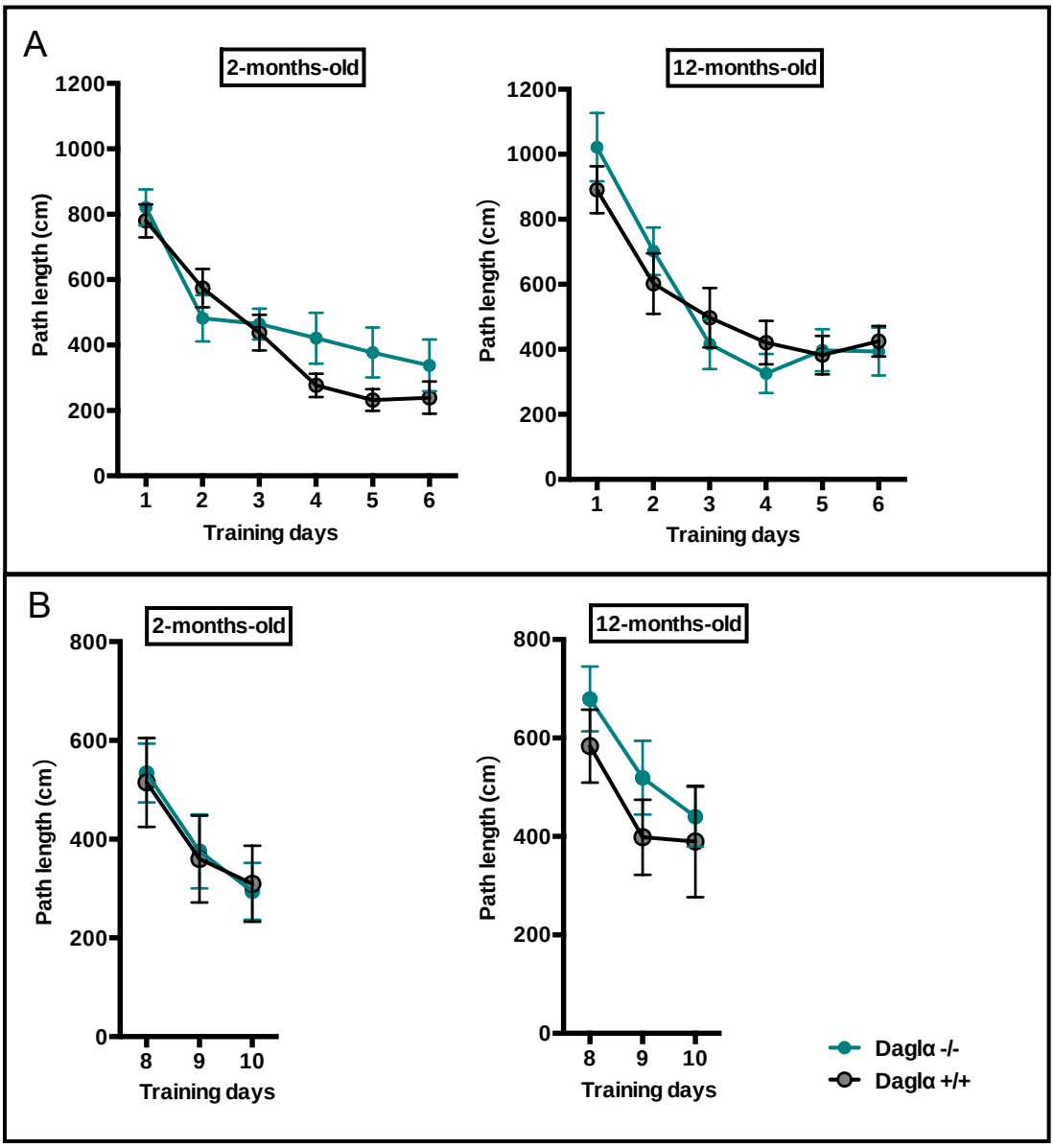


**Figure 4.3.2.2: Reduced microglia 2-AG production did not affect spatial learning ability of microglia-specific Dagla$^{-/-}$ mice.** Path length during the acquisition and reversal phase are depicted in A and B, respectively. There was no significant genotype effect in any of the age groups p > 0.05. (two-way ANOVA followed by Bonferroni's t-test; n=12 per group).

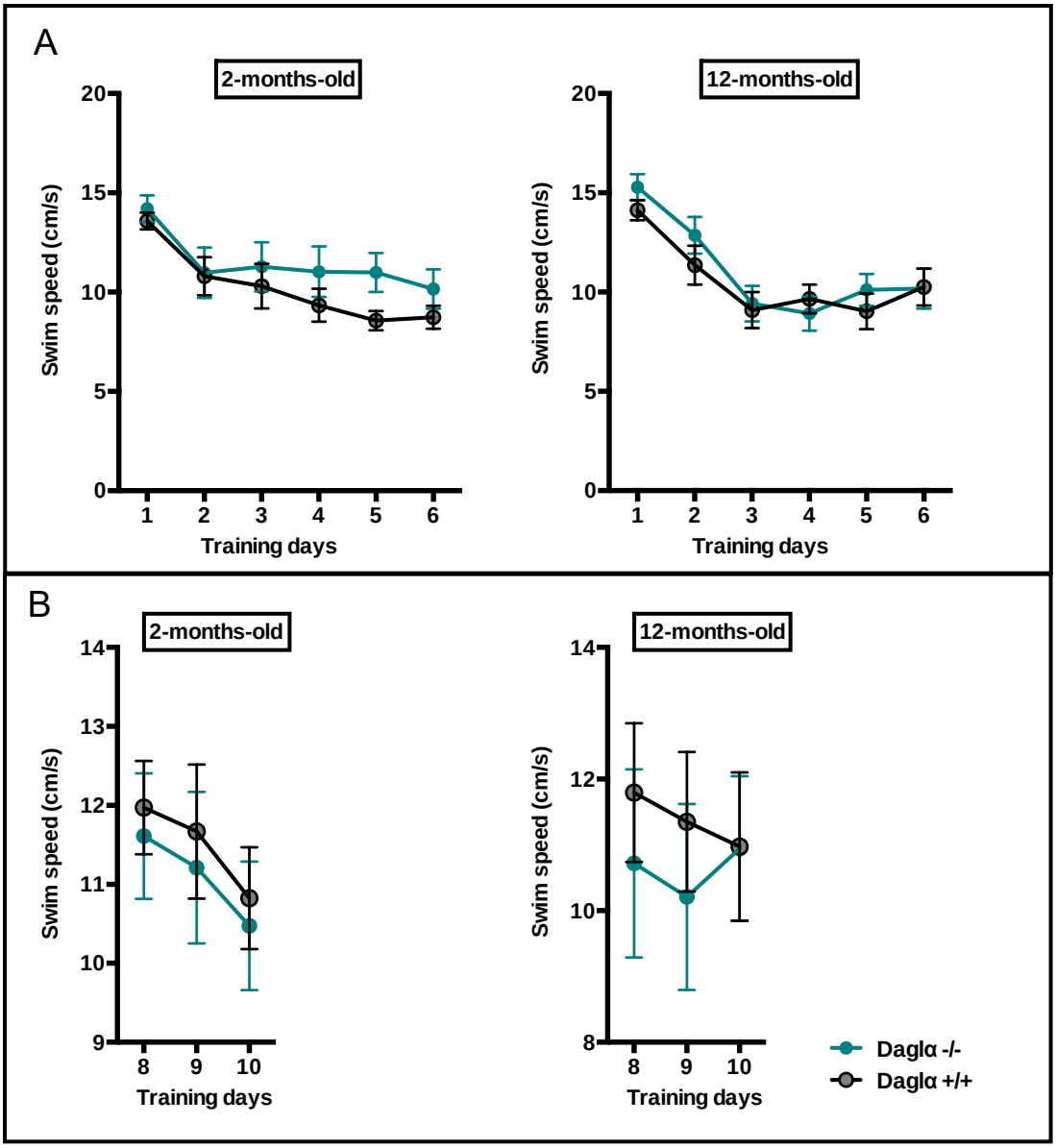


**Figure 4.3.2.3: Reduced microglia 2-AG production did not affect the swim speed of microglia-specific Dagla$^{-/-}$ mice.** The swim speed during the acquisition and reversal phase are presented in A and B, respectively. There was no significant genotype effect in any of the age groups $p > 0.05$. (two-way ANOVA followed by Bonferroni's t-test; n=12 per group).

The probe trial, which is a measure of memory strength, led to similar results for both genotypes, as mice demonstrated a significant memory strength when they were 2 months old, by spending more time in the quadrant where the platform was ($F_{(1.26)} = 9.321$, $p > 0.01$; Fig. 4.3.2.4)

The significantly high memory strength displayed during the probe trial at age 2 months was lost when the mice became 12 months old ($F_{(1.37)} = 0.01$, $p > 0.05$; Fig. 4.3.2.4).

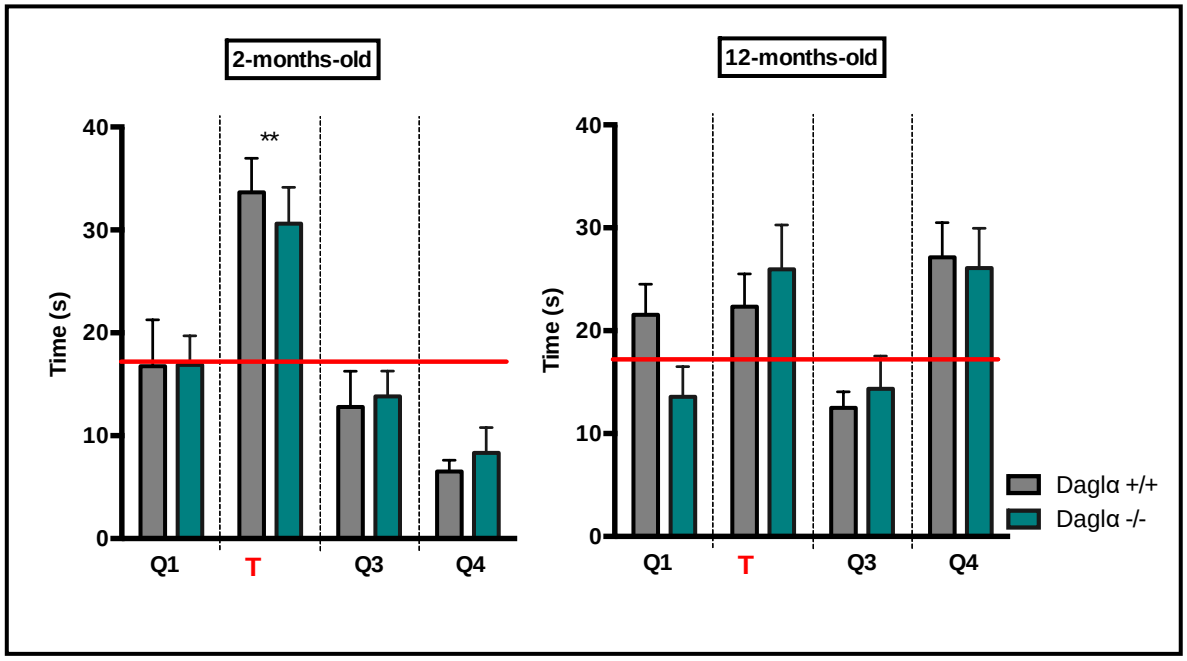


**Figure 4.3.2.4: Both microglia-specific Dagla$^{-/-}$ mice and their wild-type littermates demonstrated an age-dependent loss of memory strength.** Significance in memory strength of 2 months old mice in both genotypes.$^{**}$p< 0.01. (two-way ANOVA followed by Bonferroni's t-test; n=12 per group). Reduced memory strength when mice were 12 months old. P > 0.05. (two-way ANOVA followed by Bonferroni's t-test; n=12 per group).

### 4.3.3 Microglia reactivity in Dagla$^{-/-}$ mice

In order to investigate the possible role of the pro-inflammatory cytokines (IL-1β, IL-6 and TNFα) in learning and memory deficits of Dagla$^{-/-}$ mice, we assessed the production of the aforementioned cytokines in organotypic hippocampal slice culture (OHSC) experiments. For these experiments, a LysM-Dagla$^{-/-}$ mice line was used because OHSC is difficult to perform with mice older than a week. The inducible line we used in the behavioural part could, therefore, not be used, since induction of the knockout can begin only when the mice are already one month old. The experiments were performed as detailed in the materials and methods part.

One-way ANOVA revealed a significant LPS treatment effect in IL1β ($F_{(3, 32)} = 17.32$, $p < 0.001$), IL-6 ($F_{(3, 32)} = 12.34$, $p < 0.001$) and no significant effect for TNFα ($F_{(3, 8)} = 3.961$, $p > 0.05$) after

24h stimulation. Bonferroni's multiple comparison test, however, revealed that the significant increase in IL1β, IL-6 and TNFα production after LPS treatment is only present when the WT groups are compared, for IL1β and IL-6 ($p < 0.001$), and for TNFα ($p < 0.05$). There was no significant LPS effect observed in the Dagla$^{-/-}$ groups. IL1β and IL-6 levels were already high the Dagla$^{-/-}$ groups with significant genotype effect observed when unstimulated Dagla$^{-/-}$ mice are compared to their unstimulated WT siblings ($p < 0.001$). (Figure 4.3.3A)

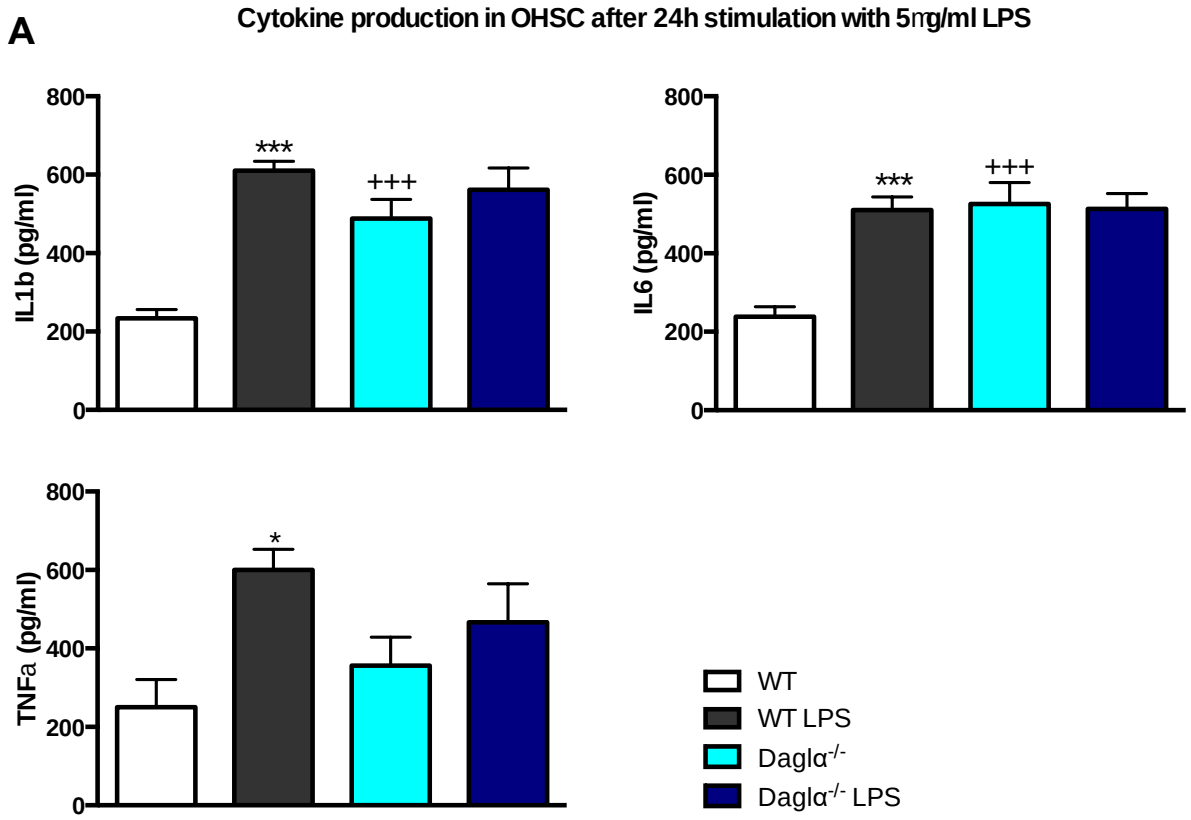


**Figure 4.3.3A: ELISA measurement of OHSC supernatants for cytokine release after 24h LPS stimulation**. Stimulation with LPS for 24h led to increased production of IL1β, IL-6 and TNFα in the WT groups (***$p < 0.001$; *$p < 0.05$) but not in the Dagla$^{-/-}$ OHSCs. IL1β and IL-6 levels were higher in the Dagla$^{-/-}$ groups even without LPS treatment; genotype effect between unstimulated groups ($^{+++}p < 0.001$). One-way ANOVA with Bonferroni's post-hoc test, values represent mean± SEM; n = 9 per group.

After 48h of stimulation, LPS stimulation did result in increase production of any of the cytokines tested. (Treatment effect: $F_{(3, 32)} = 2.101$, $p > 0.05$; $F_{(3, 32)} = 2.286$, $p > 0.05$ and $F_{(3, 8)} = 0.5097$, $p > 0.05$ for IL1β, IL-6 and TNFα respectively. Bonferroni's multiple comparison

test, nonetheless, showed a slightly significant increase in IL1β and IL-6 when WT groups stimulated and unstimulated were compared ($p < 0.05$). Figure 4.3.3B.

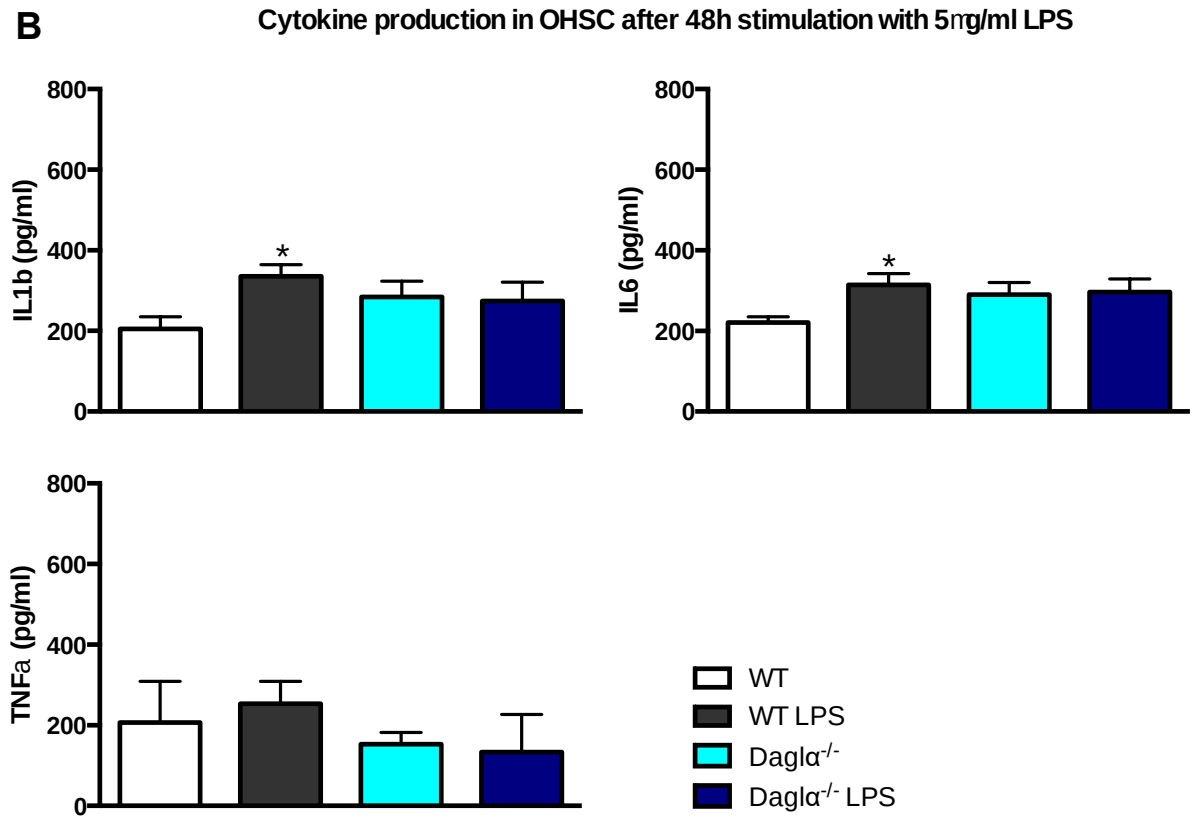


**Figure 4.3.3B: ELISA measurement of OHSC supernatants for cytokine release after 48h LPS stimulation**. Stimulation with LPS for 48h led to an increase in production of IL1β and IL-6 only in the WT group (*$p < 0.05$). One-way ANOVA with Bonferroni's post-hoc test, values represent mean ± SEM; n = 9 per group.

Now, after 72h of stimulation, LPS stimulation resulted in increase production of only IL1β ($F_{(3, 32)} = 6.372$, $p > 0.01$). No significance was recorded for IL-6 ($F_{(3, 32)} = 0.8908$, $p > 0.05$) and TNFα ($F_{(3, 8)} = 0.6778$, $p > 0.05$). Bonferroni's multiple comparisons test showed a treatment and genotype effect with the treated Dagla$^{-/-}$ group compared to untreated Dagla$^{-/-}$ group ( $p < 0.01$) and treated WT group ($p < 0.01$). Figure 4.3.3C.

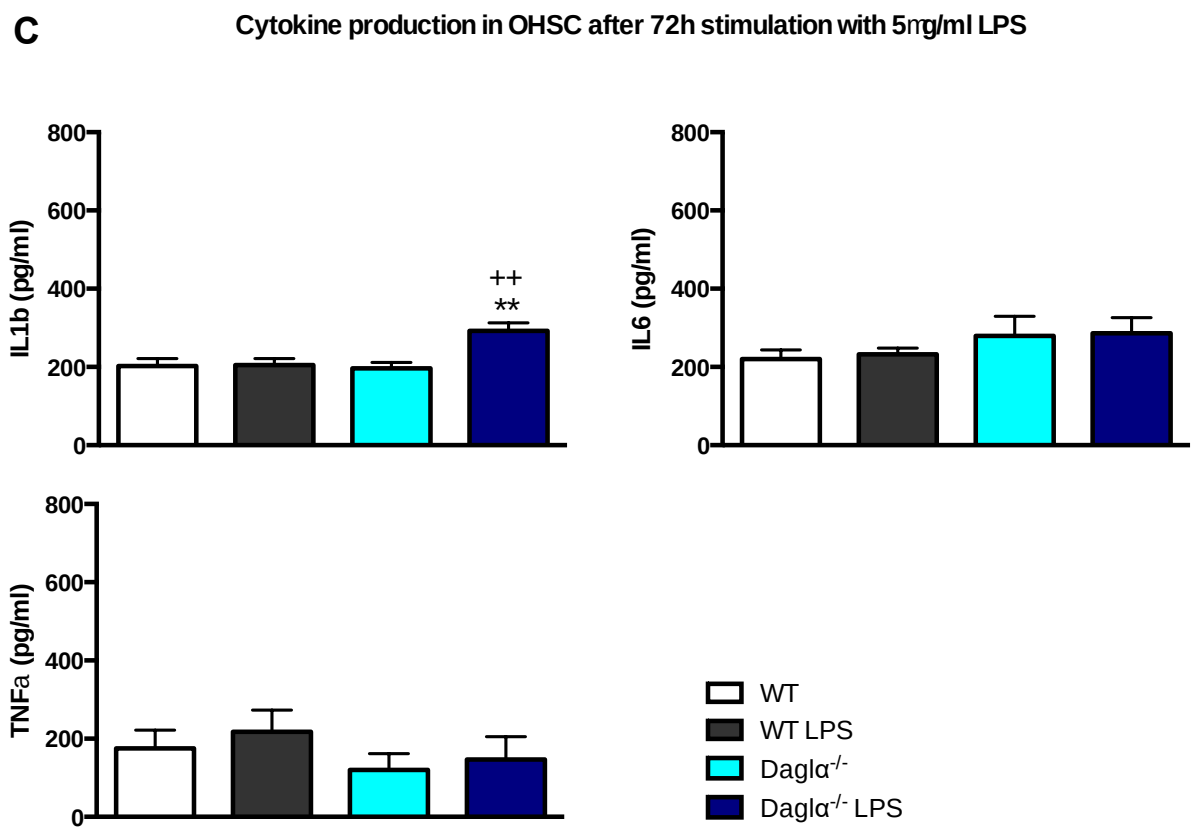


**Figure 4.3.3C: ELISA measurement of OHSC supernatants for cytokine release after 72h LPS stimulation**. Stimulation with LPS for 72h led to an increase in production of IL1β only in the Dagla$^{-/-}$ mice (**$p < 0.01$) with genotype effect when both stimulated groups were compared ($^{++}p < 0.01$). One-way ANOVA with Bonferroni's post-hoc test, values represent mean ± SEM; n = 9 per group.

## 4.4 Effects of increased AEA on microgliosis and microglia morphology in the hippocampus during ageing

The endogenous ligands of the endocannabinoid system are the 2-AG and the AEA, whereby, 2-AG is the main endocannabinoid. Excessive elevation of 2-AG levels or a complete shot down of synthesis enzymes, may lead to desensitisation of CB1 and CB2 receptors. Thus, for this experiment, we opted for a constitutive FAAH deficient mouse line age 2-3 months (young) and 12-15 months (old), where degradation of anandamide is blocked.

### 4.4.1 Age- and genotype-dependent increases in microglia density

We wanted to know how ageing and deletion of FAAH influences microglia density in the hippocampus. Here, the density of microglia was significantly higher in old than in young

animals (age: $F_{1,120} = 44.65$; $p < 0.001$), both in wild-type and FAAH$^{-/-}$ mice (age × genotype interaction $F_{1,120} = 2.588$; $p > 0.05$). However, we found a significant difference in the microglia density between the genotypes (genotype: $F_{1,120} = 5.043$; $p < 0.05$). Unexpectedly, FAAH−/− animals had a higher microglia density in the hippocampus than wild-type mice. This was significant in the young age-group according to Bonferroni's post-hoc test (Figure 4.4.1A,B) (Adopted and modified from Ativie et al, 2015).

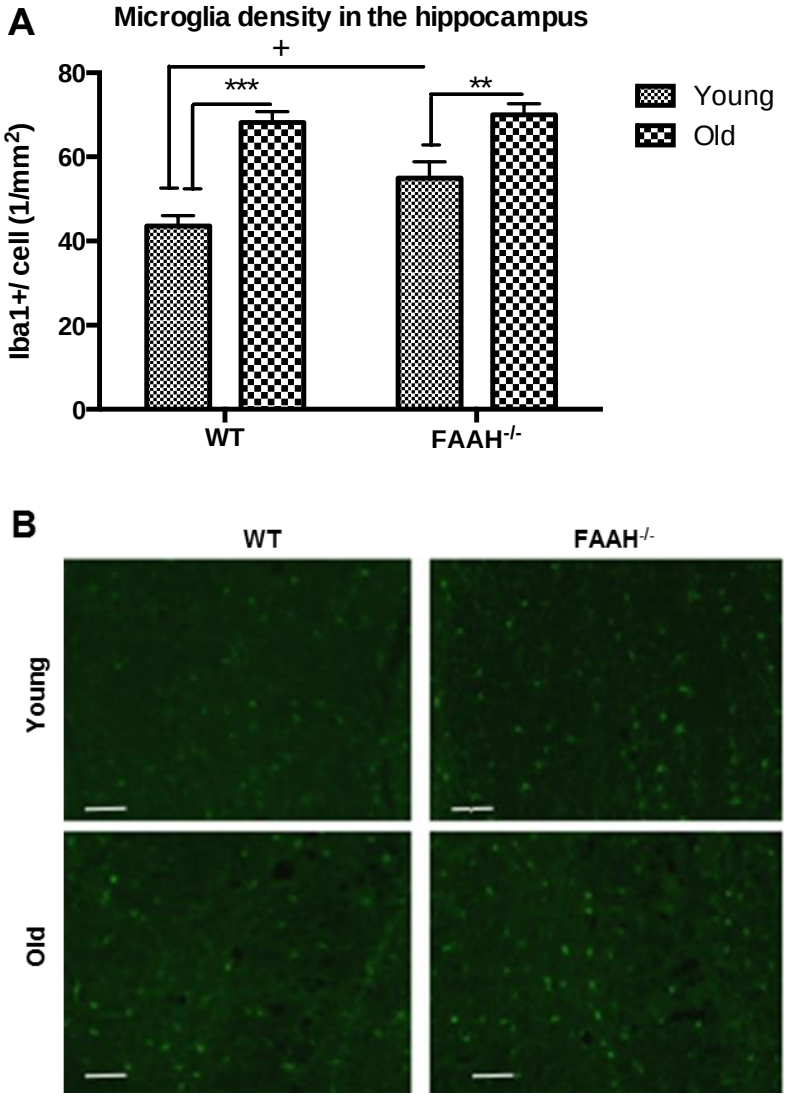


**Figure 4.4.1: Enhanced microglia density in young FAAH−/− mice.** (A) Old animals showed higher microglia densities in both genotypes. $^{+}p< 0.05$ difference between wild type (WT) and FAAH knockout mice according to Bonferroni's t-test. $^{**}p< 0.01$; $^{***}p < 0.001$ difference between young and old mice according to Bonferroni's t-test. (B) Representative microphotograph of Iba1+ microglial cells in the hippocampus. The length of the scale bars is 100 μm (modified from Ativie et al. 2015).

### 4.4.2 Ageing or genetic deletion of FAAH leads to an increase in microglia size

Since the activation of microglia is often characterized by increased cell size, we, therefore, wanted to know whether the increased microglia density in ageing due to the deletion of FAAH was accompanied by an enhanced ratio of microglia with increased cell sizes. Microglia sizes significantly increased in ageing (age: $F_{1,893} = 32.36$; $p < 0.001$), and this age-related increase was not influenced by the genotype of the animals (age × genotype interaction $F_{1,893} = 2.167$; $p > 0.05$). Genotype of the mice also had a significant effect on the sizes of microglia (genotype: $F_{1,893} = 27.70$; $p < 0.001$). Post hoc analysis of the data with Bonferroni's t-test revealed that the microglia sizes were significantly higher in $FAAH^{-/-}$ animals in both age groups (Figure 4.4.2) (Adopted and modified from Ativie et al, 2015)

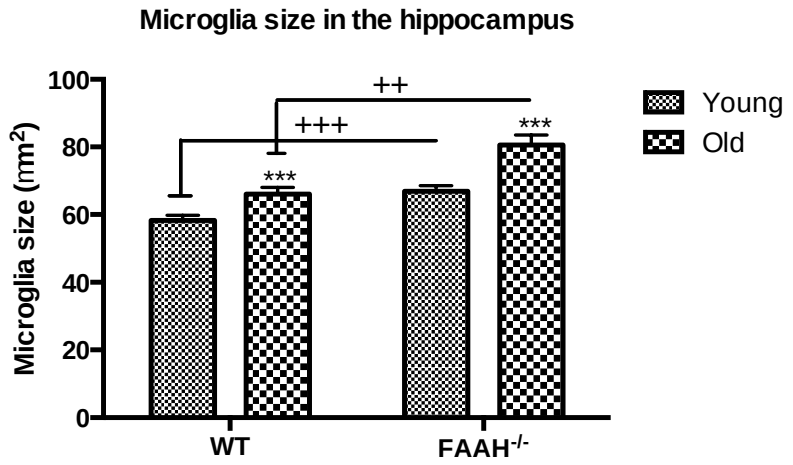


**Figure 4.4.2: Enhanced microglia size in young and old $FAAH^{-/-}$ mice**. Old animals showed higher microglia sizes in both genotypes. +++$p < 0.001$ difference between wild- type (WT) and $FAAH^{-/-}$ mice according to Bonferroni's t-test. ***$p < 0.001$ difference between young and old mice according to Bonferroni's t-test. (Modified from Ativie et al. 2015).

### 4.4.3 Altered cytokine levels in FAAH mice

Next, we wanted to know whether the larger cell bodies – morphological sign of activation – were accompanied by enhanced levels of pro-inflammatory cytokines. For this purpose, we measured the concentrations of IL-1β and IL-6. We found a significant main effect of genotype

and age on the concentration of IL-1β (genotype: $F_{1,22} = 12.10$; $p < 0.01$; age: $F_{1,22} = 11.31$; $p < 0.01$) as well as a significant age × genotype interaction ($F_{1,22} = 6.065$; $p < 0.05$). Post hoc analysis of the data revealed that IL-1β levels in young FAAH$^{-/-}$ mice were significantly higher as compared to young wild-type animals. Moreover, the age-related increase was significant in the wild-type, but not in the FAAH$^{-/-}$ mice (Figure 4.4.3A). We also found a significant main age effect for the IL-6 concentration ($F_{1,23} = 10.32$; $p < 0.01$). The genotype effect or age × genotype interaction was not significant, ($F_{1,23} = 1.855$; $p > 0.05$) and ($F_{1,23} = 0.8549$; $p > 0.05$) respectively. However, post hoc analysis of the data revealed that the age-related increase in IL-6 level was only significant in wild type but not in FAAH$^{-/-}$ mice (Figure 4.4.3B).

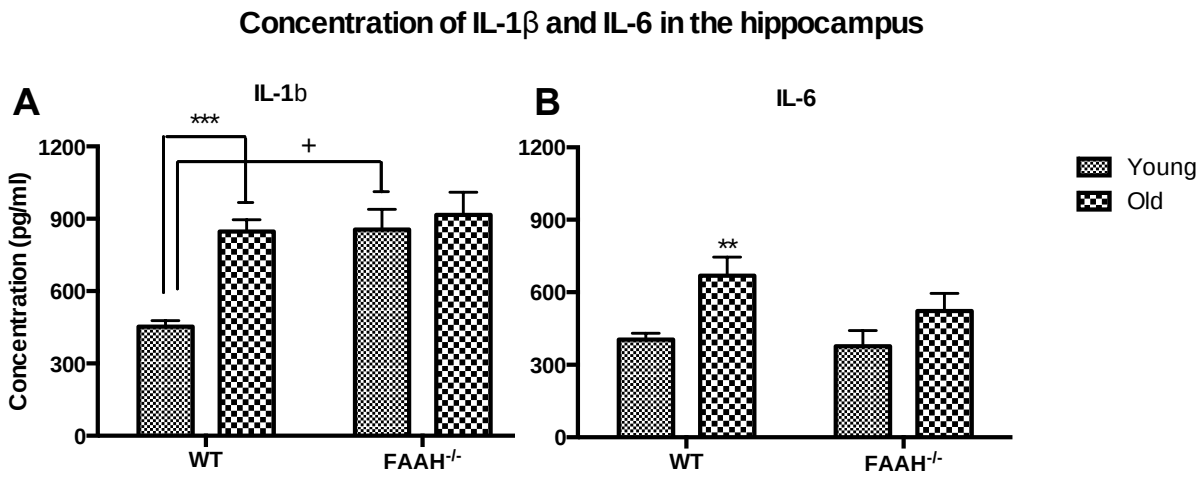


**Figure 4.4.3:** (A) Hippocampal IL-1β levels were higher in young FAAH$^{-/-}$ than in age-matched wild-type mice. Age-related increase in IL-1β levels was present in wild-type but not in FAAH$^{-/-}$ mice. (B) The elevation in IL-6 levels in ageing reached the level of significance in wild-type but not in FAAH$^{-/-}$ mice. $^{+}p < 0.05$ difference between wild-type (WT) and FAAH knockout mice according to Bonferroni's t-test. $^{**}p < 0.01$; $^{***}p < 0.001$ difference between young and old mice according to Bonferroni's t-test (Modified from Ativie et al. 2015).

# 5. Discussion

Previously published works in our lab have demonstrated that the deletion of CB1 receptor results in early onset of brain ageing, marked by memory deficit, enhanced accumulation of the ageing pigment lipofuscin, elevated neuroinflammation levels and neuronal loss (Piyanova et al. 2013; Bilkei-Gorzo et al. 2005). While these age-related changes were largely restricted to the brain, similar age-associated elevation of neuroinflammation was observed after CB1 receptor was specifically deleted from GABAergic neurons (Albayram *et al.*, 2011).These studies taken together indicated that GABAergic neurons play a crucial role in microglial activity regulation during ageing and suggested an important role for the endocannabinoid system, especially the GABA-CB1 mediated endocannabinoid signalling. In this present study, we looked closely into the role played by the GABA-CB1 mediated endocannabinoid signalling in the regulation of microglial activity during ageing but also during cases of LPS induced pathological conditions in young and old individuals. Additionally, since it is unclear from which origin, how and which endocannabinoid (2-AG or anandamide) is involved in the observed age-related changes and increased microglial reactivity in the brain, we sought to answer these questions employing microglia-specific DAGLα knockout mice as well as constitutive FAAH knockout mice in various behavioural, molecular and cellular experiments.

## 5.1 GABA CB1 deletion leads to enhanced neuroinflammation in ageing

In this study, in reflection on previous results from our lab and literature knowledge (Eljaschewitsch *et al.*, 2006), we hypothesized that reduced cannabinoid signalling between microglia and the regulatory hippocampal GABAergic neurons would lead to increased microglia activity, resulting in enhanced neuroinflammation. Indeed, in a set of experiments in organotypic hippocampal slice cultures (OHSCs) with 3 to 5 days old GABA-Cnr1$^{-/-}$ pups and

their wild type littermates, we recorded an increase in production of IL-1β, IL-6 and TNF-α levels after lipopolysaccharide (LPS) induced activation of microglia in the organotypic hippocampal slices (OHS). This is in line with literature knowledge, as LPS, a Gram-negative bacterial endotoxin has been reported to induce a rapid proinflammatory immune innate response through Toll-like receptor 4 (TLR4) signalling. Toll-like receptor 4, a pattern recognition receptor on immune cells, recognizes pathogen-associated molecular patterns (PAMPs) to which LPS is a member (Chakravarty, 2005; Mallard, Wang and Hagberg, 2009; Vaure and Liu, 2014).

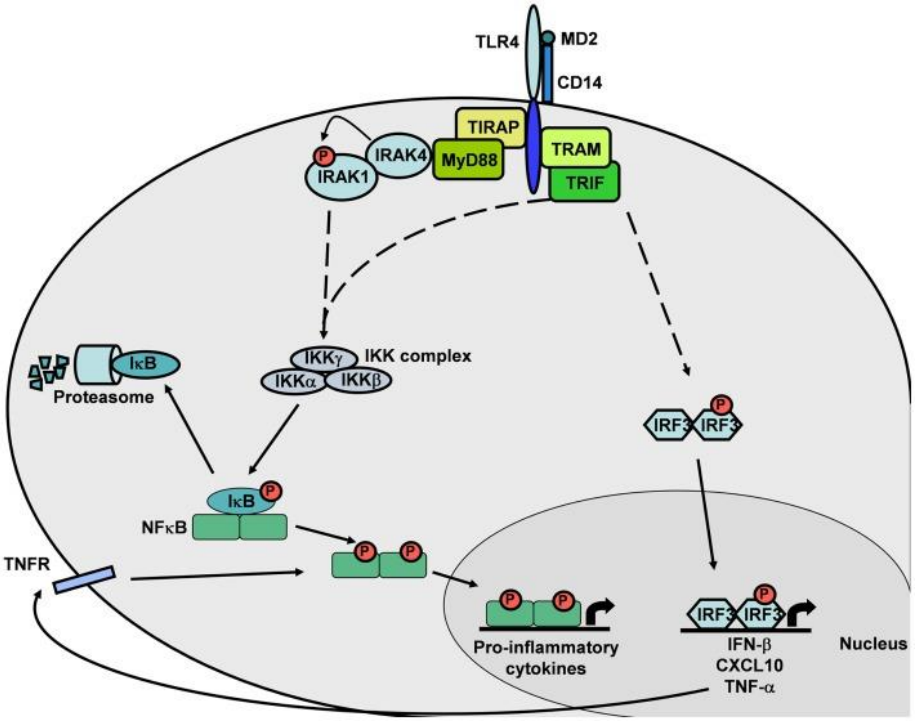


**Figure 5.1A: TLR4 intracellular signalling cascade**. The MyD88-dependent pathway induces NF-κB translocation and expression of pro-inflammatory cytokine genes. Alternatively, MyD88-independent pathway induces NF-κB or IRF3 translocation, leading to expression of pro-inflammatory cytokine genes by NF-κB or IFN-β and TNF-α genes by IRF3 (Adapted from Vaure & Liu 2014).

However, following chronic exposure of microglia/macrophage to LPS, immune cell tolerance ensues. LPS and the produced cytokines activate intracellular tyrosine kinases leading to modulation of mitogen-activated protein kinase (MAPK) cascade followed by other downstream signalling processes. Eventually, proinflammatory cytokine/chemokine release is

reduced and the microglia transit from the proinflammatory M1 to repair and regenerative M2 state, preventing neurotoxicity (Tominaga *et al.*, 1999; Ajmone-Cat, Nicolini and Minghetti, 2003; Antonietta Ajmone-Cat *et al.*, 2013) . Strikingly, this self-protection mechanism seems to be hampered in GABA-Cnr1$^{-/-}$ mice. We observed that IL-1β, IL-6 and TNF-α levels were downregulated to control levels in the WT stimulated groups, while the levels of these proinflammatory cytokines remained high in GABA-Cnr1$^{-/-}$ samples stimulated with LPS. These findings indicate a disturbed downregulation of cytokine production in GABA-Cnr1$^{-/-}$ samples after a chronic stimulation with LPS. Consequentially, increased neuroinflammation as a result of microglia overreactivity can be expected in GABA-Cnr1$^{-/-}$ mice. This implies that during chronic pathological conditions in the brain, the modulatory role of the cannabinoid system on microglia may be lost in GABA-Cnr1$^{-/-}$ individuals. This may be another explanation and a confirmation of exacerbated microglia activity, cognitive decline and other age-associated pathologies observed in previous studies with these mice (Albayram *et al.*, 2011; Piyanova *et al.*, 2013). We are aware that this experiment may be more representative if slices from older mice were included. This was, however, not achievable due to technical limitations. Organotypic hippocampal slices from older mice survive only poorly in culture using present protocols, necessitating a tenfold increase in the number of animals needed for the study, which in turn is not in conformity with existing regulatory modalities concerning studies with genetically modified animals. Modification of present protocols, which is proving very difficult at the moment, to accommodate adult slices is therefore of utmost interest. Moreover, since the cytokine levels were measured in the collected culturing media using ELISA, variations in the results from different batches of ELISA experiments are predictable due to variation from ELISA plates during plate-reading. A possible solution to this issue is to collect all samples overtime and then perform ELISA, distributing the samples evenly in the plates to reduce plate variation. The down side to this approach is, however, that one may have to collect and store

the samples for a longer period of time, which in turn could lead to degradation of the cytokines in the sample-medium.

In a further study, we evaluated the effect of CB1 deletion from GABAergic neurons on microglia activity *in situ*. Here, 2 months old GABA-Cnr1$^{-/-}$ mice and their wild type littermates were intraperitoneally injected with 0.8mg/kg LPS or saline as control. In order to mimic a broader spectrum of pathological conditions in the brain, which is usually chronic with microglia exposed to the activating stimulant for a prolonged period of time, we set out to administer LPS to the mice once which represents an acute stimulation (single injection) or on four consecutive days (multiple stimulation), representing a chronic stimulation (Ajmone-Cat, Nicolini and Minghetti, 2003). As expected, hippocampal microglia density was increased in treated mice with no particular correlation to genotype, though it appears that CB1 deletion on GABAergic neurons already showed tendencies of increased microglia density. Indeed, this is an interesting observation, as previous experiments from our lab show that in older mice microglia density in the hippocampus is increased in 12 months old GABA-Cnr1$^{-/-}$ mice as compared to 2 months old mice (Albayram *et al.*, 2011). This suggests that microglia activity increases in GABA-Cnr1$^{-/-}$ mice with increasing age, ultimately leading to microglial overreactivity and neuronal loss reported in old GABA-Cnr1$^{-/-}$ mice. Equally notable is the exacerbated microglia density in the multiple injected mice when compared to single injected individuals. Here, multiple LPS injection led to a much stronger response in the GABA-Cnr1$^{-/-}$ mice, indicating that these mice are more vulnerable to endotoxins. Literature knowledge has it, that levels of some prominent cytokines like IL-6, IL-1β and TNF-α are increased in older GABA-Cnr1$^{-/-}$ mice (Albayram et al. 2011). It is remarkable, therefore, that this present work shows that the increased cytokine level is not present in younger GABA-Cnr1$^{-/-}$ mice as cytokine levels were similar in both knockout and WT without LPS treatment and equally increased after LPS treatment. This is true for IL-1β and TNF-α in both single and multiple injection paradigms. However, the magnitude of increase of these cytokines was lower in the

multiple injection paradigm in accordance with literature (Ajmone-Cat, Nicolini and Minghetti, 2003; Antonietta Ajmone-Cat *et al.*, 2013). A decreased IL-6 expression was recorded after single injection and levels were unchanged in multiple injection paradigm for both genotypes. This observation also depicts literature knowledge as it has been reported that TNF and IL-6 are the first line of cytokines released after LPS stimulation of blood samples with IL-6 level returning back to very low concentration after 6 hours while TNF also returned to low level but was after 24 hours still 70 fold higher than IL-6 concentration (DeForge and Remick, 1991). This may explain the erratic results obtained with IL-6, indicating that we would have had to sacrifice the mice 4 to 6 hours after injection to catch actual IL-6 expression levels and not after 24 hours as we did. It is important to keep in mind that the size of LPS prevents LPS from easily crossing the blood brain barrier (Singh and Jiang, 2004). Hence, unlike stimulation in cell culture, organotypic hippocampal slice culture or intracerebroventricular (ICV) injection where LPS acting as an agonist can directly trigger TLR4 signalling in microglia, LPS administered intraperitoneally binds to TLR4 receptors on peripheral immune cells to orchestrate production of cytokines and other immune mediators that cross the blood brain barrier to activate microglia. Thus, a slight discrepancy in microglia response may occur depending on the mode of activation. The outcome of this set of experiments with reference to literature (Albayram *et al.*, 2011), confirms that CB1 knockout from GABAergic neurons unfolds its detrimental consequences with increasing age.

In another set of experiments, microglial reactivity was assessed in 3 age groups of GABA-Cnr1$^{-/-}$ mice and age-matched WT littermates. This time, however, LPS stimulation was administered bilaterally into the hippocampus. This represents a direct and acute activation of microglia, unlike in the intraperitoneal injection experiments where microglia are indirectly activated through the response from peripheral immune cells. Employing social preference test, we were able to deduce sickness behaviour in mice treated with LPS as compared to those treated with artificial cerebrospinal fluid (ACSF) in all age and genotype groups. Treated mice

showed reduced motility and sociability as they interacted less with partner mice, which is a typical response to infection in animals (Fisch, 2007; Nestler and Hyman, 2010). In cases of infection, animals change their behaviour to support physiological and metabolic conditions in the body. The phenotypic consequences of this process are expressed in reduced activity and interest alongside with responses like increased body temperature (Aubert, 1999; Wynne, Henry and Godbout, 2009). Although the sickness behaviour in WT mice was evidently strong across all age groups, in GABA-Cnr1$^{-/-}$ mice the sickness behaviour was exacerbated with increasing age. This finding is again in agreement with observations that CB1 receptor knockout becomes detrimental in ageing as evident in recorded increase in microglial reactivity in old GABA-Cnr1$^{-/-}$ mice (Albayram *et al.*, 2011; Piyanova *et al.*, 2013). And indeed, the density of microglia in the hippocampus of treated 18 months old GABA-Cnr1$^{-/-}$ mice was much higher than in the treated WT mice. In addition younger untreated GABA-Cnr1$^{-/-}$ mice always had more microglia in their hippocampus than the untreated WT. This is also in line with previously reported increase microgliosis in young GABA-Cnr1$^{-/-}$ mice. Nonetheless, it is safe to say that the increase in microglia density in young GABA-Cnr1$^{-/-}$ mice did not lead to exacerbated sickness behaviour, opening the question of the profile of these microglia. Strikingly, expression of IL-1β and TNF-α was similarly increased in WT mice after LPS treatment across all age groups. On the contrary, these cytokines increased in treated GABA-Cnr1$^{-/-}$ mice in an age-dependent manner. Although there are no morphological experiments to back this claim, one may argue that the predominant number of microglia in the young GABA-Cnr1$^{-/-}$ mice are of the M2 polarization with less detrimental effect on the brain (Chhor *et al.*, 2013). Yet, IL-6 expression was unstable as previously observed and possible reasons for this has been discussed.

Accumulation of lipofuscin has been reported to be accelerated in constitutive CB1 receptor knockout mice (Piyanova *et al.*, 2013) and accumulation of these lipopigments is wildly accepted as an ageing-marker, resulting from increasing dysfunction of cellular clearance

mechanisms (Brunk and Terman, 2002; Terman and Brunk, 2004). In most studies, lipofuscin content of the cells is examined in fixed brain sections. Lipofuscin is, however, present in virtually all cell types in the brain including neurons, though at a much lower amount compared to glial cells that account for 80 to 90 % of total lipofuscin in the brain (Riga *et al.*, 2006). In this experiment isolated microglia from young and old GABA-Cnr1$^{-/-}$ mice with their age-matched littermates were analyzed for lipofuscin content by fluorescence activated cell sorting (FACS). Mirroring previous findings, CB1 knockout from GABAergic neurons alone sufficed to elicit accelerated lipofuscin accumulation in microglia from old animals. This implies that microglia population in older GABA-Cnr1$^{-/-}$ mice contain far more dysfunctional microglia than their age-matched WT littermates. Consequentially, microglia in these mice can be overreactive, thereby harming neighbouring cells which ultimately contributes to accelerated brain ageing.

## 5.2 Reduced microglial 2-AG production leads to altered neuron-microglia interaction

A reduced endocannabinoid signalling, resulting from reduced cannabinoid receptor expression (Canas *et al.*, 2009) and coupling to $G_i$ proteins (Wang *et al.*, 2003; Feliszek, 2016) and lower 2-AG levels due to diminished Daglα activity (Piyanova, 2016) has been described in the ageing brain. Moreover, a reduced endocannabinoid production has been linked to a disturbed neuron-microglial bidirectional communication via neuroimmune regulator protein pairs such as the CD200-CD200R and CX3CL1-CX3CR1 (Hernangomez *et al.*, 2012; Justin *et al.*, 2012; Wong, 2013), leading to increased inflammation and accelerated brain ageing alongside with characteristics of various neurodegenerative diseases (Zhang *et al.*, 2011). Expectedly, expression of these neuroimmune regulator proteins is reduced in ageing (Jurgens and Johnson, 2012). In addition, unpublished findings in our lab indicated that while expression of CD200 and CD200R is reduced in the hippocampus of ageing mice both in wild type and GABA-Cnr1$^{-/-}$, old GABA-Cnr1$^{-/-}$ animals expressed higher levels of this protein pair compared to age-

matched wild type littermates. This present study showed a significant decrease or a tendential decrease in the expression of both regulator protein pairs (CD200-CD200R and CX3CL1-CX3CR1) in older mice irrespective of genotype. This is in line with literature as expression of these protein pairs have been reported to reduce during ageing. Interestingly, however, the observed decrease in expression levels of these protein pairs was less pronounced in old microglia-specific Daglα knockout mice compared to their age-match wild type littermates. This observation mirrors our findings in GABA-Cnr1$^{-/-}$ animals, though only in the CD200-CD200R protein pairs, where expression levels were higher in old knockout mice as compared to wild type in similar age. Now, the outcome of this study may appear inconsistent or even contradictory to the overall consequences of reduced or disturbed cannabinoid signalling observed so far, since these neuroimmune regulator proteins have been shown to be reduced in ageing and various CNS pathologies. On a second look, the results are consistent with literature as expression of these protein pairs is generally reduced in both old WT and knockout mice, but with an additional information that a compensatory effect attempt in response to reduced cannabinoid signalling may be induced via direct neuron-microglia interaction. The purpose of this likely compensatory response could be to offset microglia overreactivity resulting from altered cannabinoid signalling. Indeed, a further experiment with these microglia-specific Daglα knockout mice showed that some genes encoding GABA A receptor subunits are upregulated in microglia isolated from old Dagla$^{-/-}$ mice when compared to old wild type mice, while cytokine production was also increased. A possible reason for the observed expression change can either be due to increased production of GABA A receptors or change in its composition in the microglia. These findings taken together elude to the importance of the endocannabinoid signalling in the bidirectional regulation of neurons and microglia and ultimately in the regulation of microglia reactivity during ageing.

## 5. 3 Cognitive ageing and microglial reactivity in microglia-specific Dagla$^{-/-}$ mice

In this set of experiments, the consequences of a reduced 2-AG production on age-related changes in learning ability were investigated in partner and object recognition tests. A longitudinal study of microglia-specific Dagla$^{-/-}$ male mice and their age-matched wild type littermates revealed that sociability was similarly strong in all tested mice irrespective of age and genotype. Although we expected both young and old mice to show a significantly higher preference for conspecific partner mice as compared to an object, it was also important to exclude its influence on partner recognition because a normal sociability is a prerequisite for partner recognition. As expected, young and older knockout mice displayed a strong preference for partner mice similar to performances obtained with wild type mice without any age difference. Moreover, the recognition strength seemed to be reduced in older Dagla$^{-/-}$ mice as compared to young Dagla$^{-/-}$ mice. Although no significant recognition ability was obtained with young wild type mice, we, however, think that this must be due to some experimental failures or mistake on the part of the experimenter. Nonetheless, the slightly better performance, at least in the young Dagla$^{-/-}$ mice, is consistent with literature knowledge on the effect of reduced cannabinoid signalling in younger mice, as young CB1 knockout mice were reported to have a superior recognition ability compared to age-matched wild type mice (Bilkei-Gorzo *et al.*, 2005). Also consistent with literature is the intertrial interval dependent decrease in recognition ability in old mice with disturbed cannabinoid signalling (Bilkei-Gorzo *et al.*, 2005, 2012). Male microglia-specific Dagla$^{-/-}$ mice showed a weaker recognition for previously seen mice compared to age-matched wild type mice after 2 hours intertrial interval. Whereas there was no difference in the recognition ability after 30 minutes and 1 hour intertrial intervals. These results, in line with previous publications from our lab, suggest that reduced cannabinoid signalling leads to memory deficit, especially in aged mice. Although not as strong as in CB1 knockout mice, it is interesting that Daglα knock on microglia is enough to show tendencies of

memory deficits in old mice. As intended, if these mice are tested again at a much older age (18 months or older), these tendencies are likely to become even stronger and clearer, reflecting previous findings (Bilkei-Gorzo *et al.*, 2005, 2012). Male mice were solely used throughout this longitudinal object and partner recognition experiments. Female animals are often excluded from behavioural experiments with reference to hormonal fluctuation occurring during the estrous cycle that may influence female mice performance in such tests (Mogil *et al.*, 2000). The performance of female animals in object recognition test has been reported to be highly inconsistent depending on the phase of estrous cycle the animals are currently in (van Goethem *et al.*, 2012). Although female black 6 mice (C57BL/6J) have been reported to be less affected by the estrous cycle in various behavioural tests (Meziane *et al.*, 2007), their performances in recognition tests are yet unstable owing to previous experience in our lab.

In a parallel longitudinal study with female microglia-specific Dagla$^{-/-}$ mice and wild type littermates, the spatial learning and memory abilities of mice were assessed in the Morris water maze (MWM) test. It has been previously reported that a disturbance of the endocannabinoid signalling as a result of a constitutive deletion of CB1 receptor led to age-related learning and memory deficits (Albayram *et al.*, 2011). Regrettably, in this study, perturbation in the endocannabinoid system through a reduced 2-AG production as a consequence of Daglα deletion on microglia did not result in learning and/or memory deficits neither in the young nor in the old mice regardless of genotype. Although we have shown that reduced 2-AG production leads to an altered neuron-microglia crosstalk, the results indicated more of a compensation effect than a detrimental effect. Hence it is possible that the reduction in 2-AG achieved by deletion of Daglα specifically from microglia is not strong enough to provoke microglial overreactivity that in turn would lead to neuronal loss and the associated learning and memory deficits in our 2 months old mice and just about sufficient to elicit a worsened performance in 12 months old mice. Besides, the main producers of 2-AG in the brain is not established, though this is ascribed mainly to neurons and astrocytes are well capable of producing

endocannabinoids. Thus, reduction in microglial 2-AG production may alter microglia activation, but may not be sufficient to significantly affect the overall signalling of the cannabinoid system in the brain. Moreover, the MWM test is extremely dependent on hippocampal functioning (Kenney and Gould, 2009). Hence, if there is no increased neuroinflammation in the hippocampus as is the case in old CB1 receptor knockout mice (Albayram *et al.*, 2011; Piyanova *et al.*, 2013), cognitive deficits may be unlikely. Nonetheless, we observed an age-dependent loss of memory strength in the older mice, irrespective of genotype. This is in line with literature, as animals tend to have a weakening memory strength with increasing age. These results taken together suggest that reduction in 2-AG production in microglia may not be sufficient to elicit cognitive deficits, at least in 12 month old mice. Since it is a longitudinal test and the mice will be tested again when they are much older, there is a chance that the conclusion of this study at this stage might change. Lastly, the MWM test is an aversive test that could influence animal behaviour. In order to reduce this possible source of inconsistency, we used only female mice in the MWM test. Female animals have been reported to be less affected by acute stress-related impairment in spatial memory (Conrad *et al.*, 2004).

Although Daglα deletion from microglia did not lead to a significant impairment in the cognitive and social ability of tested mice as at 12 months old, we, however, yet sought to investigate any possible changes in microglial reactivity, ensuing from a reduced cannabinoid signalling. In a set of OHSC experiments, we demonstrated that the deletion of Daglα from microglia alone resulted in an increase in cytokines production similar to levels obtainable in both WT and microglia-specific Dagla$^{-/-}$ mice stimulated with LPS for 24 hours. A similar pattern was also observed with TNFα production in the GABA-Cnr1$^{-/-}$ mice. Interestingly, LPS stimulation did not seem to further exacerbate cytokines production in Dagla$^{-/-}$ mice in the first 2 days of the experiments, while LPS stimulation clearly raised cytokines production in the WT samples. As expected and in line with literature (Ajmone-Cat, Nicolini and Minghetti, 2003; Antonietta Ajmone-Cat *et al.*, 2013), cytokine release was eventually reduced to WT

unstimulated levels after 3 days. Strikingly, this time, unstimulated Dagla$^{-/-}$ samples, wherein cytokine levels was previously high, was also now downregulated. Only in IL-1β production was an LPS and genotype effect sustained in stimulated Dagla$^{-/-}$ samples. Even though these results point to a slightly dysregulated cytokines production in the Dagla$^{-/-}$ mice, this cannot be a clear-cut conclusion as was the case with results obtained from experiments with GABA-Cnr1$^{-/-}$ mice. Moreover, unpublished findings in our lab also showed that LPS intraperitoneally injected into microglia-specific Dagla$^{-/-}$ mice led to changes in cytokines expression that were similar to those obtained in their LPS-treated WT littermates. All in all, we may conclude that microglia-specific Daglα deletion only mildly if at all affects microglial reactivity.

## 5.4 Enhanced anandamide (AEA) levels lead to microgliosis and changes in microglial morphology in the hippocampus during ageing

In this set of experiments, we investigated the effects of increased AEA on microglia activity in FAAH $^{-/-}$ mice alongside the possible age-associated consequences. Now, it is crucial to note that an anti-inflammatory effect of AEA on microglia has been reported after activation with LPS (Facchinetti *et al.*, 2003; Tham *et al.*, 2007). Furthermore, a neuroprotective effect was demonstrated in hippocampal slice culture after NMDA treatment (Eljaschewitsch *et al.*, 2006). In addition, enhanced AEA levels has proven to be protective in a viral model of multiple sclerosis (Correa *et al.*, 2011) and in traumatic brain injury (Tchantchou *et al.*, 2015). However, findings in this study revealed an increase in the density and size of microglia both in wild-type and FAAH$^{-/-}$ mice in ageing. Importantly, the density of microglia was higher in the FAAH$^{-/-}$ mice as compared to wild- type animals in the young 2 months old age group. This increased microgliosis mirrors the trend observed in previous work, as a disturbance in the cannabinoid signalling often results in increased microgliosis already at an early age even though not always accompanied with pathological consequences. Furthermore, a larger microglia size was recorded in the FAAH$^{-/-}$ mice as compared to wild-type in both 2 and 12 months old mice. Moreover, we demonstrated that ageing led to an increased expression of two prominent pro-

inflammatory cytokines; IL-1β and IL-6 in wild-type mice. Interestingly, this age- related increase was totally absent (IL-1β) or failed to reach the level of significance (IL-6) in FAAH$^{-/-}$ mice. Again and importantly, IL-1β level was already high in young FAAH$^{-/-}$ mice, which may suggest higher inflammation. We have previously argued that IL-6 is rapidly degraded after production (DeForge and Remick, 1991), preventing accurate detection of the actual level of expression if samples were collected later than 4 hours after induction of release. This argument, however, does not hold here as the deletion of FAAH continues to have effect and the samples were not additionally treated with any stimulant like LPS. Hence, a possible reason why IL-1β and IL-6 are differently affected by FAAH could be that IL-1β is secreted through a non-classical export mechanism, whereas IL-6 through the classical mechanism (Eder, 2009). So, it is conceivable that anandamide differentially affects these secretory pathways. Alternatively, since IL-1β and IL-6 are produced in a premature form, it is also possible that anandamide differentially affects their maturation process (Akdis *et al.*, 2011).Taken together, these changes are indicative of a more pronounced pro- inflammatory activity state of microglia in young FAAH$^{-/-}$ mice. Therefore, it can be concluded from these results that increased AEA levels due to the genetic deletion of FAAH leads to pro-inflammatory changes in the brain of young animals and these changes are akin to those observed during the normal ageing process. Consequentially, it is evident that a balance in endocannabinoid levels is essential for proper functioning of the endocannabinoid system, while excessive or reduced production of endocannabinoids may prove detrimental. Although the implications of FAAH deletion inferable from our experiment does not entirely replicate literature knowledge, one can argue that our work may not be completely comparable to other studies where an acute stimulation with LPS or brain injury was employed. In normal ageing, a pro-inflammatory milieu develops slowly over an extended period of time and the neuroinflammation is weaker than under most pathological conditions. Thus, it is possible that AEA blocks the acute induction of

inflammatory processes after a strong trigger, whereas it does not counteract slowly progressing pro-inflammatory changes. (Adapted and modified from Ativie et al. 2015).

## 5.5 Conclusion and outlook

The crucial role of microglia in host-defence against pathogens in the brain and the consequences of microglial overreactivity in the initiation and progression of neuroinflammatory processes are well established. Furthermore, the importance of neuron-microglial bidirectional regulation in maintenance of homeostasis in the CNS especially during ageing and the role of the endocannabinoid system are all reinforced by a body of growing evidence. In addition, the importance of CB1 receptor activity and GABA-CB1 receptor activity in supporting a balance between pro- and anti-inflammatory processes in the ageing brain has been reported. This present work further strengthens the aforementioned findings and provides a better understanding of which particular cell types and how the endocannabinoid signalling may be involved in the regulation of "normal" brain ageing process as well as in pathological processes. This study has shown that GABA-CB1 mediated endocannabinoid signalling is indispensable for a healthy brain ageing. We established that the reported downregulation of proinflammatory cytokines after an insult to the brain which is important to prevent damage to cells in the CNS especially neurons is disturbed in GABA-CB1 knockout mice. Furthermore, we showed that microgliosis and proinflammatory cytokines are slightly higher in GABA-CB1 receptor knockout individuals and become worsened after treatment with LPS in aged mice. This implies that pathological conditions are exacerbated in mice lacking GABA-CB1 receptors, particularly during ageing. Moreover, we demonstrated an increased accumulation of lipofuscin in microglia of old GABA-CB1 knockout mice, indicating an exacerbated senescent property in microglia and so with accelerated ageing in these mice. However, these changes did not result in heightened sickness behaviour or cognitive deficits distinct to the

GABA-CB1 knockout mice. This study also showed that a reduced 2-AG level leads to upregulation of direct neuron-microglial communication proteins during ageing, suggesting a compensation attempt for reduced cannabinoid signalling. Nevertheless, a reduced 2-AG level and the observed upregulation in neuroimmune regulator proteins were not accompanied by significant social or cognitive deficits in mice lacking Daglα. Although, reduced 2-AG level did not affect microglial activity in every case, increased AEA led to increased microgliosis and microglia activity irrespective of age. Now, with the exception of behavioural experiments, this study has shown that the genetic deletion of CB1 receptors on GABAergic neurons was sufficient to replicate findings reported in constitutive CB1 knockout mice, underlining the importance of GABAergic neurons in the regulation of microglial activity in the ageing and diseased brain. Nonetheless, further experiments most now focus on the dynamics of epigenetics and gene expression profile in these mice and the role of astrocytes should be looked into. The longitudinal behavioural experiments that are still ongoing should continue at least till mice are 24 months old. There is a good chance that the effect of reduced 2-AG level is only achievable at a much-advanced age.

# 6. Publications

Ativie, F., Albayram, O., Bach, K., Pradier, B., Zimmer, A. and Bilkei-Gorzo, A. (2015) 'Enhanced microglial activity in FAAH-/- animals', *Life Sciences*. Elsevier Inc., 138, pp. 52–56. doi: 10.1016/j.lfs.2014.12.01

# 7. Acknowledgement

In a community of benefactors, some truly stand out. So, I am most grateful and indebted to my supervisor PD Dr. Andras Bilkei-Gorzo; You are indeed a teacher in all ramifications with the patients of a father which makes you a natural “Doktorvater”. I consider myself most fortunate to have been under your tutelage. Thank you.

A worker needs a workshop. In light of these words, I am very thankful to Prof. Andreas Zimmer for accepting and giving me the opportunity to engage in this exciting research in his lab and also for providing a workplace that is accommodating to all. Thank you for the support.

How can I forget my first teacher in the lab Dr. Önder Albayram a.k.a “Dr. Love”. Although you were not in the lab to see me finish the work we started together, your inspiration, dedication and support during my first days in the lab saw me through the years. You are a truly loyal friend and mentor. I am for ever indebted to you buddy. Thank you for being you.

I will also like to thank Prof. Gerhard von der Emde for obliging to be my second reviewer. It might not occur to you, but you were one of the first persons to teach me the basic principles of neuroscience in the master program in neurosciences. So, you were practically with me all the way to see the seed you have planted grow. I am most grateful.

The lab is the second home of a scientist, so I will like to thank my friends and colleagues at the Institute of Molecular Psychiatry of the University Bonn for the friendly and enabling work-atmosphere. I appreciate your kindness and support.

It is often said that an accomplished child was certainly not guided by the parents alone, but also by the community at large. So, let me express my deepest gratitude to all legal and natural persons that have contributed one way or the other in building me up over the years.

Lastly, to my family and friends, the journey was long and sometimes rocky; very rocky indeed, but you stood by me. Thank you all for believing in me. Getting there folks, getting there.

# 8. Curriculum Vitae

## Frank Ativie

## Education

# 9. References

Ajmone-Cat, M. A., Nicolini, A. and Minghetti, L. (2003) 'Prolonged exposure of microglia to lipopolysaccharide modifies the intracellular signaling pathways and selectively promotes prostaglandin E 2 synthesis', *Journal of Neurochemistry*, 87(5), pp. 1193–1203. doi: 10.1046/j.1471-4159.2003.02087.x.

Akdis, M., Burgler, S., Crameri, R., Eiwegger, T., Fujita, H., Gomez, E., Klunker, S., Meyer, N., O'Mahony, L., Palomares, O., Rhyner, C., Quaked, N., Schaffartzik, A., Van De Veen, W., Zeller, S., Zimmermann, M. and Akdis, C. A. (2011) 'Interleukins, from 1 to 37, and interferon-γ: Receptors, functions, and roles in diseases', *Journal of Allergy and Clinical Immunology*, 127(3), pp. 701–721. doi: 10.1016/j.jaci.2010.11.050.

Albayram, O., Alferink, J., Pitsch, J., Piyanova, A., Neitzert, K., Poppensieker, K., Mauer, D., Michel, K., Legler, A., Becker, A., Monory, K., Lutz, B., Zimmer, A. and Bilkei-Gorzo, A. (2011) 'Role of CB1 cannabinoid receptors on GABAergic neurons in brain aging', *Proceedings of the National Academy of Sciences of the United States of America*, 108(27), pp. 11256–11261. doi: 10.1073/pnas.1016442108.

Albayram, O., Bilkei-Gorzo, A. and Zimmer, A. (2012) 'Loss of CB1 receptors leads to differential age-related changes in reward-driven learning and memory', *Frontiers in Aging Neuroscience*, 4(DEC), pp. 1–8. doi: 10.3389/fnagi.2012.00034.

Antonietta Ajmone-Cat, M., Mancini, M., De Simone, R., Cilli, P. and Minghetti, L. (2013) 'Microglial polarization and plasticity: Evidence from organotypic hippocampal slice cultures', *Glia*, 61(10), pp. 1698–1711. doi: 10.1002/glia.22550.

Ashton, J. C., Friberg, D., Darlington, C. L. and Smith, P. F. (2006) 'Expression of the cannabinoid CB2 receptor in the rat cerebellum: An immunohistochemical study', *Neuroscience Letters*. doi: 10.1016/j.neulet.2005.11.038.

Ativie, F., Albayram, O., Bach, K., Pradier, B., Zimmer, A. and Bilkei-Gorzo, A. (2015) 'Enhanced microglial activity in FAAH-/- animals', *Life Sciences*. Elsevier Inc., 138, pp. 52–56. doi:

10.1016/j.lfs.2014.12.016.

Atwood, B. K. and Mackie, K. (2010) 'CB2: a cannabinoid receptor with an identity crisis.', *British journal of pharmacology*. doi: 10.1111/j.1476-5381.2010.00729.x.

Aubert, A. (1999) 'Sickness and behaviour in animals: A motivational perspective', *Neuroscience and Biobehavioral Reviews*, 23(7), pp. 1029–1036. doi: 10.1016/S0149-7634(99)00034-2.

Bachstetter, A. D., Morganti, J. M., Jernberg, J., Schlunk, A. and Staten, H. (2012) 'NIH Public Access', 32(11), pp. 2030–2044. doi: 10.1016/j.neurobiolaging.2009.11.022.Fractalkine.

Bilkei-Gorzo, A. (2012) 'The endocannabinoid system in normal and pathological brain ageing', *Philos Trans R Soc Lond B Biol Sci*, 367(1607), pp. 3326–3341. doi: 10.1098/rstb.2011.0388.

Bilkei-Gorzo, A., Albayram, O., Draffehn, A., Michel, K., Piyanova, A., Oppenheimer, H., Dvir-Ginzberg, M., Rácz, I., Ulas, T., Imbeault, S., Bab, I., Schultze, J. L. and Zimmer, A. (2017) 'A chronic low dose of Δ9-tetrahydrocannabinol (THC) restores cognitive function in old mice', *Nature Medicine*. Nature Publishing Group, (July 2015). doi: 10.1038/nm.4311.

Bilkei-Gorzo, A., Drews, E., Albayram, Ö., Piyanova, A., Gaffal, E., Tueting, T., Michel, K., Mauer, D., Maier, W. and Zimmer, A. (2012) 'Early onset of aging-like changes is restricted to cognitive abilities and skin structure in Cnr1 -/- mice', *Neurobiology of Aging*. Elsevier Inc., 33(1), p. 200.e11-200.e22. doi: 10.1016/j.neurobiolaging.2010.07.009.

Bilkei-Gorzo, A., Racz, I., Valverde, O., Otto, M., Michel, K., Sarstre, M. and Zimmer, A. (2005) 'Early age-related cognitive impairment in mice lacking cannabinoid CB1 receptors', *Proceedings of the National Academy of Sciences*, 102(43), pp. 15670–15675. doi: 10.1073/pnas.0504640102.

Billadeau, D. D. and Leibson, P. J. (2002) 'ITAMs versus ITIMs: Striking a balance during cell regulation', *Journal of Clinical Investigation*, 109(2), pp. 161–168. doi: 10.1172/JCI200214843.

Bishop, N. A., Lu, T. and Yankner, B. A. (2010) 'Neural mechanisms of ageing and cognitive decline', *Nature*, 464(7288), pp. 529–535. doi: 10.1038/nature08983.

Bisogno, T., Howell, F., Williams, G., Minassi, A., Cascio, M. G., Ligresti, A., Matias, I., Schiano-

Moriello, A., Paul, P., Williams, E. J., Gangadbaran, U., Hobbs, C., Di Marzo, V. and Doherty, P. (2003) 'Cloning of the first sn1-DAG lipases points to the spatial and temporal regulation of endocannabinoid signaling in the brain', *Journal of Cell Biology*, 163(3), pp. 463–468. doi: 10.1083/jcb.200305129.

Bisogno, T. and Di Marzo, V. (2010) 'Cannabinoid receptors and endocannabinoids: role in neuroinflammatory and neurodegenerative disorders.', *CNS & neurological disorders drug targets*. doi: BSP/CDTCNSND/E-Pub/00056 [pii].

Blankman, J. L., Simon, G. M. and Cravatt, B. F. (2007) 'A Comprehensive Profile of Brain Enzymes that Hydrolyze the Endocannabinoid 2-Arachidonoylglycerol', *Chemistry and Biology*, 14(12), pp. 1347–1356. doi: 10.1016/j.chembiol.2007.11.006.

Block, M. L., Zecca, L. and Hong, J. S. (2007) 'Microglia-mediated neurotoxicity: uncovering the molecular mechanisms', *Nat Rev Neurosci*, 8(1), pp. 57–69. doi: 10.1038/nrn2038.

Brunk, U. T. and Terman, A. (2002) 'The mitochondrial-lysosomal axis theory of aging: Accumulation of damaged mitochondria as a result of imperfect autophagocytosis', *European Journal of Biochemistry*, 269(8), pp. 1996–2002. doi: 10.1046/j.1432-1033.2002.02869.x.

Burtner, C. R. and Kennedy, B. K. (2010) 'Progeria syndromes and ageing: what is the connection?', *Nature reviews. Molecular cell biology*. Nature Publishing Group, 11(8), pp. 567–578. doi: 10.1038/nrm2944.

Canas, P. M., Duarte, J. M. N., Rodrigues, R. J., Köfalvi, A. and Cunha, R. A. (2009) 'Modification upon aging of the density of presynaptic modulation systems in the hippocampus', *Neurobiology of Aging*, 30(11), pp. 1877–1884. doi: 10.1016/j.neurobiolaging.2008.01.003.

Carson, M. J., Doose, J. M., Melchior, B., Schmid, C. D. and Ploix, C. C. (2006) 'CNS immune privilege: Hiding in plain sight', *Immunological Reviews*, 213(1), pp. 48–65. doi: 10.1111/j.1600-065X.2006.00441.x.

Chakravarty, S. (2005) 'Toll-Like Receptor 4 on Nonhematopoietic Cells Sustains CNS Inflammation during Endotoxemia, Independent of Systemic Cytokines', *Journal of Neuroscience*, 25(7), pp. 1788–1796. doi: 10.1523/JNEUROSCI.4268-04.2005.

Chhor, V., Le Charpentier, T., Lebon, S., Oré, M. V., Celador, I. L., Josserand, J., Degos, V., Jacotot, E., Hagberg, H., Sävman, K., Mallard, C., Gressens, P. and Fleiss, B. (2013) 'Characterization of phenotype markers and neuronotoxic potential of polarised primary microglia In vitro', *Brain, Behavior, and Immunity*. Elsevier Inc., 32, pp. 70–85. doi: 10.1016/j.bbi.2013.02.005.

Conrad, C. D., Jackson, J. L., Wieczorek, L., Baran, S. E., Harman, J. S., Wright, R. L. and Korol, D. L. (2004) 'Acute stress impairs spatial memory in male but not female rats: Influence of estrous cycle', *Pharmacology Biochemistry and Behavior*, 78(3), pp. 569–579. doi: 10.1016/j.pbb.2004.04.025.

Correa, F., Hernangómez-Herrero, M., Mestre, L., Loría, F., Docagne, F. and Guaza, C. (2011) 'The endocannabinoid anandamide downregulates IL-23 and IL-12 subunits in a viral model of multiple sclerosis: Evidence for a cross-talk between IL-12p70/IL-23 axis and IL-10 in microglial cells', *Brain, Behavior, and Immunity*. Elsevier Inc., 25(4), pp. 736–749. doi: 10.1016/j.bbi.2011.01.020.

Dalton, G. D., Bass, C. E., Van Horn, C. G. and Howlett, A. C. (2009) 'Signal transduction via cannabinoid receptors', *CNS Neurol Disord Drug Targets*. doi: HT-3 (Puffenbarger) [pii].

DeForge, L. E. and Remick, D. G. (1991) 'Kinetics of TNF, IL-6, and IL-8 gene expression in LPS-stimulated human whole blood', *Biochemical and Biophysical Research Communications*, 174(1), pp. 18–24. doi: 10.1016/0006-291X(91)90478-P.

Delaney, J. R., Chou, A., Olsen, B., Carr, D., Murakami, C., Ahmed, U., Sim, S., An, E. H., Castanza, A. S., Fletcher, M., Higgins, S., Holmberg, M., Hui, J., Jelic, M., Jeong, K. S., Kim, J. R., Klum, S., Liao, E., Lin, M. S., Lo, W., Miller, H., Moller, R., Peng, Z. J., Pollard, T., Pradeep, P., Pruett, D., Rai, D., Ros, V., Schleit, J., Schuster, A., Singh, M., Spector, B. L., Sutphin, G. L., Wang, A. M., Wasko, B. M., Vander Wende, H., Kennedy, B. K. and Kaeberlein, M. (2013) 'End-of-life cell cycle arrest contributes to stochasticity of yeast replicative aging', *FEMS Yeast Research*, 13(3), pp. 267–276. doi: 10.1111/1567-1364.12030.

Devane, W. A., Dysarz, F. A. d, Johnson, M. R., Melvin, L. S. and Howlett, A. C. (1988) 'Determination and characterization of a cannabinoid receptor in rat brain', *Mol Pharmacol*.

Eder, C. (2009) 'Mechanisms of interleukin-1?? release', *Immunobiology*. Elsevier, 214(7), pp. 543–

553. doi: 10.1016/j.imbio.2008.11.007.

Eljaschewitsch, E., Witting, A., Mawrin, C., Lee, T., Schmidt, P. M., Wolf, S., Hoertnagl, H., Raine, C. S., Schneider-Stock, R., Nitsch, R. and Ullrich, O. (2006) 'The endocannabinoid anandamide protects neurons during CNS inflammation by induction of MKP-1 in microglial cells', *Neuron*, 49(1), pp. 67–79. doi: 10.1016/j.neuron.2005.11.027.

Facchinetti, F., Del Giudice, E., Furegato, S., Passarotto, M. and Leon, A. (2003) 'Cannabinoids ablate release of TNFα in rat microglial cells stimulated with lypopolysaccharide', *Glia*, 41(2), pp. 161–168. doi: 10.1002/glia.10177.

Felder, C. C., Briley, E. M., Axelrod, J., Simpson, J. T., Mackie, K. and Devane, W. A. (1993) 'Anandamide, an endogenous cannabimimetic eicosanoid, binds to the cloned human cannabinoid receptor and stimulates receptor-mediated signal transduction.', *Proceedings of the National Academy of Sciences of the United States of America*, 90(16), pp. 7656–60. doi: 10.1073/pnas.90.16.7656.

Fisch, G. S. (2007) 'Animal models and human neuropsychiatric disorders', *Behavior Genetics*, 37(1), pp. 1–10. doi: 10.1007/s10519-006-9117-0.

Freund, T. F., Katona, I. and Piomelli, D. (2003) 'Role of endogenous cannabinoids in synaptic signaling.', *Physiological reviews*, 83(3), pp. 1017–66. doi: 10.1152/physrev.00004.2003.

Gaoni, Y. and Mechoulam, R. (1964) 'Isolation, Structure, and Partial Synthesis of an Active Constituent of Hashish', *Journal of the American Chemical Society*, 86, pp. 1646–1647. doi: 10.1021/ja01062a046.

García-Gutiérrez, M. S., Pérez-Ortiz, J. M., Gutiérrez-Adán, A. and Manzanares, J. (2010) 'Depression-resistant endophenotype in mice overexpressing cannabinoid CB 2 receptors', *British Journal of Pharmacology*. doi: 10.1111/j.1476-5381.2010.00819.x.

Gellman, S. H., Conza, M., Nold, M., Krattiger, P., Demarcus, M., Fessmann, T., Mcateer, S., Schrader, T., Tsukube, H., Nishimura, Y., Yamazaki, I., Osuka, A., Horner, J. H., Newcomb, M., Kramer, R., Simova, S., Schneider, U., Chemie, V., Dobson, C. M. and Poulsen, F. M. (2002) 'Synthese und Struktur von Na 3 N', (10), pp. 2001–2003.

Ginhoux, F., Greter, M., Leboeuf, M., Nandi, S., See, P., Gokhan, S., Mehler, M. F., Conway, S. J., Ng, L. G., Stanley, E. R., Samokhvalov, I. M. and Merad, M. (2010) 'Fate Mapping Analysis Reveals That Adult Microglia Derive from Primitive Macrophages', *Science*, 330(6005), pp. 841–845. doi: 10.1126/science.1194637.

van Goethem, N. P., Rutten, K., van der Staay, F. J., Jans, L. A. W., Akkerman, S., Steinbusch, H. W. M., Blokland, A., van't Klooster, J. and Prickaerts, J. (2012) 'Object recognition testing: Rodent species, strains, housing conditions, and estrous cycle', *Behavioural Brain Research*. Elsevier B.V., 232(2), pp. 323–334. doi: 10.1016/j.bbr.2012.03.023.

Grabert, K., Michoel, T., Karavolos, M. H., Clohisey, S., Baillie, J. K., Stevens, M. P., Freeman, T. C., Summers, K. M. and McColl, B. W. (2016) 'Microglial brain region-dependent diversity and selective regional sensitivities to aging.', *Nature neuroscience*, 19(3), pp. 504–516. doi: 10.1038/nn.4222.

Hellwig, S., Brioschi, S., Dieni, S., Frings, L., Masuch, A., Blank, T. and Biber, K. (2016) 'Altered microglia morphology and higher resilience to stress-induced depression-like behavior in CX3CR1-deficient mice', *Brain, Behavior, and Immunity*, 55. doi: 10.1016/j.bbi.2015.11.008.

Hernangomez, M., Mestre, L., Correa, F. G., Lor??a, F., Mecha, M., I??igo, P. M., Docagne, F., Williams, R. O., Borrell, J. and Guaza, C. (2012) 'CD200-CD200R1 interaction contributes to neuroprotective effects of anandamide on experimentally induced inflammation', *GLIA*. doi: 10.1002/glia.22366.

Hoeffel, G., Wang, Y., Greter, M., See, P., Teo, P., Malleret, B., Leboeuf, M., Low, D., Oller, G., Almeida, F., Choy, S. H. Y., Grisotto, M., Renia, L., Conway, S. J., Stanley, E. R., Chan, J. K. Y., Ng, L. G., Samokhvalov, I. M., Merad, M. and Ginhoux, F. (2012) 'Adult Langerhans cells derive predominantly from embryonic fetal liver monocytes with a minor contribution of yolk sac-derived macrophages.', *The Journal of experimental medicine*, 209(6), pp. 1167–81. doi: 10.1084/jem.20120340.

Hoek, R. M. (2000) 'Down-Regulation of the Macrophage Lineage Through Interaction with OX2 (CD200)', *Science*, 290(5497), pp. 1768–1771. doi: 10.1126/science.290.5497.1768.

Jung, K. M., Astarita, G., Yasar, S., Vasilevko, V., Cribbs, D. H., Head, E., Cotman, C. W. and Piomelli, D. (2012) 'An amyloid ?? 42-dependent deficit in anandamide mobilization is associated with cognitive dysfunction in Alzheimer's disease', *Neurobiology of Aging*. Elsevier Inc., 33(8), pp. 1522–1532. doi: 10.1016/j.neurobiolaging.2011.03.012.

Jurgens, H. A. and Johnson, R. W. (2012) 'Dysregulated neuronal-microglial cross-talk during aging, stress and inflammation', *Experimental Neurology*. Elsevier Inc., 233(1), pp. 40–48. doi: 10.1016/j.expneurol.2010.11.014.

Justin, T. R., Josh, M. M., Adam, D. B., Charles, E. H., Melinda, P., Bethany, A. G., Edwin, J. W., Paula, C. B., Gemma, C., Vamc, A. H. and Fl, T. (2012) 'NIH Public Access', 31(45), pp. 16241–16250. doi: 10.1523/JNEUROSCI.3667-11.2011.CX3CR1.

Kano, M., Ohno-shosaku, T., Hashimotodani, Y. and Uchigashima, M. (2009) 'Endocannabinoid-Mediated Control of Synaptic Transmission', pp. 309–380. doi: 10.1152/physrev.00019.2008.

Katona, I., Sperlágh, B., Sík, A., Käfalvi, A., Vizi, E. S., Mackie, K. and Freund, T. F. (1999) 'Presynaptically located CB1 cannabinoid receptors regulate GABA release from axon terminals of specific hippocampal interneurons.', *The Journal of neuroscience : the official journal of the Society for Neuroscience*, 19(11), pp. 4544–4558. doi: 10.1523/JNEUROSCI.4587-05.2006.

Keimpema, E., Straiker, A., Mackie, K., Harkany, T. and Hjerling-Leffler, J. (2012) 'Sticking out of the crowd: the molecular identity and development of cholecystokinin-containing basket cells', *J Physiol The Journal of Physiology S*, 5904(November 2011), pp. 703–714. doi: 10.1113/jphysiol.2011.224386.

Kenney, J. W. and Gould, T. J. (2009) 'Plasticity by Nicotine', *Molecular Neurology*, 38(1), pp. 101–121. doi: 10.1007/s12035-008-8037-9.Modulation.

Köfalvi, K. S. and A. (2016) 'Cannabis: A Treasure Trove or Pandora's Box?', *Mini-Reviews in Medicinal Chemistry*, pp. 1–70. doi: http://dx.doi.org/10.2174/1389557516666161004162133.

Lee, M., Schwab, C. and Mcgeer, P. L. (2011) 'Astrocytes are GABAergic cells that modulate microglial activity', *Glia*, 59(1), pp. 152–165. doi: 10.1002/glia.21087.

Lee, S.-H. and Soltesz, I. (2011) 'Requirement for CB1 but not GABAB receptors in the cholecystokinin mediated inhibition of GABA release from cholecystokinin expressing basket cells.', *The Journal of physiology*, 589(Pt 4). doi: 10.1113/jphysiol.2010.198499.

Lefebvre, J. L., Kostadinov, D., Chen, W. V, Maniatis, T. and Sanes, J. R. (2012) 'Protocadherins Mediate Dendritic Self-Avoidance in the Mammalian Nervous System', *Nature*. Nature Publishing Group, 488(7412), pp. 517–521. doi: 10.1038/nature11305.

Lopez-Otin, C., Blasco, M. A., Partridge, L., Serrano, M. and Kroemer, G. (2013) 'The hallmarks of aging', *Cell*, 153(6). doi: 10.1016/j.cell.2013.05.039.

Lucin, K. M. and Wyss-Coray, T. (2009) 'Immune Activation in Brain Aging and Neurodegeneration: Too Much or Too Little?', *Neuron*. Elsevier Inc., 64(1), pp. 110–122. doi: 10.1016/j.neuron.2009.08.039.

Maccarrone, M., Bab, I., Bíró, T., Cabral, G. A., Dey, S. K., Di Marzo, V., Konje, J. C., Kunos, G., Mechoulam, R., Pacher, P., Sharkey, K. A. and Zimmer, A. (2015) 'Endocannabinoid signaling at the periphery: 50 years after THC', *Trends in Pharmacological Sciences*, 36(5), pp. 277–296. doi: 10.1016/j.tips.2015.02.008.

Mackie, K., Devane, W. A. and Hille, B. (1993) 'Anandamide, an endogenous cannabinoid, inhibits calcium currents as a partial agonist in N18 neuroblastoma cells.', *Molecular pharmacology*.

Mackie, K. and Hille, B. (1992) 'Cannabinoids inhibit N-type calcium channels in neuroblastoma-glioma cells.', *Proceedings of the National Academy of Sciences of the United States of America*, 89(9), pp. 3825–3829. doi: 10.1073/pnas.89.9.3825.

Mallard, C., Wang, X. and Hagberg, H. (2009) 'The Role of Toll-like Receptors in Perinatal Brain Injury', *Clinics in Perinatology*, 36(4), pp. 763–772. doi: 10.1016/j.clp.2009.07.009.

Di Marzo, V., Bifulco, M. and De Petrocellis, L. (2004) 'The endocannabinoid system and its therapeutic exploitation.', *Nature reviews. Drug discovery*. doi: 10.1038/nrd1495.

Di Marzo, V. and De Petrocellis, L. (2010) 'Endocannabinoids as regulators of transient receptor

potential (TRP) channels: A further opportunity to develop new endocannabinoid-based therapeutic drugs.', *Current medicinal chemistry*. doi: BSP/CMC/E-Pub/ 094 [pii].

Di Marzo, V. and De Petrocellis, L. (2012) 'Why do cannabinoid receptors have more than one endogenous ligand?', *Philosophical Transactions of the Royal Society B: Biological Sciences*, 367(1607), pp. 3216–3228. doi: 10.1098/rstb.2011.0382.

Massberg, S., Schaerli, P., Knezevic-Maramica, I., Köllnberger, M., Tubo, N., Moseman, E. A., Huff, I. V., Junt, T., Wagers, A. J., Mazo, I. B. and von Andrian, U. H. (2007) 'Immunosurveillance by Hematopoietic Progenitor Cells Trafficking through Blood, Lymph, and Peripheral Tissues', *Cell*, 131(5), pp. 994–1008. doi: 10.1016/j.cell.2007.09.047.

McHugh, D., Page, J., Dunn, E. and Bradshaw, H. B. (2012) 'Δ 9-tetrahydrocannabinol and N-arachidonyl glycine are full agonists at GPR18 receptors and induce migration in human endometrial HEC-1B cells', *British Journal of Pharmacology*, 165(8), pp. 2414–2424. doi: 10.1111/j.1476-5381.2011.01497.x.

Mecha, M., Feliú, A., Carrillo-Salinas, F. J., Rueda-Zubiaurre, A., Ortega-Gutiérrez, S., de Sola, R. G. and Guaza, C. (2015) 'Endocannabinoids drive the acquisition of an alternative phenotype in microglia', *Brain, Behavior, and Immunity*. Elsevier Inc., 49, pp. 233–245. doi: 10.1016/j.bbi.2015.06.002.

Meziane, H., Ouagazzal, A. M., Aubert, L., Wietrzych, M. and Krezel, W. (2007) 'Estrous cycle effects on behavior of C57BL/6J and BALB/cByJ female mice: Implications for phenotyping strategies', *Genes, Brain and Behavior*. doi: 10.1111/j.1601-183X.2006.00249.x.

Miller, L. K. L. and Devi, L. a (2011) 'The highs and lows of cannabinoid receptor expression in disease: mechanisms and their therapeutic implications', *Pharmacological Reviews*, 63(3), pp. 461–470. doi: 10.1124/pr.110.003491.461.

Milligan, E. D., Sloane, E. M. and Watkins, L. R. (2008) 'Glia in pathological pain: A role for fractalkine', *Journal of Neuroimmunology*, 198(1–2), pp. 113–120. doi: 10.1016/j.jneuroim.2008.04.011.

Miron, V. E., Boyd, A., Zhao, J.-W., Yuen, T. J., Ruckh, J. M., Shadrach, J. L., van Wijngaarden, P.,

Wagers, A. J., Williams, A., Franklin, R. J. M. and ffrench-Constant, C. (2013) 'M2 microglia and macrophages drive oligodendrocyte differentiation during CNS remyelination.', *Nature neuroscience*, 16(9), pp. 1211–8. doi: 10.1038/nn.3469.

Mogil, J. S., Chesler, E. J., Wilson, S. G., Juraska, J. M. and Sternberg, W. F. (2000) 'Sex differences in thermal nociception and morphine antinociception in rodents depend on genotype', *Neuroscience and Biobehavioral Reviews*. doi: 10.1016/S0149-7634(00)00015-4.

Munro, S., Thomas, K. L. and Abu-Shaar, M. (1993) 'Molecular characterization of a peripheral receptor for cannabinoids.', *Nature*. doi: 10.1038/365061a0.

Murataeva, N., Straiker, A. and MacKie, K. (2014) 'Parsing the players: 2-arachidonoylglycerol synthesis and degradation in the CNS', *British Journal of Pharmacology*, 171(6), pp. 1379–1391. doi: 10.1111/bph.12411.

Murray, R. M., Morrison, P. D., Henquet, C. and Di Forti, M. (2007) 'Cannabis, the mind and society: the hash realities.', *Nature Reviews Neuroscience*. doi: 10.1038/nrn2253.

Nakane, S., Oka, S., Arai, S., Waku, K., Ishima, Y., Tokumura, A. and Sugiura, T. (2002) '2-Arachidonoyl-sn-glycero-3-phosphate, an arachidonic acid-containing lysophosphatidic acid: Occurrence and rapid enzymatic conversion to 2-arachidonoyl-sn-glycerol, cannabinoid receptor ligand, in rat brain', *Archives of Biochemistry and Biophysics*. doi: 10.1016/S0003-9861(02)00038-3.

Nestler, E. J. and Hyman, S. E. (2010) 'Animal models of neuropsychiatric disorders', *Nature Neuroscience*. Nature Publishing Group, 13(10), pp. 1161–1169. doi: 10.1038/nn.2647.

Neumann, H. (2001) 'Control of glial immune function by neurons', *Glia*, 36(2), pp. 191–199. doi: 10.1002/glia.1108.

Neumann, H., Misgeld, T., Matsumuro, K. and Wekerle, H. (1998) 'Neurotrophins inhibit major histocompatibility class II inducibility of microglia: Involvement of the p75 neurotrophin receptor', *Neurobiology and approved*, 95(May), p. 57795784. doi: 10.1073/pnas.95.10.5779.

Niraula, A., Sheridan, J. F. and Godbout, J. P. (2016) 'Microglia Priming with Aging and Stress',

*Neuropsychopharmacology*. doi: 10.1038/npp.2016.185.

Ohno-Shosaku, T., Maejima, T. and Kano, M. (2001) 'Endogenous cannabinoids mediate retrograde signals from depolarized postsynaptic neurons to presynaptic terminals', *Neuron*, 29(3), pp. 729–738. doi: 10.1016/S0896-6273(01)00247-1.

Ortega-Gutiérrez, S., Molina-Holgado, E. and Guaza, C. (2005) 'Effect of anandamide uptake inhibition in the production of nitric oxide and in the release of cytokines in astrocyte cultures', *Glia*, 52(2), pp. 163–168. doi: 10.1002/glia.20229.

Ousman, S. S. and Kubes, P. (2012) 'Immune surveillance in the central nervous system', *Nature Neuroscience*. Nature Publishing Group, 15(8), pp. 1096–1101. doi: 10.1038/nn.3161.

Palazuelos, J., Aguado, T., Pazos, M. R., Julien, B., Carrasco, C., Resel, E., Sagredo, O., Benito, C., Romero, J., Azcoitia, I., Fernández-Ruiz, J., Guzmán, M. and Galve-Roperh, I. (2009) 'Microglial CB2 cannabinoid receptors are neuroprotective in Huntington's disease excitotoxicity', *Brain*, 132(11), pp. 3152–3164. doi: 10.1093/brain/awp239.

Perry, V. H. and Holmes, C. (2014) 'Microglial priming in neurodegenerative disease.', *Nature reviews. Neurology*, 10(4). doi: 10.1038/nrneurol.2014.38.

De Petrocellis, L. and Di Marzo, V. (2010) 'Non-CB1, Non-CB2 receptors for endocannabinoids, plant cannabinoids, and synthetic cannabimimetics: Focus on G-protein-coupled receptors and transient receptor potential channels', *Journal of Neuroimmune Pharmacology*. doi: 10.1007/s11481-009-9177-z.

Piyanova, A., Albayram, O., Rossi, C. A., Farwanah, H., Michel, K., Nicotera, P., Sandhoff, K. and Bilkei-Gorzo, A. (2013) 'Loss of CB1 receptors leads to decreased cathepsin D levels and accelerated lipofuscin accumulation in the hippocampus', *Mechanisms of Ageing and Development*. doi: 10.1016/j.mad.2013.08.001.

Piyanova, A., Lomazzo, E., Bindila, L., Lerner, R., Albayram, O., Ruhl, T., Lutz, B., Zimmer, A. and Bilkei-Gorzo, A. (2015) 'Age-related changes in the endocannabinoid system in the mouse hippocampus', *Mechanisms of Ageing and Development*, 150. doi: 10.1016/j.mad.2015.08.005.

Ransohoff, R. M. (2016) ‘A polarizing question: do M1 and M2 microglia exist?’, *Nature neuroscience*, 19(8). doi: 10.1038/nn.4338.

Ransohoff, R. M. and Cardona, A. E. (2010) ‘The myeloid cells of the central nervous system parenchyma’, *Nature*, 468(7321), pp. 253–262. doi: 10.1038/nature09615.

Reibaud, M., Obinu, M. C., Ledent, C., Parmentier, M., Böhme, G. a and Imperato, a (1999) ‘Enhancement of memory in cannabinoid CB1 receptor knock-out mice.’, *European journal of pharmacology*, 379(1), pp. R1–R2. doi: S0014299999004963 [pii].

Riga, D., Riga, S., Halalau, F. and Schneider, F. (2006) ‘Brain lipopigment accumulation in normal and pathological aging’, *Annals of the New York Academy of Sciences*, 1067(1), pp. 158–163. doi: 10.1196/annals.1354.019.

Rowinska, Z., Koeppel, T. A., Sanati, M., Schelzig, H., Jankowski, J., Weber, C., Zernecke, A. and Liehn, E. A. (2017) ‘Role of the CX3C chemokine receptor CX3CR1 in the pathogenesis of atherosclerosis after aortic transplantation’, *Plos One*, 12(2), p. e0170644. doi: 10.1371/journal.pone.0170644.

Schulz, C., Gomez Perdiguero, E., Chorro, L., Szabo-Rogers, H., Cagnard, N., Kierdorf, K., Prinz, M., Wu, B., Jacobsen, S. E. W., Pollard, J. W., Frampton, J., Liu, K. J. and Geissmann, F. (2012) ‘A lineage of myeloid cells independent of Myb and hematopoietic stem cells.’, *Science (New York, N.Y.)*, 336(6077), pp. 86–90. doi: 10.1126/science.1219179.

Sheridan, G. K. and Murphy, K. J. (2013) ‘Neuron-glia crosstalk in health and disease: fractalkine and CX3CR1 take centre stage.’, *Open biology*, 3(12), p. 130181. doi: 10.1098/rsob.130181.

Singh, A. K. and Jiang, Y. (2004) ‘How does peripheral lipopolysaccharide induce gene expression in the brain of rats?’, *Toxicology*, 201(1–3), pp. 197–207. doi: 10.1016/j.tox.2004.04.015.

Soreq, L., Rose, J., Soreq, E., Hardy, J., Trabzuni, D., Cookson, M. R., Smith, C., Ryten, M., Patani, R. and Ule, J. (2017) ‘Major Shifts in Glial Regional Identity Are a Transcriptional Hallmark of Human Brain Aging’, *Cell Reports*. ElsevierCompany., 18(2), pp. 557–570. doi: 10.1016/j.celrep.2016.12.011.

Stella, N. (2009) ‘Endocannabinoid signaling in microglial cells’, *Neuropharmacology*. Elsevier Ltd, 56(SUPPL. 1), pp. 244–253. doi: 10.1016/j.neuropharm.2008.07.037.

Streit, W. J. and Xue, Q. S. (2014) ‘Human CNS immune senescence and neurodegeneration’, *Current Opinion in Immunology*. doi: 10.1016/j.coi.2014.05.005.

Suárez, J., Llorente, R., Romero-Zerbo, S. Y., Mateos, B., Bermúdez-Silva, F. J., De Fonseca, F. R. and Viveros, P. (2009) ‘Early maternal deprivation induces gender-dependent changes on the expression of hippocampal CB1 and CB2 cannabinoid receptors of neonatal rats’, *Hippocampus*. doi: 10.1002/hipo.20537.

Tchantchou, F., Tucker, L. B., Fu, A. H., Bluett, R. J., Joseph, T., Patel, S., Zhang, Y. and Sciences, H. (2015) ‘HHS Public Access’, pp. 427–439. doi: 10.1016/j.neuropharm.2014.06.006.The.

Terman and Brunk (2004) ‘Lipofuscin’, *International Journal of Biochemistry and Cell Biology*.

Tham, C. S., Whitaker, J., Luo, L. and Webb, M. (2007) ‘Inhibition of microglial fatty acid amide hydrolase modulates LPS stimulated release of inflammatory mediators’, *FEBS Letters*, 581(16), pp. 2899–2904. doi: 10.1016/j.febslet.2007.05.037.

Tominaga, K., Saito, S., Matsuura, M. and Nakano, M. (1999) ‘Lipopolysaccharide tolerance in murine peritoneal macrophages induces downregulation of the lipopolysaccharide signal transduction pathway through mitogen-activated protein kinase and nuclear factor-kappaB cascades, but not lipopolysaccharide-incorporatio’, *Biochimica et biophysica acta*, 1450(2), pp. 130–44. Available at: http://www.ncbi.nlm.nih.gov/pubmed/10354505.

Trezza, V., Cuomo, V. and Vanderschuren, L. J. M. J. (2008) ‘Cannabis and the developing brain: Insights from behavior’, *European Journal of Pharmacology*, 585(2–3), pp. 441–452. doi: 10.1016/j.ejphar.2008.01.058.

UNODC (2015) *World Drug Report 2015, United Nations publication*. doi: 10.1017/CBO9781107415324.004.

Vaure, C. and Liu, Y. (2014) ‘A comparative review of toll-like receptor 4 expression and functionality

in different animal species', *Frontiers in Immunology*, 5(JUL), pp. 1–15. doi: 10.3389/fimmu.2014.00316.

Villeda, S. A., Luo, J., Mosher, K. I., Zou, B., Britschgi, M., Bieri, G., Stan, T. M., Fainberg, N., Ding, Z., Eggel, A., Lucin, K. M., Czirr, E., Park, J. S., Couillard-Despres, S., Aigner, L., Li, G., Peskind, E. R., Kaye, J. A., Quinn, J. F., Galasko, D. R., Xie, X. S., Rando, T. A. and Wyss-Coray, T. (2011) 'The ageing systemic milieu negatively regulates neurogenesis and cognitive function', *Nature*, 477(7362), pp. 90–94. doi: 10.1038/nature10357.

Vinet, J., van Weering, H. R., Heinrich, A., Kälin, R. E., Wegner, A., Brouwer, N., Heppner, F. L., van Rooijen, N., Boddeke, H. W., Biber, K., Bechmann, I., Galea, I., Perry, V., Kreutzberg, G., Rossum, D. Van, Hanisch, U., Hanisch, U., Kettenmann, H., S, Z. (2012) 'Neuroprotective function for ramified microglia in hippocampal excitotoxicity', *Journal of Neuroinflammation*. BioMed Central Ltd, 9(1), p. 27. doi: 10.1186/1742-2094-9-27.

Wang, L., Liu, J., Harvey-White, J., Zimmer, A. and Kunos, G. (2003) 'Endocannabinoid signaling via cannabinoid receptor 1 is involved in ethanol preference and its age-dependent decline in mice.', *Proceedings of the National Academy of Sciences of the United States of America*, 100(3), pp. 1393–8. doi: 10.1073/pnas.0336351100.

Wei, R. and Jonakait, G. M. (1999) 'Neurotrophins and the anti-inflammatory agents interleukin-4 (IL-4), IL- 10, IL-11 and transforming growth factor-??1 (TGF-??1) down-regulate T cell costimulatory molecules B7 and CD40 on cultured rat microglia', *Journal of Neuroimmunology*, 95(1–2), pp. 8–18. doi: 10.1016/S0165-5728(98)00248-3.

Wong, W. T. (2013) 'Microglial aging in the healthy CNS: phenotypes, drivers, and rejuvenation.', *Frontiers in cellular neuroscience*, 7(22), p. 10.3389/fncel.2013.00022. doi: 10.3389/fncel.2013.00022.

World Health Organization (2015) 'World Report on Ageing and Health', pp. 1–247.

Wynne, A. M., Henry, C. J. and Godbout, J. P. (2009) 'Immune and behavioral consequences of microglial reactivity in the aged brain', *Integrative and Comparative Biology*, 49(3), pp. 254–266. doi: 10.1093/icb/icp009.

Wyss-Coray, T. (2016) ‘Ageing, neurodegeneration and brain rejuvenation’, *Nature*, 539(7628), pp. 180–186. doi: 10.1038/nature20411.

Zhang, H., Hayashi, T., Tsuru, K., Deguchi, K., Nagahara, M., Hayakawa, S., Nagai, M., Kamiya, T., Osaka, A. and Abe, K. (2007) ‘Vascular endothelial growth factor promotes brain tissue regeneration with a novel biomaterial polydimethylsiloxane-tetraethoxysilane’, *Brain Research*, 1132(1), pp. 29–35. doi: 10.1016/j.brainres.2006.09.117.

Zhang, S., Wang, X.-J., Tian, L.-P., Pan, J., Lu, G.-Q., Zhang, Y.-J., Ding, J.-Q. and Chen, S.-D. (2011) ‘CD200-CD200R dysfunction exacerbates microglial activation and dopaminergic neurodegeneration in a rat model of Parkinson’s disease’, *Journal of Neuroinflammation*. BioMed Central Ltd, 8(1), p. 154. doi: 10.1186/1742-2094-8-154.